

Olefin Hydrotreating and Characterization of Olefins in Thermally Cracked Naphtha

by

Annapoorna Shruthi Budnar Subramanya

A thesis submitted in partial fulfillment of the requirements for the degree of

Master of Science

in

Chemical Engineering

Department of Chemical and Materials Engineering
University of Alberta

© Annapoorna Shruthi Budnar Subramanya, 2020

Abstract

Bitumen partial upgrading technologies aim to produce a product that meets viscosity and density specifications for pipeline transport with little to no addition of diluents. Thermal cracking processes are attractive for partial upgrading since they result in an increase in the light fractions. Thermal cracking, however, results in the formation of olefins that are concentrated in the lower boiling cuts of the cracked product. The olefin content must be reduced sufficiently to improve the storage stability of the cracked product and to meet the regulatory specifications for transportation by pipelines. The BituMaxTM partial upgrading process makes use of an olefin-aromatic alkylation process to reduce the olefin content in the product. Determination of the nature and abundance of olefins provides knowledge that is needed to support the development of the BituMaxTM olefin treatment process.

One objective of this study was to characterize olefins in thermally cracked naphtha (boiling point 15 – 240 °C) obtained from a bitumen upgrader facility located in Alberta, Canada. The cracked naphtha was sub-fractionated into smaller boiling cuts in a lab-scale atmospheric distillation column. The sub-fractions were analyzed using gas chromatography with mass spectrometer (GC-MS) and flame ionization detector (GC-FID). Identification of olefinic species was confirmed by subjecting the cracked naphtha to mild hydrotreatment and comparison of chromatograms before and after hydrotreatment. This was necessary because assignment of compound identity based solely on the suggestions of the Mass Spectral Library was unreliable for distinguishing between olefins and cycloparaffins with the same molecular formula.

A reaction study was conducted with model compounds to evaluate the hydrogenation activity of Ni/Al₂O₃ catalytic systems, with an aim to better understand olefin hydrotreating in the presence of aromatics, which also had some relevance to the naphtha characterization.

Hydrogenation reactions with model naphtha were conducted in the temperature range 60 to 280 °C, 1 MPa H₂ pressure at 1000 mL H₂/mL liquid ratio and weight hourly space velocity of 0.5 h⁻¹ based on the liquid feed. Model naphtha was made of 1-hexene (10 wt%), toluene (5 wt%) and *n*-octane (85 wt%). The reactions were studied over both reduced and sulfided Ni/Al₂O₃ catalysts. For the study of sulfided Ni/Al₂O₃, the catalyst was subjected to in situ sulfiding, and the feed was spiked with dimethyl disulfide (0.5 wt%) to keep the catalyst in a sulfided state. Hydrogenation of the model naphtha over reduced Ni/Al₂O₃ catalyst resulted in near complete conversion of 1-hexene to *n*-hexane at temperatures as low as 80 °C and near complete conversion of toluene to methylcyclohexane at 160 °C. Hydrogenation over sulfided Ni/Al₂O₃ catalyst resulted in selective conversion of 1-hexene compared to toluene, but the products formed below 240 °C were *n*-hexane and internal isomers *cis*-3-hexene, *trans*-3-hexene, *cis*-2-hexene and *trans*-2-hexene. Conversion to *n*-hexane was higher than 20% only at temperatures above 240 °C. Trace concentrations of a skeletal isomerization product of 1-hexene was also detected at temperatures above 240 °C.

A first-pass identification of compounds in the cracked naphtha by GC-MS was verified using model compounds and by spiking sub-fractions. The identification of olefinic species was checked by comparison of chromatograms before and after mild hydrotreatment coupled with comparison of non-isothermal retention indices with the values reported in literature, when such data was available. The concentration of the species was calculated by evaluating average FID response factors for various compound classes identified in the cracked naphtha sample. Approximately 74 wt% of compounds that made up the cracked naphtha were identified by the characterization study.

The identified species consisted of 40 wt% paraffins, 13 wt% olefins, 12 wt% cycloparaffins, 4 wt% aromatic compounds and 5 wt% sulfur compounds. The majority of the olefinic species found were in the C₅-C₇ range. The nature of the olefinic species was determined – straight chained (~6 wt%), branched olefins (~4 wt%), cyclic olefins (~3 wt%) and diolefins (~0.2 wt%).

Preface

(Mandatory due to collaborative work)

The characterization of cracked naphtha (Chapter 5 of this thesis) was done in collaboration with Cloribel Santiago, former research assistant at University of Alberta. Cloribel was in-charge of developing suitable method conditions for GC analyses and preparing a preliminary database of compounds based on GC-MS identification. I was responsible for sub-fractionation, hydrotreatment and preparation of samples for GC-MS and GC-FID studies and subsequently updating the database by tracking the changes post hydrotreatment, to confirm the identity of the olefins. Arno De Klerk supervised the entire study and was involved in concept formation and reviewing the results of the study.

Cibele Halmenschlager, research associate at University of Alberta, supervised the operation of the continuous flow reactor for catalytic hydrogenation (Chapter 3). Giselle Uzcategui and Shirley Fong, graduate students at the University of Alberta, helped with distillation of cracked naphtha samples (Chapter 4). Garima Chauhan, post-doctoral research associate at University of Alberta, performed the SimDis analyses (Chapter 4).

Dedication

To Appa,

For your sacrifices that helped me access higher education – a privilege that you were denied.

You loved me enough to let me go and explore my dreams.

Acknowledgement

At the onset, I would like to express my heartfelt gratitude to my thesis supervisor, Dr Arno De Klerk for providing me the opportunity to learn and grow as an engineer. Thank you, especially, for all the thought-provoking conversations that went beyond engineering and graduate studies. I would also like to thank NSERC, CNOOC International Ltd and Alberta Innovates for funding my thesis project.

Many thanks to Cloribel Santiago and Cibele Halmenschlager for your patience and guidance with my thesis project. I am grateful that I got the opportunity to work closely with not one, but two wonderful female scientists who handle multiple responsibilities with absolute grace.

I would like to thank all the graduate students and research associates who are part of my research group for being the most supportive and friendly bunch to work with. A special mention to Adriana, Shirley and Natalia for your kindness and empathy that have reassured me during times of distress. An extra special mention to Felipe for all the love and support. Thank you for brightening up my days with your geniality and humor.

I am extremely grateful to Charity Slobod and all the amazing staff of FGSR for helping me become a better communicator and providing multiple opportunities to speak about my research to a wide-ranging audience. I am indebted to you all for helping me overcome cultural barriers and gain self-confidence.

My parents Jyothi and Subramanya Bhat and aunts Shuba and Radha are the reason I am here today. Your unconditional love, encouragement and belief in me is a beacon of light that guides all my decisions and successes in life. I hope to always make you proud with my work.

I want to acknowledge the support and love of my best friends Vidya and Arshitha. Words cannot express how grateful I am to have you both in my life. Thank you for standing by me and enriching my graduate school experience even without physically being by my side. Same goes for my partner, Sid. Thank you, Sid, for your unending support and understanding that helps me to aim for the skies. I am glad that you have the conviction in my abilities even when I lose sight of them. I could not have asked for a better support system through my journey of migrating to a new country and experiencing the challenges of graduate studies.

Table of Contents

CHAPTER 1 – INTRODUCTION	1
1.1 Background.....	1
1.2 Objective.....	5
1.3 Scope of work.....	6
1.4 References.....	6
CHAPTER 2: LITERATURE REVIEW	8
2.1 Partial upgrading of bitumen	8
2.1.1 Thermal cracking for partial upgrading.....	8
2.1.2 BituMax™ olefin treatment by Friedel Crafts alkylation.....	10
2.2 Characterization of olefins in complex organic mixtures.....	12
2.2.1 Characterization by high resolution gas chromatography integrated with detectors...	13
2.2.2 Compositional studies of cracked naphtha	16
2.3 Catalytic hydrogenation.....	18
2.3.1 Catalyst selection for olefin hydrogenation.....	19
2.3.2 Olefin hydrogenation with reduced Ni catalyst.....	20
2.3.3 Olefin hydrogenation with sulfided nickel catalyst.....	20
2.4 References.....	21
CHAPTER 3: HYDROGENATION OF OLEFIN-CONTAINING FEED OVER Ni/Al₂O₃ CATALYST	25
Abstract.....	25
3.1 Introduction.....	26
3.2 Experimental.....	27
3.2.1 Materials	27
3.2.2 Catalyst preparation and characterization.....	28
3.2.3 Catalyst reduction	29
3.2.4 Catalyst presulfiding.....	29
3.2.5 Reactor design.....	32
3.2.6 Reactor operation.....	37
3.2.7 Analyses.....	38
3.2.8 Calculations.....	41

3.2.9 Calibration.....	42
3.3 Results.....	43
3.3.1 GC-MS identification of reaction products.....	43
3.3.1.1 Unsulfided model feed hydrogenation.....	43
3.3.1.2 Sulfided model feed hydrogenation.....	46
3.3.2 Conversion of 1-hexene and toluene into hydrogenated products.....	50
3.3.2.1 Reactions over unsulfided Ni/Al ₂ O ₃	50
3.3.2.2 Reactions over sulfided Ni/Al ₂ O ₃	53
3.3.3 Spent catalyst analysis.....	56
3.4 Discussion.....	58
3.4.1 Equilibrium of olefin and aromatic hydrogenation reactions.....	58
3.4.1 Hydrogenation of olefins over reduced Ni/Al ₂ O ₃ catalyst.....	60
3.4.2 Hydrogenation of olefins over sulfided Ni/Al ₂ O ₃ catalyst.....	60
3.4.3 Effect of catalyst pretreatment on hydrogenation of aromatic compounds.....	61
3.4.4 Reactions of sulfur compounds in the feed.....	62
3.5 Conclusions.....	62
3.6 References.....	63
CHAPTER 4: ATMOSPHERIC DISTILLATION OF THERMALLY CRACKED PRODUCT BEFORE AND AFTER HYDROTREATMENT	65
4.1 Introduction.....	65
4.2 Experimental.....	66
4.2.1 Materials.....	66
4.2.2 Distillation column design.....	67
4.2.3 Distillation column operation.....	69
4.2.4 Analyses.....	71
4.2.5 Calculations.....	73
4.3 Results.....	73
4.4 Discussions.....	78
4.4.1 Boiling point distribution of cracked naphtha – Comparison of simulated distillation and atmospheric distillation.....	78
4.4.2 Effect of hydrotreatment on boiling point distribution of cracked naphtha.....	81

4.4.3 Effect of hydrotreatment on density and refractive indices of sub-fractions.....	83
4.5 Conclusions.....	84
4.6 References.....	85
CHAPTER 5: CHARACTERIZATION OF CRACKED NAPHTHA TO IDENTIFY AND MEASURE CONCENTRATION OF OLEFINIC SPECIES.....	86
Abstract.....	86
5.1 Introduction.....	87
5.2 Experimental.....	88
5.2.1 Materials.....	88
5.2.2 Analyses.....	89
5.3 Results.....	92
5.3.1 GC-MS compound identification.....	92
5.3.2 Compound verification with model compounds.....	94
5.3.3 Verification of compounds by hydrotreatment.....	96
5.3.4 Verification of compounds by spiking sub-fractions.....	97
5.3.5 Concentration of various compound classes in cracked naphtha.....	99
5.4 Discussion.....	100
5.4.1 Verification of nature of identified olefins.....	100
5.4.2 Implications for Bitumax™ partial upgrading process.....	103
5.5 Conclusions.....	104
5.6 References.....	105
CHAPTER 6 – CONCLUSIONS.....	107
6.1 Conclusions.....	107
6.2 Future work.....	108
BIBLIOGRAPHY.....	109
APPENDIX A: Determination of Average Response Factors for Compound Classes.....	114
APPENDIX B: Quantification of hydrogenation reaction products using GC-FID.....	118
APPENDIX C: Model mass balance calculations for hydrogenation reactions.....	120
APPENDIX D: Supplementary information for identification of unknown peaks.....	123
APPENDIX E: List of compounds identified in cracked naphtha.....	127
APPENDIX F: Concentration of compounds identified in cracked naphtha.....	165

List of Tables

Table 1.1 Pipeline specifications for Alberta bitumen products	1
Table 2.1 Characterization of cracked naphthas from Gujarat region in India	17
Table 2.2 Characterization of FCC naphtha from Scanraff refinery in Lysekil, Sweden	17
Table 2.3 Characterization of FCC naphtha from mid-continent petroleum	18
Table 3.1 Materials used for hydrogenation reaction study	27
Table 3.2 Operating conditions for hydrogenation reactions	38
Table 3.3 Average response factors relative to cyclohexane for GC-FID	39
Table 3.4 Compounds in unsulfided feed for hydrogenation reactions	44
Table 3.5 Compounds in hydrogenated product over unsulfided catalyst	45
Table 3.6 Compounds in sulfided feed for hydrogenation reactions	47
Table 3.7 Compounds in hydrogenated product over sulfided catalyst	49
Table 3.8 Mass balances of hydrogenation reactions over unsulfided catalyst	51
Table 3.9 GC-FID results for composition of unsulfided feed and hydrogenated products	51
Table 3.10 Equilibrium vapor-phase compositions of reaction products over unsulfided catalyst at various reaction temperatures	52
Table 3.11 Molar balance of species for reactions over unsulfided catalyst.....	52
Table 3.12 Conversion of 1-hexene and toluene on hydrogenation over unsulfided catalyst	53
Table 3.13 Mass balances of hydrogenation reactions over sulfided catalyst	53
Table 3.14 GC-FID results for composition of sulfided feed and hydrogenated products	54
Table 3.15 Equilibrium vapor-phase compositions of reaction products over sulfided catalyst at various reaction temperatures	54
Table 3.16 Molar balance of species for reactions over sulfided catalyst.....	55
Table 3.17 Conversion of 1-hexene and selectivity towards <i>n</i> -hexane on hydrogenation over sulfided catalyst	56
Table 3.18 TGA results for catalyst samples	56
Table 3.19 Elemental analysis of catalyst samples	57
Table 3.20 Equilibrium constants for formation of compounds from 1-hexene at various temperatures ⁹	59
Table 3.21 Equilibrium constants for hydrogenation of toluene into methylcyclohexane	59
Table 4.1 Properties of cracked naphtha and hydrotreated product used for distillation studies. 66	

Table 4.2 Chemicals and gases used for hydrotreatment and distillation	67
Table 4.3 Process parameters for atmospheric distillation of cracked naphtha and hydrotreated product	71
Table 4.4 Average mass balance over 1 hour for hydrotreatment of cracked naphtha over sulfided Ni/Al ₂ O ₃	73
Table 4.5 Equilibrium phase compositions of hydrotreated product in the reaction product tank	74
Table 4.6 Fractional yields of cracked naphtha and hydrotreated product distillation cuts.....	75
Table 4.7 Densities and refractive indices of the distilled sub-fractions at 20 °C.....	77
Table 4.8 Theoretical distillation yields of hydrotreated product by accounting for the liquid yield lost due to migration to vapor-phase.....	82
Table 5.1 Materials used for cracked naphtha characterization study	88
Table 5.2 Average response factors relative to <i>n</i> -octane for GC-FID	91
Table 5.3 Compound suggestions given by the MS Library for peaks in figure 5.1b	94
Table 5.4 Verification of MS Library suggestions with model compounds	95
Table 5.5 Model compounds chosen for spiking sub-fractions of cracked naphtha	97
Table 5.6 Concentration of olefinic compounds in cracked naphtha.....	99
Table 5.8 Assignment of compounds based on effect of hydrotreatment and retention indices	102
Table 5.9 Nature and concentration of olefinic species identified in cracked naphtha.....	103
Table A.1 Compounds used for preparation of standard solutions	114
Table A.2 Average relative response factors of various compound classes for FID	116
Table B.1 Average response factors relative to cyclohexane for GC-FID.....	118
Table B.2 Quantification of reaction products of hydrogenation over sulfided catalyst at 200 °C.	119
Table C.1 Composition of outlet gas stream for sulfided hydrogenation at 200 °C	121
Table C.2 Summary of mass balance for sulfided hydrogenation at 200 °C	122

List of Figures

Figure 1.1 CNOOC International BituMax™ scheme for bitumen partial upgrading	2
Figure 2.1 Simplified free-radical chain reaction mechanism for cracking of long-chained hydrocarbons.....	9
Figure 2.2 Reaction scheme of olefin-aromatic alkylation over an acid catalyst	10
Figure 2.3 Reaction products typical for acid catalyzed reaction of benzene with ethylene.....	12
Figure 2.4 Typical chromatogram obtained after GC separation of an organic mixture	14
Figure 3.1 Ni/ γ -Al ₂ O ₃ catalyst pellets used for hydrogenation reactions	29
Figure 3.2 Process flow diagram of the reactor used for hydrogenation reactions.....	35
Figure 3.3 Images of the continuous flow reactor designed for hydrogenation reactions	36
Figure 3.4 Calibration curve of the HPLC pump for <i>n</i> -octane	42
Figure 3.5 Calibration curve of the drum-type gas flowmeter for hydrogen gas at 293 K and 93.27 kPa absolute	43
Figure 3.6 Chromatogram for GC-MS analysis of unsulfided model feed.....	44
Figure 3.7 Chromatogram for GC-MS analysis of hydrogenated product over unsulfided catalyst at 120 °C	45
Figure 3.8 Chromatogram for GC-MS analysis of sulfided model feed.....	46
Figure 3.9 Chromatogram for GC-MS analysis of hydrogenated product over sulfided catalyst at 200 °C	48
Figure 3.10 TGA weight loss profiles of Ni/Al ₂ O ₃ catalysts.....	57
Figure 3.11 FTIR Spectra of pyridine treated catalysts in the 1400 to 1600 cm ⁻¹ region.....	58
Figure 4.1 BR M690 Distillation system used for fractionation of cracked naphtha	69
Figure 4.2 Simulated distillation curve of thermally cracked naphtha	76
Figure 4.3 Simulated distillation curve of hydrotreated product	76
Figure 4.4 Atmospheric and Simulated distillation curves of thermally cracked naphtha	78
Figure 4.5 Boiling point distribution based on number of carbon atoms	79
Figure 4.6 Boiling point deviation of non-normal paraffin compounds in methylpolysiloxane stationary phase.....	80
Figure 4.7 Boiling point distribution curves of cracked naphtha and hydrotreated product	83
Figure 5.1a GC-MS chromatogram of cracked naphtha fraction (B.P 85 – 100 °C) up to 50 mins	93

Figure 5.1b A segment of the above-mentioned chromatogram between 14.2 to 17.2 mins	93
Figure 5.2 GC-FID chromatograms of a sub-fraction showing increase in the peak area after spiking with 1-heptene	98
Figure 5.3 GC-MS chromatograms of cracked naphtha before and after hydrotreatment – segments with retention time 14.2 to 17.2 minutes	102

CHAPTER 1 – INTRODUCTION

1.1 Background

Naturally occurring bitumen, found in the oil sands reserves of western Canada, is characterized by high density ($>1000 \text{ kg/m}^3$ at $15 \text{ }^\circ\text{C}$) and viscosity ($>100 \text{ Pa}\cdot\text{s}$ at $15 \text{ }^\circ\text{C}$)¹. Western Canadian bitumen is extracted and shipped to various refineries across provincial and international borders via pipelines or rails. Pipelines are believed to be the safer mode of transport since they hold a better record over rail transport for environmental concerns such as accidental oil spills.² Once extracted, bitumen needs to undergo certain pretreatment processes to reduce its density, viscosity and solids and water content to produce a material that is fit for transportation via pipelines. The extent of quality improvement is dictated by the North American oil pipeline specifications, listed in Table 1.1.

Table 1.1 Pipeline specifications for Alberta bitumen products ³

Property	Units	Pipeline Specification
Viscosity	Centistokes (cSt)	$<350 \text{ cSt at } 15 \text{ }^\circ\text{C}$
Density	kg/m^3	<940
API Gravity	-	>19
Solids and Water content	vol %	<0.5
Olefin content	wt %	<1.0

Currently, one of the approaches to reduce density and viscosity is to blend bitumen with diluents such as natural gas condensates. This approach, however, has resulted in high operating expenses involved with purchase, addition and removal of diluents, ultimately diminishing the value of bitumen (by as much as US \$14/bbl of bitumen) in a competitive market.⁴ Furthermore, the added diluent makes up about 30 vol% of the material in the pipeline leading to severe transportation bottlenecks caused by having a limited number of pipelines.⁴

There is thus a need to develop economically viable alternatives to produce bitumen that meets specifications for pipeline transport to various refineries. *Partial upgrading technologies* aim to achieve this goal with little or no addition of diluents, with special emphasis on lowering the overall capital and operating costs. Feasible partial upgrading processes propose to use a

combination of unit operations – reactions such as thermal cracking, separation technologies such as solvent deasphalting and minimal addition of diluents – that can be used pairwise to produce partially upgraded bitumen that meets pipeline specifications (refer to table 1.1).⁵ One such technology is the BituMax™ Process, developed by CNOOC International Ltd. (formerly Nexen Energy ULC). The process scheme, shown in Figure 1.1, employs solvent deasphalting followed by mild thermal cracking (i.e., visbreaking) to convert most of the heavy compounds in bitumen into lighter compounds, in order to reduce the density and viscosity of the product with minimum loss in liquid product yield. However, the product stream from the thermal cracker contains olefins, which are undesirable due to potential fouling associated with olefins and diolefins, especially during transportation and downstream processing.⁵ Thus, the olefins in cracked naphtha must be treated before pipeline transportation.

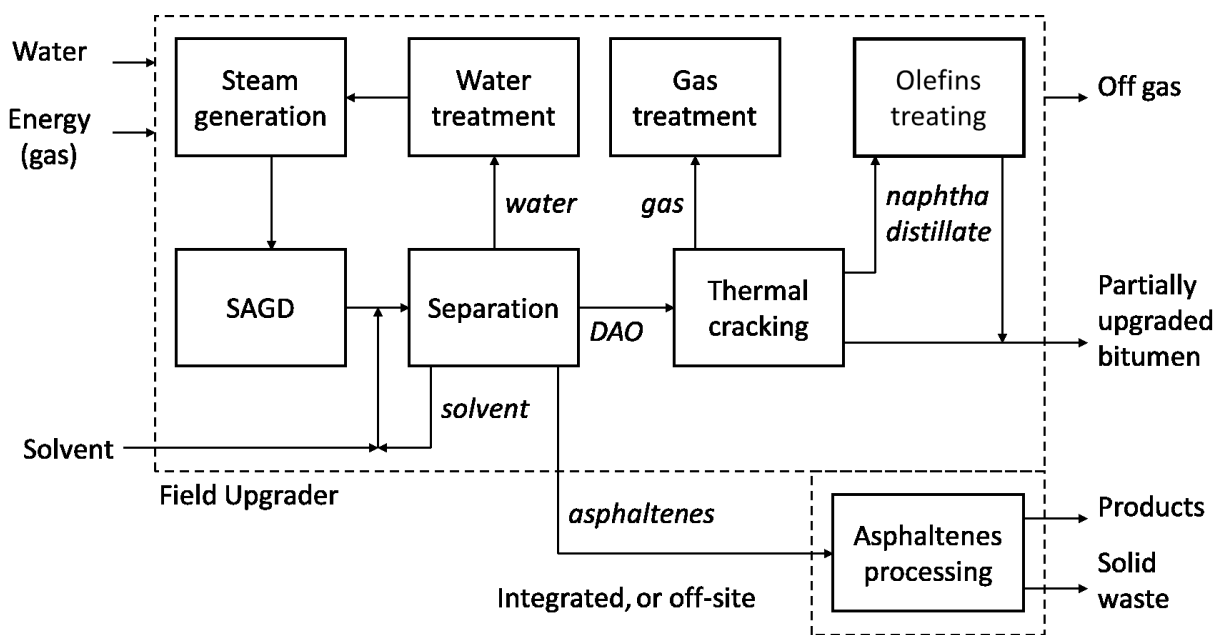


Figure 1.1 CNOOC International BituMax™ scheme for bitumen partial upgrading⁶

Olefins in cracked feedstocks are conventionally treated by hydroprocessing, which requires additional capital and operating costs associated with hydrogen production. Instead, the BituMax™ Process proposes to treat the olefins in the naphtha (material with boiling range 15 – 200 °C) from the thermal cracker with aromatics-containing distillate (boiling range 200 – 350 °C) to form alkyl aromatics via a Friedel-Crafts alkylation pathway. Sufficient olefin conversion must be achieved so that the partially upgraded bitumen meets pipeline specifications which require the

bitumen to contain < 1 wt% 1-decene equivalent olefins based on a proton nuclear magnetic resonance (¹H NMR) method of analysis.³

To understand the motivations and the objectives for this thesis, it is first important to note the differences between the BituMax™ olefin conversion process and the more conventionally used Friedel-Crafts olefin-aromatic alkylation in petrochemical industries. These are detailed below:

- Catalysts: First, the conventional process uses catalysts such as Lewis acids and zeolites to achieve the alkyl-aromatic conversion of petroleum feeds.^{7,8} These catalysts cannot be employed for bitumen-derived thermally cracked feeds, however, since they contain nitrogen bases that can poison these catalysts. Therefore, the olefin aromatic alkylation in BituMax™ uses an amorphous silica-alumina catalyst to enable operation in the presence of nitrogen bases.⁹
- Process Objectives: Secondly, the conventional Friedel-Crafts olefin-aromatic alkylation processes are aimed at production of specific aromatic products (e.g. ethylbenzene, cumene). The process parameters are selected to suppress the formation of oligomers and polyalkylated aromatics. In the BituMax™ process, the sole purpose is the removal of olefins via conversion to aromatics. The nature of the converted aromatic products is not relevant.
- Feed composition: Lastly, and most importantly, in the conventional process, the feed is devoid of potential catalyst poisons. Furthermore, the ratio of aromatics to olefins is carefully controlled in order to achieve selective formation of the desired alkyl-aromatic product. This is not the case for BituMax™ Process, where the composition of the feed depends on the complex reactions in the thermal cracking unit and thus, cannot be independently controlled.

These differences in the feed materials, catalysts, and process objectives between the BituMax™ process and conventional olefin-aromatic alkylation processes mean that fresh investigations need to be conducted regarding the above-mentioned aspects in order to develop a robust olefin treatment process for bitumen partial upgrading.

Understanding of the nature and abundance of olefins present in the cracked naphtha is a first step towards answering some fundamental questions surrounding reaction selectivity and conversions

that can be achieved by Friedel-Crafts alkylation over an amorphous silica-alumina catalyst. A detailed investigation of cracked naphtha at the species level would help gain insight into the nature of olefins, i.e., number of carbon atoms, position of double bond etc., ultimately providing elementary knowledge regarding the feed for the olefin treatment process. Determination of concentration of the species will provide clarity regarding the conversions that must be achieved in order to meet the pipeline specifications (refer to table 1.1). This cannot be accomplished merely by conducting certain standard tests such as Bromine Number (ASTM D1159) and $^1\text{H-NMR}$ analysis. Cracked naphtha sourced from bitumen contains heteroatomic compounds such as thiols and pyrroles and these compounds interfere with Bromine Number tests to measure olefin content, leading to results that overestimate the olefin content. $^1\text{H-NMR}$ analysis quantifies the amount of olefinic hydrogen in the sample but does not offer much insight into the structural composition of the olefinic species.

The current study employs a detail-oriented approach to characterize thermally cracked naphtha (B.P 15 – 240 °C) obtained from a bitumen upgrader facility located in Alberta, Canada. Separation techniques such as atmospheric distillation and gas chromatography (GC) with mass spectroscopic and flame ionization detectors have been used in addition to hydrogenation of cracked naphtha in order to identify and quantify the olefinic species present.

The cracked naphtha is first distilled into sub-fractions having narrow boiling cuts using an atmospheric distillation column. Doing so reduces the complexity of the mixture, with each cut containing fewer compounds than the original sample. Each sub-fraction is then subjected to further separation in a chromatographic column, where the separation occurs based on differential adsorption affinities towards the stationary phase material that is present in the GC column. The two-dimensional separation procedure (one based on boiling point and the other based on differential adsorption) enables the individual species in cracked naphtha to be distinguished with a high resolution.

The species that elute from the GC column are then analyzed using a mass spectroscopic (MS) detector to identify compounds based on the electron impact mass spectrum. However, assigning the identity of compounds based on the mass spectrum is challenging with potential misidentification of structural and functional isomers. For example, a peak that is identified as a compound with the formula C_7H_{14} by the MS library, could in fact be any isomer of *n*-heptene

(e.g. 2-heptene), branched acyclic heptene (e.g. 2-methyl-3-hexene) or cycloparaffin (e.g. methylcyclohexane). This raises a significant challenge since the species in thermally cracked product are expected to possess high isomeric diversity. The current study aims to understand the exact nature and abundance of olefinic species in cracked naphtha, thus there is a need to confirm the compound class identity of the compounds in the sub-fractions that are suggested to be olefins by the MS library.

The identity of the compounds can be deduced by subjecting the cracked naphtha to a chemical treatment such as mild hydrogenation and tracking the concentration of the species before and after the reaction. Olefinic species are reactive to hydrogenation, whereas cycloparaffins will remain unchanged. Hydrogenation of a complex feedstock such as cracked naphtha could potentially result in multiple reactions including saturation of olefinic and aromatic species and hydrodesulfurization. When the objective is to achieve selective conversion of olefins and not aromatics, it is valuable to conduct a study with synthetic cracked naphtha (made with model compounds) to evaluate the conversion and product selectivity for olefin hydrogenation. The hydrogenation reactions of model feed are studied over a Ni/Al₂O₃ catalytic system in a continuous packed-bed reactor, the results of which help in establishing reaction conditions for the hydrotreatment of olefins in cracked feedstocks using the same catalytic reactor.

Once the compounds that are identified by GC-MS are confirmed by hydrotreatment, the next step involves quantification of the compounds by GC coupled with a flame ionization detector (GC-FID). The concentrations of the compounds are determined by measuring the area of the corresponding peak in the chromatogram, which is a function of the response of the FID. The FID response varies from one compound class to another. Thus, the quantification studies are done by evaluating average response factors for the respective compound classes.

1.2 Objective

One objective of this thesis project is to deduce the nature of the olefins (such as number of carbon-atoms, position of the double-bonds and skeletal structure i.e., linear, branched or cyclic) and the concentration of olefins (in wt%) in thermally cracked naphtha from a bitumen upgrader facility, in order to better understand the feed for the olefin treatment unit of the BituMaxTM Process. Characterization studies are done by gas chromatography with mass spectrometer (GC-MS) and

flame ionization detector (GC-FID), aided by sub-fractionation and hydrotreatment of the cracked naphtha.

Another objective is to gain a better understanding of the hydrogenation activity of Ni/Al₂O₃ catalytic systems and to evaluate the conditions for olefin hydrotreating in the presence of aromatics. Though not directly applicable for the envisioned partial upgrading process, lab-scale catalytic hydrogenation of olefins complements the characterization studies.

1.3 Scope of work

The first part of the experimental study uses model compounds to understand the effect of temperature and catalyst pre-treatment on hydrogenation of olefin-containing feed over Ni/Al₂O₃ catalyst (*Chapter 3*). The rest of the study focusses on sub-fractionation and hydrotreatment of cracked naphtha (*Chapter 4*) and characterization of the same cracked naphtha by gas chromatography coupled with various detectors, i.e., GC-MS and GC-FID (*Chapter 5*).

The characterization studies were done in collaboration with Cloribel Santiago, who developed suitable method conditions for GC analyses and catalogued a preliminary database of compounds based on GC-MS identification. I was responsible for sub-fractionation, hydrotreatment and preparation of samples for GC-MS and GC-FID studies and subsequently updating the database by tracking the changes post hydrotreatment, to confirm the identity of the olefins. The updated databases are provided in Appendix E and Appendix F.

1.4 References

- (1) Gray, M. R. *Upgrading Oilsands Bitumen and Heavy Oil*; Pica Pica Press: Edmonton, 2015.
- (2) Green, K. P.; Jackson, T. Pipelines are the safest way to transport oil and gas <https://www.fraserinstitute.org/article/pipelines-are-safest-way-transport-oil-and-gas> (accessed Dec 15, 2019).
- (3) Enbridge. *Enbridge Quality Pooling Specification Package*; Edmonton, 2019.
- (4) Gieseman, J.; Keesom, W. *Bitumen Partial Upgrading 2018 Whitepaper AM0401A*; Calgary, 2018.
- (5) Gray, M. R. Fundamentals of Partial Upgrading of Bitumen. *Energy and Fuels* **2019**, *33*, 6843–6856.
- (6) De Klerk, A. *Annual Report 2016-2017 (Year 1), Progress Report on Industrial Research*

Chair Program; Edmonton, 2017.

- (7) Ingallina, P.; Perego, C. Recent Advances in the Industrial Alkylation of Aromatics: New Catalysts and New Processes. *Catal. Today* **2002**, *73*, 3–22.
- (8) Degnan, T. F.; Smith, C. M.; Venkat, C. R. Alkylation of Aromatics with Ethylene and Propylene: Recent Developments in Commercial Processes. *Appl. Catal. A Gen.* **2001**, *221*, 283–294.
- (9) Xia, Y. Acid Catalyzed Aromatic Alkylation in the Presence of Nitrogen Bases, MSc Thesis, University of Alberta, 2012.

CHAPTER 2: LITERATURE REVIEW

This chapter provides a general background on key topics discussed in the development of this thesis project. Some works found in literature are cited in order to explain the concepts. The main topics reviewed are divided into three sections. The first section provides a brief description about partial upgrading of bitumen and sets the context in which this study was undertaken. The second section provides details regarding analytical techniques and relevant studies related to characterization of olefins in thermally cracked material. The last section provides a brief explanation of certain aspects of catalytic hydrogenation of olefin-containing feedstocks. The concepts reviewed in this section include the hydrogenation reactivity of various olefins over metal catalysts and the pretreatment of catalysts for hydrogenation in the presence of sulfur compounds.

2.1 Partial upgrading of bitumen

2.1.1 Thermal cracking for partial upgrading

Partial upgrading technologies aim to remove contaminants from bitumen and produce a partially upgraded material that meets pipeline specifications for density and viscosity, listed in table 1.1, with little to no addition of diluents.¹ Partial upgraders are expected to be integrated with extraction facilities on the field where fresh bitumen from in-situ production would be subjected to relatively low cost, mild chemical processes such as thermal cracking and solvent deasphalting to upgrade the value of the product. For this reason, partial upgrading technologies have also come to be known as “field upgrading” technologies. Thermal cracking processes convert part of the vacuum residue fraction into lighter components. Depending on the severity of the cracking process, the product may contain unstable asphaltenes, or coke precursors. Thus, partial upgrading technologies aim to use a combination of thermal cracking and partial deasphalting techniques to produce a stable material that meets pipeline specifications (Refer to table 1.1).²

The technology that is relevant for this thesis project is the CNOOC International Bitumax™ partial upgrading technology that uses a thermal cracking unit, i.e., a visbreaker at the heart of the process to thermally decompose most of the heavy molecules in bitumen into lighter products.³ Visbreaking is a relatively low-cost technology, widely employed in the petroleum industry to produce fuel oil that meets specifications.^{4,5} The thermal cracking process of visbreaking is characterized by mild temperature conditions (350 – 500 °C) and short residence times. The low

severity of the operating conditions favors a high yield of liquid-phase products in the naphtha and distillate boiling ranges while simultaneously limiting the production of solid coke.⁶ These factors make it a very attractive process for bitumen partial upgrading – to potentially produce a low-viscosity and low-density product that meets pipeline specifications, listed in table 1.1.

During the process of thermal cracking, the heat energy supplied initiates homolytic dissociation of covalent bonds to form reactive free radical species with an unpaired electron.⁷ The free radicals then undergo a number of parallel and successive intermediate reactions leading to the formation of smaller molecules. Non-catalytic cracking of molecules in petroleum feedstocks takes place via free radical intermediates. The intermediate reaction network is very complex, a simplified description is illustrated in figure 2.1. The highly reactive free radicals propagate by hydrogen abstraction and β -scission, the latter resulting in the formation of molecules with a double bond, i.e., olefins.⁸ The beta-scission reactivity of carbon free radicals decreases with decrease in chain length and they eventually combine with each other in the termination step that ceases the cracking mechanism.

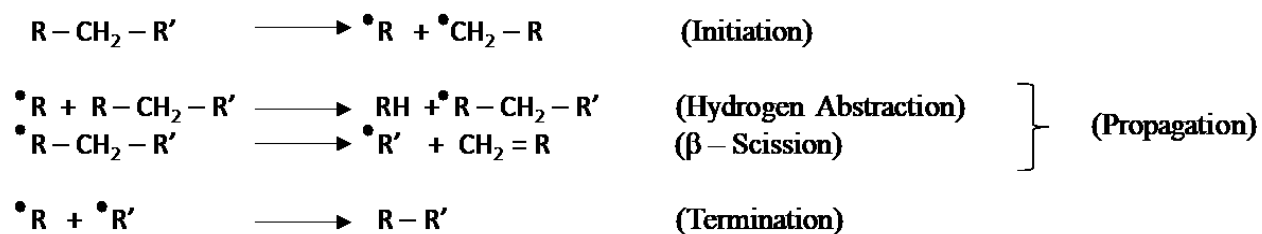


Figure 2.1 Simplified free-radical chain reaction mechanism for cracking of long-chained hydrocarbons

As explained above, the process of thermal cracking results in the formation of olefins. Unfortunately, the pipeline specifications limit the presence of olefins to less than 1 wt% equivalent of 1-decene based on a proton nuclear magnetic resonance (¹H NMR) method of analysis.⁹ Thus, the product from the thermal cracking operation must go through further treatment for conversion of olefins.

2.1.2 BituMaxTM olefin treatment by Friedel Crafts alkylation

The olefins formed during thermal cracking have considerably shorter chain lengths than the parent molecules. Consequently, they have lower boiling points. In fact, studies conducted on bitumen-derived cracked feedstocks have reported that olefins tend to be concentrated in the low boiling fractions, i.e., naphtha and distillate.^{8,10} In order to meet the pipeline specifications for olefin content (refer to table 1.1), the BituMaxTM partial upgrading process focusses on treating the olefins in the cracked streams boiling below 350 °C before blending all the streams to form partially upgraded bitumen (refer to figure 1.1).

Catalytic hydrogenation is widely employed in oilsands upgrading due to the versatility of the process to achieve benefits including, but not limited to increase in the H:C ratio by saturation of diolefins, olefins and aromatics and removal of heteroatoms such as oxygen, sulfur and nitrogen.¹¹ However, the incorporation of a hydrotreating unit and a hydrogen production unit is associated with high operating costs and large space requirements. Thus, hydrogenation is not an attractive option for a partial upgrader facility that is located near a bitumen extraction site. The olefins must therefore be treated by a pathway that does not rely on hydroprocessing. Instead, the BituMaxTM process aims to achieve this goal by reacting the olefins with the aromatic compounds in the naphtha and distillate streams to form alkyl aromatics via a Friedel-Crafts alkylation pathway.

Friedel-Crafts olefin aromatic alkylation is an electrophilic aromatic substitution reaction, catalyzed by an acid catalyst. The olefin is protonated by an acid catalyst to form a carbonium ion. The electron-rich aromatic molecule acts as a nucleophile, enabling the addition of the carbonium ion to form the alkyl aromatic. In the reaction scheme shown in Figure 2.2, A represents an olefin. The presence of an acid catalyst (H⁺) leads to formation of carbonium ion A⁺, which then interacts with aromatic molecule B to form alkyl aromatic compound AB.

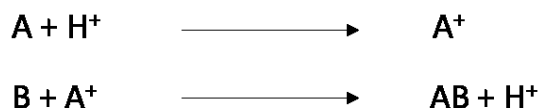


Figure 2.2 Reaction scheme of olefin-aromatic alkylation over an acid catalyst

Friedel-Crafts alkylation reaction is catalyzed by a variety of catalysts including AlCl_3 , BF_3 , phosphoric acid on kieselguhr, silica-alumina and zeolites.¹²⁻¹⁶ Solid state acid catalysts are extensively employed in petroleum refining industries since they can be operated in fixed bed reactors for alkylation processes. Over the span of the last few decades, the stability of alkylation catalysts has seen tremendous developments with increased catalyst lifetimes and low rates of deactivation.^{14,17} However, it must be noted that the feeds used for these industrial processes contain pure reactants and are free of potential catalyst inhibitors and poisons such as nitrogen bases and dienes. This is hardly the case for the BituMaxTM alkylation process, since characterization studies have revealed that bitumen-sourced thermally cracked naphtha have pyridines, pyrroles and diolefins.^{18,19}

Yuhan Xia conducted olefin aromatic alkylation studies over silica-alumina catalysts in the presence of nitrogen bases. The catalyst with the highest medium strength acid sites (Siral 30) was identified as the most suitable for alkylation in the presence of nitrogen bases.²⁰ The operating temperature of the alkylation process of the BituMaxTM olefin treatment unit is limited to 300 – 350 °C to obtain the best compromise between the highest olefins-aromatics alkylation activity and least catalyst inhibition by nitrogen bases in the feed.²¹

Apart from olefin aromatic alkylation, typical acid catalysts also enable side reactions such as transalkylation, isomerization and oligomerization, as shown in figure 2.3. For commercial synthesis of alkyl aromatics, the process operating conditions and catalysts are chosen to enable selective conversion to mono-alkyl aromatics (for E.g. ethylbenzene and cumene) and suppress the formation of oligomers and polyalkylated aromatics. However, the objective of the BituMaxTM process is the conversion of olefinic species, hence transalkylation and multiple alkylation of aromatics are also desirable outcomes. In fact, one of the most strictly controlled process parameters in the industry – the molar ratio of olefins and aromatics in the feed – cannot be independently controlled in the BituMaxTM process since the process feed is determined by the highly complex reactions taking place in the thermal cracker. The vastly different feed material to what is conventionally employed for olefin-aromatic alkylation, as well as the difference in process objective, means that there are aspects related to the chemistry and catalysis of the process that need to be further investigated in order to develop a robust process for partial upgrading. The current study is focused on investigating the nature and abundance of olefinic species in the

thermally cracked naphtha as the first step towards better understanding the complex feed material of the BituMax™ olefin treatment unit.

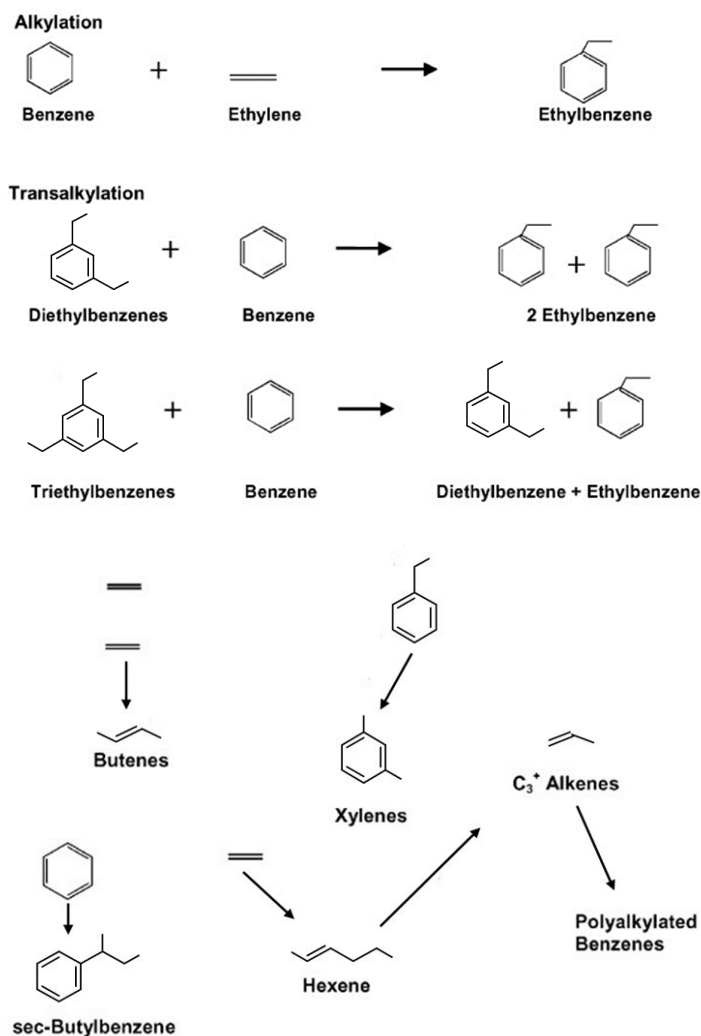


Figure 2.3 Reaction products typical for acid catalyzed reaction of benzene with ethylene¹⁷

2.2 Characterization of olefins in complex organic mixtures

Significant advances have been achieved over the past few decades in the development of analytical techniques for the characterization of species in complex organic mixtures that are typically encountered in petroleum and biochemical industries. The determination of the structure of compounds or functional groups is done by chemical methods or by instrumental methods. This section reviews analytical techniques and some relevant characterization studies based on physical separation of organic mixtures.

2.2.1 Characterization by high resolution gas chromatography integrated with detectors

Techniques such as NMR-spectroscopy and IR-spectroscopy are widely used for analysis of organic samples to determine the functional groups of the species based on the characteristic spectra that can be used to distinguish various functional groups.²² These methods do not provide details regarding the individual components that make up complex samples like cracked naphtha. Instead, detailed characterization studies of complex petroleum-based mixtures are done by subjecting the sample to physical separation methods such as chromatography, followed by detection of the separated individual species.

Gas chromatography (GC) is an effective technique for compound separation in mixtures consisting of volatile compounds. Compound separation is achieved in a long, thin capillary column whose inner wall is coated with a material, i.e., stationary phase, which exhibits different adsorption affinity to different molecules in the mixture. An inert gas, i.e., mobile phase carries the volatile organic sample into the capillary column, where the components of the mixture adsorb on the stationary phase. Based on the extent of their affinity with the stationary phase, the components desorb from the stationary phase at different rates, and the components are then detected. The rate and degree of separation depends upon the chemical affinity of the individual species towards the stationary phase and vapor pressure of the species – which is governed by the column temperature. The compound with the least affinity and vapor pressure elutes first from the column. When a GC device is integrated with special detectors, it can be used for identification and quantification of the separated species.

This section provides a brief background on concepts of gas-chromatography and various detectors that are used for determining the identity and concentration of compounds in complex mixtures such as cracked naphtha.

Partition Coefficient (K_c): The tendency of an analyte to get adsorbed on the stationary phase is measured by a factor known as partition coefficient, as shown in equation (1). The partition coefficient for a compound depends on the chemical nature of the stationary phase as well as the vapor pressure of the compound.²³ High resolution separation is achieved by selection of a suitable material as the stationary phase and maintaining optimum temperature conditions in the GC column. GC capillary columns made up of non-polar stationary phases such as (1)

dimethylpolysiloxane have the capability to achieve separation of isomeric compounds such as *m*-xylene and *p*-xylene, despite the compounds having almost identical vapor pressures.²⁴

$$K_c = \frac{\text{Concentration of analyte in stationary phase}}{\text{Concentration of analyte in mobile phase}}$$

Retention time: When a sample is introduced into the GC column, the components in the mixture interact with the stationary phase to varying extents, depending on the partition coefficient. The resulting separation of individual components causes them to traverse the length of the column at varying rates with the help of the carrier gas. The time taken for an analyte in the mixture to pass through the column is known as retention time. The retention time of a component depends on the carrier gas velocity, the length and temperature program of the GC column as well as the material of the stationary phase.

Chromatogram: As the separated components elute through the GC column, they pass through a detector that measures a response based on a physicochemical property (such as molecular mass or thermal conductivity). The response of the detector is recorded as a function of time, resulting in a plot known as a chromatogram, as shown in figure 2.4. The straight line – called the “base line”, corresponds to the pure carrier gas. The deflections – called “peaks” represent the compounds that elute at the corresponding retention times.

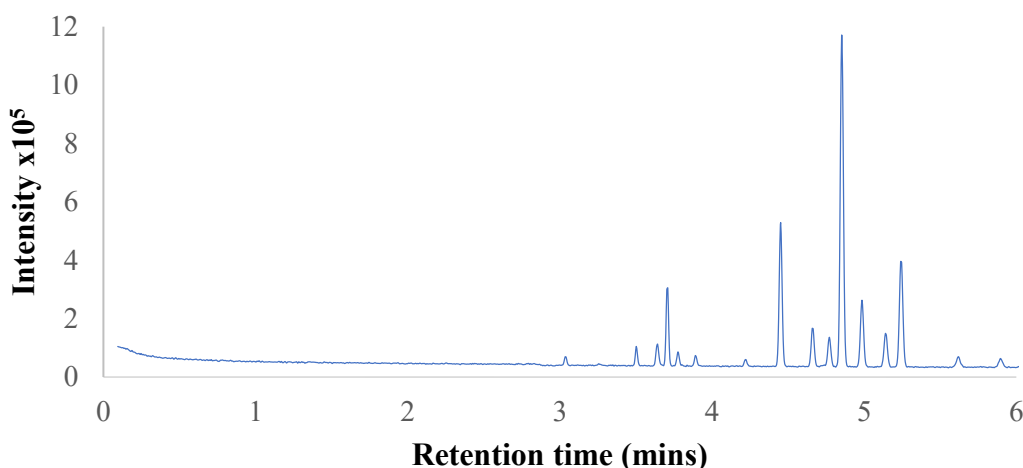


Figure 2.4 Typical chromatogram obtained after GC separation of an organic mixture

The detector, located at the exit of a GC column, is used to obtain information regarding the identity and concentration of the analyte as it elutes from the column. There are many types of detectors that can be integrated with a GC device. The operating principles of the detectors that were used in the current study are mentioned below:

Mass-spectroscopic detector (MSD): This detector is used widely for determination of the nature of the analyte, based on the mass to charge ratio. When the analyte elutes from the GC column, the mass spectroscopic detector subjects the analyte to ionization and fragmentation with the aid of an electron impact source. The fragmented ions then pass through a mass analyzer where they are sorted based on their mass to charge ratios. Since most ions are singly charged, the resulting peaks in the mass spectrum indicate the molecular mass of the corresponding ions. The structural identity of the compound is determined by examining the fragmentation pattern of the ions generated.²² High-resolution mass spectroscopic detectors provide useful information on the molecular formula of volatile organic compounds based on their molecular weights.

Flame-ionization detector (FID): These detectors are useful for quantitative studies of components present in hydrocarbon mixtures. The eluted compounds are burned in a flame generated by hydrogen and air, resulting in combustion of the compound. The thermally decomposed compound releases ions that can carry electric current that is measured by a high-impedance picoammeter and registers a response.²³ The concentration of the compound can be measured as a function of the peak area in the resulting chromatogram. The FID detector registers a poor response for compounds containing heteroatoms such as halogens, oxygen and sulfur. Thus, it is important to measure the response factor (RF) for the corresponding compound or compound class with standard solutions, according to equation (2), prior to measuring the concentration (mass per volume) of analytes in unknown samples.

$$RF = \frac{\text{Peak area in chromatogram}}{\text{Concentration of analyte in standard solution}} \quad (2)$$

Measurement of the concentration of analytes in a sample can also be achieved by spiking the sample with a known concentration of a standard compound and using pre-determined relative response factors (RRF) between the two compounds.²⁵ The RRF between two analytes (A and B) is determined by analyzing the two analytes simultaneously within the same (3)

solution. Firstly, the peak area and concentration of the analytes are used to calculate the response for each analyte, as in Equation 2. The response factors calculated for each analyte are then used to establish the RRF between the two analytes as in Equation 3.

$$RRF = \frac{RF \text{ of analyte A}}{RF \text{ of analyte B}}$$

The RRF can be used to calculate the unknown concentration of analyte A in the presence of a known concentration of analyte B, as in Equation 4.

$$\text{Concentration A} = \frac{\text{Peak area A}}{\text{Peak area B}} \times \frac{1}{RRF} \times \text{Concentration B} \quad (4)$$

2.2.2 Compositional studies of cracked naphtha

Studies to enhance knowledge of the composition of petroleum mixtures using the various analytical techniques discussed above began appearing in scientific literature as early as the 1930's. Such compositional studies became more rigorous and extensive in the next few decades, aided by improvements in the compound separation and identification capabilities of analytical methods such as chromatography and spectroscopy. The increase in the complexity and number of components in hydrocarbon mixtures that have undergone thermal treatments, such as visbreaking and catalytic cracking, makes it more challenging for extensive characterization of the individual species in the mixture. A few studies that analyzed the composition of cracked naphtha mixtures from various petroleum sources around the world have been reviewed in this section.

Nagpal et al.²⁶ analyzed the distribution of compounds belonging to various functional groups in cracked naphthas from fluid-catalytic and visbreaking processes, obtained from a refinery in Gujarat, India. The identification of compounds was done by GC-MS analyses. The results, shown in table 2.1, showed that the concentration of olefins was lower in cracked naphtha from the visbreaker as compared to that from a fluid catalytic cracker (FCC). However, the isomeric species with different functional groups (e.g. diolefins vs. cyclic olefins) could not be distinguished due to the similarity in their mass spectra.

Table 2.1 Characterization of cracked naphthas from Gujarat region in India²⁶

Compound class	FCC naphtha	Visbroken naphtha
	(vol%)	(vol%)
Paraffins	32.2	42.9
Cyclic paraffins	9.1	17.8
Mono olefins	37.2	18.9
Tri olefins + Acetylenes	0.2	2.2
Di olefins + Cyclic olefins	15.0	11.0
Aromatics	6.3	7.2

Ramnas et al.²⁷ conducted extensive characterization studies by analyzing FCC naphtha from desulfurized vacuum gas oil, obtained from the Scanraff refinery in Sweden. The compounds were identified by GC-MS analysis using two different stationary phases on the GC column. The study identified various compounds in the C₅-C₉ range. The concentration of the compounds was calculated with a flame ionization detector. However, the authors of this study did not use correction factors (response factors) for the various hydrocarbon classes. Table 2.2 summarizes the results of this study.

Table 2.2 Characterization of FCC naphtha from Scanraff refinery in Lysekil, Sweden²⁷

Compound class	Number of carbon atoms						Total (wt%)
	4	5	6	7	8	9	
Paraffins	0.1	9.6	8.8	5.6	3.5	2.0	29.6
Olefins	0.6	13.6	10.4	5.8	1.3	0.0	31.7
Diolefins	0.0	0.3	0.4	0.0	0.0	0.0	0.7
Cyclic paraffins	0.0	0.2	2.8	3.7	2.5	0.0	9.2
Cyclic olefins	0.0	0.7	2.2	2.4	1.5	0.0	6.8
Cyclic diolefins	0.0	0.1	0.2	0.0	0.0	0.0	0.3
Aromatics	0.0	0.0	1.0	4.3	6.7	2.7	14.7

Cady et al.²⁸ conducted elaborate analyses of FCC naphtha sourced from mid-continent crude petroleum. The naphtha was further separated by superfractionation to obtain several small fractions with boiling points 2 °C apart. The components in the fractions were then identified by

methods such as bromination of olefins, maleic anhydride addition to conjugated diolefins, sulfonation of aromatics combined with mass-spectrometry and ultraviolet spectrometry. The concentration of the compounds was determined based on the distillation yields. The compound-wise classification of the various species identified in the FCC naphtha is listed in table 2.3.

Table 2.3 Characterization of FCC naphtha from mid-continent petroleum²⁸

Compound class	Number of carbon atoms				Total (vol%)
	5	6	7	8	
Paraffins	23.3	21.8	7.7	1.9	54.7
Cyclic paraffins	0.3	1.5	3.5	0.6	6.0
Cyclic olefins	0.7	1.3	0.6	0.3	2.9
Olefins	14.2	10.1	5.2	1.5	31.0
Diolefins	0.0	0.1	0.1	0.0	0.2
Aromatics	0.0	0.3	1.3	0.2	1.8

Based on the studies discussed above, it is evident that the nature of compounds in cracked naphtha is influenced by the original source of the hydrocarbon mixture as well as the severity of the conditions employed during thermal cracking process. The current study will aim to replicate these characterization studies for thermally cracked naphtha from visbreaking operation at a bitumen upgrader facility, with a special focus on identifying the nature and concentration of olefinic species.

2.3 Catalytic hydrogenation

Determination of olefinic content in cracked mixtures could be achieved by taking advantage of the reactive C=C bond. One such conventional technique is by bromine number analysis, whereby the amount of bromine consumed for titration is a measure of the olefinic content. However, this technique is not reliable for mixtures with sulfur compounds since they react with bromine, resulting in an overestimation of the concentration of olefins present. Instead, this study uses catalytic hydrogenation as a reaction pathway to treat cracked naphtha. This is useful for two main reasons. Firstly, hydrogenation can assist the MS identification of species, because it can help with differentiating between olefins (which are unsaturated and therefore react with hydrogen) and cyclic paraffins (which are saturated and hence are not reactive to hydrogenation). Secondly, it is

the fall-back technology for olefin treatment although it is not a technology that is preferred for partial upgrading owing to the costs associated with hydrogen production.

The following subsections explain the basis for catalyst selection and catalyst subtypes that are used for the hydrogenation studies.

2.3.1 Catalyst selection for olefin hydrogenation

Hydrogenation of unsaturated compounds can be carried out by various catalysts. For example, metals such as platinum, palladium, ruthenium, cobalt, and molybdenum are used on a supporting material such as activated carbon or alumina are commonly used in the petroleum industry.⁵ The catalyst chosen in this thesis was nickel supported on porous alumina as it is relatively inexpensive and readily available. The pre-treatment procedure followed during catalyst activation influences the hydrogenation activity of a given metal catalyst. Two such methods were used to treat the catalyst:

- Prereduction: Most hydroprocessing catalysts are supported metal catalysts manufactured by precipitation of one or more metal oxide oxides such as NiO, MoO₃ and WO₃ on carriers such as SiO₂, Al₂O₃ and zeolites. They are activated with a stream of hydrogen at temperatures in the range of 300 °C.²⁹ This process reduces the metal oxides to their metallic states and they become highly active centers for the formation of metal hydride complexes that enable adsorption of the reactants on the surface for hydrogenation.³⁰
- Presulfiding: Reduced metal catalysts deactivate rapidly if the feedstock contains sulfur species. The effect of catalyst poisoning by sulfur is overcome by pretreating the highly active reduced metal catalyst with sulfiding agents such as H₂S or dimethyl disulfide (DMDS). This process, known as presulfiding (or sulfiding), converts the active metal sites into metal sulfides.³¹ Controlled adsorption of sulfur on the active metal surface creates a diffusion barrier against bulk poisoning by the sulfur compounds in the reactants, thus preserving hydrogenation activity of the catalyst. The process of sulfiding results in lowering the hydrogenation activity of the catalytic surface. Thus, sulfide catalysts are typically used for reactions at higher temperatures compared to reduced catalysts.³¹

2.3.2 Olefin hydrogenation with reduced Ni catalyst

Various kinetic studies of metal catalyzed olefin hydrogenation have revealed that the reaction occurs through the formation of an alkyl intermediate which results in hydrogen exchange and double bond migration, as well as addition of hydrogen to saturate the olefinic species.³²⁻³⁴ Figure 2.5 illustrates the alkyl intermediates that can be formed during hydrogenation of 1-butene over a reduced Ni catalyst.

2.3.3 Olefin hydrogenation with sulfided nickel catalyst

Unlike reduced catalysts, sulfided catalysts exhibit polyfunctional catalytic behavior, i.e., in addition to properties of metal catalysts as well as those of acid catalysts.³¹ Such behaviour in hydrogenation reactions could potentially result in side reactions like isomerization and hydrocracking. However, acid catalytic behavior is expected to become significant at higher temperatures (above 400 °C) and do not interfere with hydrogenation of olefins at typical hydrotreating conditions, i.e., below 330 °C.³⁵

Elements such as carbon and sulfur adsorb rapidly and strongly on nickel. The binding energies of these elements with nickel metal is high relative to those of typical reactants (e.g. CO and hydrogen) and relative to the energies of bonds involved in bulk compounds of nickel with these contaminants, e.g. nickel sulfides and carbides.³⁶ Generally, species that are more strongly bound to a catalytic surface than reactants and products function as poisons and reduce the catalytic efficiency. Thus, the process of deliberate sulfiding is expected to significantly lower the hydrogenation activity of the Ni/Al₂O₃ catalyst. At sufficiently high concentrations, sulfur and carbon form bulk nickel sulfide and carbide.

Nickel containing catalysts such as NiS on Al₂O₃ have been used for selective hydrogenation of polyolefins to monoolefins.^{37,38} However, the conversions and selectivity for monoolefin hydrogenation using NiS/Al₂O₃ are expected to be very different from that of conjugated diolefins. Since sulfide catalysts are typically high temperature catalysts, the reaction rates of aromatic compounds are markedly lower than that of olefins. Hence, NiS/Al₂O₃ is potentially attractive for selective conversion of olefins.

2.4 References

- (1) Keesom, B.; Gieseeman, J. *Bitumen Partial Upgrading 2018 Whitepaper*; Edmonton, 2018.
- (2) Gray, M. R. Fundamentals of Partial Upgrading of Bitumen. *Energy and Fuels* **2019**, *33*, 6843–6856.
- (3) De Klerk, A. *Annual Report 2016-2017 (Year 1), Progress Report on Industrial Research Chair Program Issued to NSERC, Nexen Energy ULC, and Alberta Innovates*; Edmonton, 2017.
- (4) Joshi, J. B.; Pandit, A. B.; Kataria, K. L.; Kulkarni, R. P.; Sawarkar, A. N.; Tandon, D.; Ram, Y.; Kumar, M. M. Petroleum Residue Upgrading via Visbreaking: A Review. *Ind. Eng. Chem. Res.* **2008**, *47*, 8960–8988.
- (5) Speight, J. G.; Ozum, B. *Petroleum Refining Processes*; Marcel Dekker, Inc: New York, 2002.
- (6) Speight, J. G. Visbreaking: A Technology of the Past and the Future. *Sci. Iran.* **2012**, *19* (3), 569–573.
- (7) Raseev, S. *Thermal and Catalytic Processes in Petroleum Refining*; Marcel Dekker, Inc: New York, 2003.
- (8) Gray, M. R.; Mccaffrey, W. C. Role of Chain Reactions and Olefin Formation in Cracking, Hydroconversion, and Coking of Petroleum and Bitumen Fractions. **2002**, *16* (7), 756–766.
- (9) Enbridge. *Enbridge Quality Pooling Specification Package*; Edmonton, 2019.
- (10) Xin, Q.; Alvarez-Majmutov, A.; Dettman, H. D.; Chen, J. Hydrogenation of Olefins in Bitumen-Derived Naphtha over a Commercial Hydrotreating Catalyst. *Energy Fuels* **2018**, *32* (5), 6167–6175.
- (11) Gray, M. R. *Upgrading Oilsands Bitumen and Heavy Oil*; Pica Pica Press: Edmonton, 2015.

- (12) Ipatieff, V. N.; Grosse, A. V. Alkylation of Aromatic Compounds with Olefins in the Presence of Boron Fluoride. *J. Am. Chem. Soc.* **1936**, *58*, 233–239.
- (13) Ipatieff, V. N.; Schmerling, L. Ethylation of Benzene in the Presence of Solid Phosphoric Acid. *Ind. Eng. Chem.* **1946**, *38*, 400–402.
- (14) Ingallina, P.; Perego, C. Recent Advances in the Industrial Alkylation of Aromatics: New Catalysts and New Processes. *Catal. Today* **2002**, *73*, 3–22.
- (15) O’Kelly, A. A.; Kellett, J.; Plucker, J. Monoalkylbenzenes by Vapor-Phase Alkylation with Silica-Alumina Catalyst. *Ind. Eng. Chem.* **1947**, *39*, 154–158.
- (16) Garner, F. R.; Iverson, R. L. How Ethylbenzene Is Made. 1. By the High-Pressure Process. *Oil Gas J.* **1954**, *53* (25), 86–88.
- (17) Degnan, T. F.; Smith, C. M.; Venkat, C. R. Alkylation of Aromatics with Ethylene and Propylene: Recent Developments in Commercial Processes. *Appl. Catal. A Gen.* **2001**, *221*, 283–294.
- (18) Paez Cardenas, Y. Identification, Conversion and Reactivity of Diolefins in Thermally Cracked Naphtha, MSc Thesis, University of Alberta, 2016.
- (19) Rao, Y.; De Klerk, A. Characterization of Heteroatom-Containing Compounds in Thermally Cracked Naphtha from Oilsands Bitumen. *Energy and Fuels* **2017**, *31* (9), 9247–9254.
- (20) Xia, Y. Acid Catalyzed Aromatic Alkylation in the Presence of Nitrogen Bases, MSc Thesis, University of Alberta, 2012.
- (21) De Klerk, A.; Zerpa Reques, N.; Xia, Y.; Omer, A. A. Integrated Central Processing Facility (CFU) in Oil Field Upgrading (OFU). Canada Patent 20140138287, 2014.
- (22) Silverstein, R. M.; Bassler, G. C.; Morill, T. C. *Spectrometric Identification of Organic Compounds*, 4th ed.; John Wiley & Sons, Inc: New York, 1981.
- (23) Littlewood, A. B. *Gas Chromatography - Principles, Techniques and Applications*, 1st

- ed.; Academic Press Inc: New York, 1962.
- (24) Agilent Technologies Inc. Application specific GC-columns - HP-PONA Columns
<https://www.agilent.com/en/product/gc-columns/application-specific-gc-columns/hp-pona-columns> (accessed Dec 15, 2019).
- (25) Rome, K.; McIntyre, A.; Astra Zeneca. Intelligent Use of Relative Response Factors in Gas Chromatography-Flame Ionisation Detection. *Chromatography Today*. Macclesfield 2012, pp 52–56.
- (26) Nagpal, J. M.; Joshi, G. C.; Singh, J.; Rastogi, S. N.; Joshi, G. C.; Singh, J.; Rastogi, S. Gum Forming Olefinic Precursors in Motor Gasoline, A Model Compound Study. *Fuel Sci. Technol. Int.* **2007**, *12* (6), 873–894.
- (27) Ramnas, O.; Ostermark, U.; Petersson, G. Characterization of Sixty Alkenes in a Cat-Cracked Gasoline Naphtha by Gas Chromatography. *Chromatographia* **1994**, *38* (3/4), 222–226.
- (28) Cady, W. E.; Marschner, R. F.; Cropper, W. P. Composition of Virgin, Thermal, and Catalytic Naphthas from Mid-Continent Petroleum. *Ind. Eng. Chem.* **1952**, *44* (8), 1859–1864.
- (29) Monteiro-Gezork, A. C.; Effendi, A.; Winterbottom, J. M. Hydrogenation of Naphthaene on NiMo and Ni/Al₂O₃ Catalysts: Pretreatment and Deactivation. *Catal. Today* **2007**, *128*, 63–73.
- (30) Pernicone, N.; Traina, F. Catalyst Activation by Reduction. *Stud. Surf. Sci. Catal.* **1979**, *3*, 321–351.
- (31) Weisser, O.; Landa, S. *Sulphide Catalysts, Their Properties and Applications*; Academia publishing house: Prague, 1973.
- (32) Twigg, G. H.; Wood, W. A. The Catalytic Isomerization of Butene-1. In *Proceedings of the Royal Society A*; 1941; pp 106–117.

- (33) Hirota, K.; Teratani, S.; Yoshida, N.; Kitayama, T. On the Hyperfine Reaction Deuterium with Distribution Deuterium of the Catalytic Powders of Propene on Copper. *J. Catal.* **1969**, *13* (3), 306–315.
- (34) Bond, G. C. *Metal-Catalysed Reactions of Hydrocarbons*, 1st ed.; Springer US, 2005.
- (35) Meerbot, W. K.; Hinds, G. P. Reaction Studies with Mixtures of Pure Compounds. *Ind. Eng. Chem.* **1955**, *47* (April), 749–752.
- (36) Bartholomew, C. H. Mechanisms of Nickel Catalyst Poisoning. In *Catalyst Deactivation*; Delmon, B., Froment, G. F., Eds.; Elsevier Science Publishers B.V.: Amsterdam, 1987; pp 81–104.
- (37) Kasperik, A. S.; Fuchs, H. A. Selective Hydrogenation of Butadienes and Ethyl-Acetylene. France Patent 1493227, 1967.
- (38) Anderson, J.; McAllsiter, S. H.; Derr, E. L.; Peterson, W. H. Diolefins in Alkylation Feedstocks - Conversion to Monoolefins by Selective Hydrogenation. *Ind. Eng. Chem.* **1948**, *40*, 2295–2301.

CHAPTER 3: HYDROGENATION OF OLEFIN-CONTAINING FEED OVER Ni/Al₂O₃ CATALYST

Abstract

The objective of this experimental study was to evaluate the effect of reaction temperature and catalyst pretreatment on hydrogenation of olefins over a 3.3 wt% Ni/Al₂O₃ catalyst in a packed bed flow reactor. Hydrogenation reactions were conducted in the temperature range 60 to 280 °C, 1 MPa H₂ pressure at 1000 mL H₂/mL liquid ratio and weight hourly space velocity of 0.5 h⁻¹ based on the liquid feed. For the evaluation, a model naphtha was employed consisting of 1-hexene (10 wt%), toluene (5 wt%) and *n*-octane (85 wt%). The reactions were studied over both unsulfided and sulfided Ni/Al₂O₃ catalysts. For the study of sulfided Ni/Al₂O₃, the catalyst was subjected to in situ sulfiding, and the feed was spiked with dimethyl disulfide (0.5 wt%) to keep the catalyst in a sulfided state.

Hydrogenation of the model naphtha over unsulfided Ni/Al₂O₃ catalyst resulted in near complete conversion of 1-hexene to *n*-hexane at temperatures as low as 80 °C. It was also noteworthy that near complete conversion of toluene to methylcyclohexane was achieved at 160 °C. Hydrogenation over sulfided Ni/Al₂O₃ catalyst resulted in selective conversion of 1-hexene compared to toluene but temperatures up to 280 °C were needed for 96.5% conversion of 1-hexene. Hydrogenation of 1-hexene over sulfided catalyst at lower temperatures (<200 °C) predominantly formed internal isomers *cis*-3-hexene, *trans*-3-hexene, *cis*-2-hexene and *trans*-2-hexene. Sulfur species in the feed reacted with olefins to form addition products such as thiols and thioethers at temperatures below 200 °C. Trace concentrations of skeletal isomerization product of 1-hexene was detected at temperatures above 240 °C. FTIR analysis to determine the presence of Brønsted acid sites that may have catalyzed skeletal isomerization in the sulfided catalyst was inconclusive. Sulfided Ni/Al₂O₃ was not sufficiently active for aromatic hydrogenation at mild temperatures, i.e., below 280 °C. Thus, hydrogenation of feed containing aromatics over sulfided Ni/Al₂O₃ at 1MPa H₂ pressure resulted in selective hydrogenation of olefins.

3.1 Introduction

Cracking of petroleum and synthetic oil feedstocks to convert heavy hydrocarbons into lighter compounds results in an olefin-containing product.¹ Depending on the application, the olefins in the cracked product may be undesirable and hydrotreating is employed to convert the olefins to paraffins. The cracked products may or may not contain sulfur compounds. For treatment of sulfur-free feedstocks, such as products from fluid catalytic cracking of Fischer-Tropsch wax, hydrogenation via supported metal catalysts such as Ni/Al₂O₃ and Pt/SiO₂ can be employed, resulting in conversion of olefins to paraffins. Thermally cracked products of bitumen partial upgrading processes such as BitumaxTM are known for relatively high sulfur concentrations.² When olefin-rich feedstock contains sulfur compounds, the supported metal catalyst must be presulfided in order to employ the catalyst as a sulfided catalyst, although this strategy is not always useful. In such cases bimetallic sulfided metal catalysts are more commonly employed, such as NiMo/Al₂O₃.³

When the olefins in cracked feedstocks are to be treated, it is important to design hydrotreating conditions that enable maximum conversion of olefins into paraffins by eliminating or reducing the rate of other side reactions such as isomerization. Reaction selectivity and conversion of olefins are dependent on various factors such as metal loading on catalyst, pore volume of the support, reaction temperature, space velocity of feed and partial pressure of hydrogen gas.⁴

The following study uses model compounds to evaluate the hydrogenation conversions and selectivity of conversion of olefin-containing feedstock at various reaction temperatures, in a continuous packed bed reactor that is loaded with Ni/Al₂O₃ catalyst. Another parameter that is studied is the effect of catalyst pretreatment on overall olefin conversion to compare performance when converting sulfur-free and sulfur-containing feed materials. The catalyst bed is prereduced with hydrogen gas for reactions with feedstock that does not contain sulfur; the catalyst bed is presulfided with dimethyl disulfide (DMDS) for reactions with feedstock containing sulfur compounds. The results of this study will help in establishing reaction conditions for hydrotreatment of olefins in cracked feedstocks using the existing Ni/Al₂O₃ catalytic system and when the aim is to hydrotreat only olefins in mixtures containing aromatics.

3.2 Experimental

3.2.1 Materials

The list of chemicals is shown in Table 3.1. Nickel nitrate hexahydrate and alumina pellets were used for catalyst preparation. The γ -Al₂O₃ pellets were cylindrical with 4.87 mm in diameter and 5.60 mm in length. Carborex® 16 silicon carbide abrasive was used as inert material for catalyst packing. The abrasives were supplied by Ritchey Supply. The SiC abrasives were of size mesh 16 (1.19 mm) with a density of 1.52 g/mL. 1-Hexene, toluene and *n*-octane were used in the model feed for the hydrogenation reactions. Dimethyl disulfide (DMDS) and *n*-heptane were used to sulfide the catalyst bed. DMDS was also used to spike the model feed for reactions over the sulfided catalyst. Cyclohexane was used as an internal standard for GC-FID analysis of all samples. Methyl cyclohexane was used for verification of a compound suggested by the mass spectral library in GC-MS.

Table 3.1 Materials used for hydrogenation reaction study

Compound	Formula	CASRN ^a	Mass Fraction Purity ^b	Supplier
<i>Chemicals</i>				
<i>n</i> -Octane	C ₈ H ₁₈	111-65-9	0.98	Sigma-Aldrich
Toluene	C ₇ H ₈	108-88-3	0.999	Fisher Chemical
1-hexene	C ₆ H ₁₂	592-41-6	0.97	Aldrich Chemistry
<i>n</i> -heptane	C ₇ H ₁₆	142-82-5	0.999	Fisher Chemical
Dimethyl disulfide	C ₂ H ₆ S ₂	624-92-0	0.99	Aldrich Chemistry
Methylcyclopentane	C ₆ H ₁₂	96-37-7	0.96	TCI America
Cyclohexane	C ₆ H ₁₂	110-82-7	0.995	Sigma-Aldrich
Methylcyclohexane	C ₇ H ₁₄	108-87-2	- ^c	Millipore Sigma
Nickel (II) nitrate hexahydrate	Ni(NO ₃) ₂ ·6H ₂ O	13478-00-7	0.999985	Fisher Scientific
Alumina tablets 5x5 mm	γ -Al ₂ O ₃	-	- ^c	Sasol

Compound	Formula	CASRN ^a	Mass Fraction Purity ^b	Supplier
<i>Gas cylinders</i>				
Hydrogen	H ₂	1333-74-0	0.99999 ^d	Praxair
Nitrogen	N ₂	7727-37-9	0.99999 ^d	Praxair

^a CASRN = Chemical Abstracts Services Registry Number

^b Purity of the material guaranteed by the supplier; material used without further purification

^c Mass fraction purity not specified

^d Mole fraction purity

3.2.2 Catalyst preparation and characterization

The nickel catalyst was prepared by incipient wet impregnation of nickel nitrate hexahydrate on the alumina support.⁵ A known quantity of Ni(NO₃)₂·6H₂O was mixed with deionized water. The solution was added dropwise to fresh γ -Al₂O₃ pellets and stirred continuously with a glass rod. Excess water was evaporated by heating the wet pellets at 80 °C for 5 hours. The dried catalyst was then calcined in a CWF 1100 Carbolite chamber furnace at 600 °C for 3 hours under constant flow of air.

The Brunauer–Emmett–Teller (BET) surface area analysis using Autosorb iQ reported the surface area of the Ni catalyst to be 151 m²/g. The average pore size of the impregnated catalyst was 4.6 nm. Analysis with the ZIESS SIGMA Field Emission Scanning Electron Microscope (FESEM), equipped with Energy Dispersive X-ray (EDX) detector reported 3.3 wt% Ni spread over the surface of γ -Al₂O₃ support.⁵

X-Ray fluorescence (XRF) spectrometry was performed as part of the current study in order to quantify bulk concentration of nickel on the alumina support. The XRF instrument was a Bruker S2 Ranger that employed a Peltier cooled silicon drift detector and Pd-target as primary X-ray source. Analyses were performed at 50 kV. Quantification was performed using an external calibration curve. The measurement was done by placing 3 g of finely crushed catalyst particles in XRF cups assembled using thin films supplied by Chemplex Industries. The bulk composition of Ni was reported to be 3.3±0.6 wt%. Figure 3.1 shows the fresh Ni/Al₂O₃ catalyst pellets that were loaded in the reactor for further pretreatment and hydrogenation reactions.



Figure 3.1 Ni/ γ -Al₂O₃ catalyst pellets used for hydrogenation reactions

3.2.3 Catalyst reduction

The impregnated Ni catalyst was activated in the continuous packed bed reactor that was used for reaction studies. The reactor was loaded with alternating layers of Ni/ γ -Al₂O₃ catalyst pellets and SiC abrasives (inert material). The packed bed was made up of 4 layers each of 9 g of catalyst and 3 layers each of 4 g of SiC inerts. The layered distribution was done to ensure better heat distribution during activation and hydrogenation reactions. The packed bed reactor was placed in the furnace and connected to the rest of the plant. The system was pressurized to 1 MPa and leak tests were conducted – first with nitrogen gas and then with hydrogen gas – as a safety measure, to prevent leakage of flammable gases. The furnace was then heated to 120 °C for 1 h to remove traces of moisture from the catalyst from exposure to ambient air after calcination. The temperature was then gradually increased at the rate of 30 °C/h and operated isothermally at 300 °C for 3 h. A constant flow of hydrogen gas was maintained at 100 mL/min. The hydrogen gas acts as a reducing medium and converts nickel oxide into its metal form which becomes the active center for hydrogenation. The heat was turned off after 3 hours, but the hydrogen supply was maintained until the reactor cooled to 80 °C, to prevent oxidation of the activated catalyst.

3.2.4 Catalyst presulfiding

For hydrogenation studies over sulfided Ni catalyst, the impregnated Ni/ γ -Al₂O₃ catalyst was pretreated by following the guidelines for in situ catalyst presulfiding.⁶ The process was performed

in the hydrogenation reactor using 0.5 wt% DMDS diluted in *n*-heptane as the in situ sulfiding agent. The DMDS solution was prepared in a fumehood since it had an unpleasant odor. The catalyst was sulfided in two steps: low temperature sulfiding (at 220 – 230 °C) followed by high temperature sulfiding (at 340 – 350 °C).

Packing of catalysts in the reactor and leak tests were done as described in section 3.2.3. The catalysts had to be dried completely to remove all traces of moisture before in situ sulfiding. The reactor was pressurized to 1 MPa and hydrogen was introduced at 500 mL/min. Temperature in the furnace was set to 80 °C and raised to 170 °C in discrete steps of 30 °C/h. The gradual increase in temperature prevented potential exotherms by absorption of condensed hydrocarbons that could be present in the reactor. The reactor was held at 170 °C for 1 h to ensure complete removal of traces of moisture. The reactor was then cooled to 120 °C and heptane was introduced at the rate of 2 mL/min. The temperature was held at 120 °C, in order to control the potential exotherm from the heat of absorption, until the catalyst bed was completely wetted by heptane. The temperature inside the reactor was continuously monitored through the LabVIEW interface. After 3 hours of pumping heptane, the heat was turned off. The hydrogen supply was stopped after the temperature in the reactor reached 80 °C. The system was shut down, ensuring that the hydrogen in the reactor was locked in place to prevent oxidation of the catalyst bed.

The system was restarted the next day. Temperature of the furnace was set to 120 °C and hydrogen was reintroduced at 500 mL/min. Heptane was pumped into the reactor at 0.5 mL/min. The temperature was increased at a rate of 20 °C/h until it reached 180 °C. When the temperature inside the reactor reached 180 °C, the heptane solution was replaced with 0.5 wt% DMDS solution in heptane. This initiated the sulfiding of the catalyst bed. The system pressure, temperature and flow rates of inlet and outlet streams were continuously monitored. The temperature was increased at the rate of 20 °C/h until the highest temperature in the reactor reached 220 °C. From this point on, the system was maintained at 220 °C. Liquid and gas samples were collected from the product stream once every hour.

The gas samples were analyzed using gas-phase GC to measure concentration of hydrogen sulfide. The instrument conditions used for analysis are described in section 3.2.7. The reactor was operated at 220 °C for 10 hours but there was no hydrogen sulfide detected in the product gas

stream. At this point, the furnace was switched off and hydrogen supply was shut down after the reactor cooled to 80 °C.

The process of catalyst sulfiding was resumed on the third day. It was anticipated that the first stage of sulfiding at 220 °C would take up to 6 hours, resulting in a breakthrough of hydrogen sulfide concentration in the outlet gas stream. Since hydrogen sulfide gas remained undetected in the outlet gas stream even after 10 hours of sulfiding, the system pressure was raised from 1 MPa to 2 MPa. Hydrogen was supplied at 500 mL/min and furnace temperature set to 220 °C. DMDS solution was pumped at 0.5 mL/min. Liquid and gas samples were collected one hour after the reactor temperature reached steady state. GC analysis of gas sample showed the presence of hydrogen sulfide gas. Samples were collected and measured for the next 2 hours. The concentration of hydrogen sulfide in the gas stream remained constant (~0.08 mol %). Mass balance of sulfur was calculated to ensure that sulfur was no longer being adsorbed on the catalyst. The catalyst was ready for high temperature sulfiding.

The furnace temperature was raised to 330 °C while maintaining gas and liquid flow. Temperatures inside the reactor were continuously monitored. When the highest temperature in the reactor reached 340 °C, temperature was manually controlled on the furnace controller to ensure that the reactor operated in isothermal condition. One hour after the reactor reached steady state, liquid and gas samples were collected and gas samples were analyzed. The concentration of hydrogen sulfide was found to be ~0.08 mol %. Mass balances and sample analysis for the next 3 hours showed that all the sulfur in the feed was in the product stream. Hydrogen sulfide breakthrough was achieved. The catalyst bed was sulfided to a sufficient extent. The heat supply was shut off and liquid feed pumping was stopped. Hydrogen supply was stopped after 3 h when the reactor cooled to 100 °C. Thus, the catalyst remained in the sulfided state for reactions with sulfur-containing feed.

Appropriate personal protective equipment such as eye glasses, respirator, protective gloves and lab coat were used while collection and handling of samples due to the hazardous nature of the hydrogen sulfide in the gaseous stream. Hydrogen sulfide is a colorless, poisonous and flammable gas with the smell of rotten eggs. It can be detected by smell at very low concentrations ranging from 0.01 – 0.3 parts per million. The Alberta Occupational Exposure Limit (OEL) is 10 parts per million (ppm) for 8 hours and 15 ppm as a ceiling limit.⁷ Exposure to higher than recommended

levels of hydrogen sulfide results in severe health hazards such as nausea, loss of consciousness and even death.

3.2.5 Reactor design

A continuous flow packed bed reactor was used for the hydrogenation reactions. Some design modifications were done on an existing plant to enable operation at the specific conditions required for the current reaction studies. A process flow diagram of the reactor set-up is shown in Figure 3.2. The images of the actual flow-reactor set-up in the laboratory are shown in Figure 3.3.

The feed tank (F-1) was an amber glass bottle of 1L capacity, supplied by Fisher. The lid had a drilled hole of 0.32 cm diameter to facilitate insertion of an inlet pump hose. The lid prevented evaporation of volatile feed material. The feed tank was placed on a Mettler Toledo Model ML 3002E electronic weighing balance with a measuring range of 0.00-3200.00 g and a precision of 0.01 g. The weighing balance was used to monitor the amount of feed that had entered the system. Feed was pumped into the system through a LabAlliance positive displacement pump, i.e., HPLC pump with a volumetric flow range of 0.01 – 10.00 mL/min. The feed temperature was measured by an Omega (Model KMQXL-062U-12) K-type thermocouple (T1) that was installed after the feed inlet. The thermocouple was 30.5 cm in length and 0.16 cm in diameter, with a measurement range of 0 – 1335 °C. The co-feed gas line had a Brooks SLA5800 series mass flow controller (MF-1) that was calibrated for a volumetric flow rate of 0 – 1500 mL/min to supply a precise volume of hydrogen for the reactions. An alternate gas line for nitrogen gas was present in order to purge the system when needed. The nitrogen gas line was also connected to a Groove-type back pressure regulator (BP-1) in order to control and set the total pressure inside the reactor. The back-pressure regulator, manufactured by Equilibar, had a 316 stainless steel body with a Viton® O-ring seal. It could regulate pressures up to 4.13 MPa and was designed to operate at temperatures up to 300 °C. The inlet pressure of hydrogen and nitrogen gases were monitored by pressure gauges P1 and P2 respectively.

Check valves (CV-1, CV-2, CV-3) were installed after the liquid feed inlet, hydrogen gas inlet and nitrogen gas inlet respectively to prevent backflow of inlet fluids. Two relief valves (RV-1, RV-2) designed for set pressure of 11 MPa were present before and after the reactor as a safety measure, in the event of excess pressure buildup in the system. The relief valves were connected to the fume hood. The check valves and relief valves were made of Swagelok 316 stainless steel.

The reactions took place in a Swagelok 316 stainless steel, cylindrical packed bed reactor of length 17 cm and diameter 2.54 cm (RX-1). A stainless steel thermowell was installed in the reactor vessel to enable temperature measurements at various points inside the reactor. Three Omega K-type thermocouples (Model KMQXL-062U-36), labelled T2, T3 and T4 were placed inside the thermowell at the top (4.2 cm), middle (10.3 cm) and bottom (15.5 cm) of the reactor vessel respectively. The reactor was packed with catalysts and inerts as explained in section 3.2.3. The height of packing in the reactor was 15 cm. Glass wool was placed at the top and bottom of the packed bed to insulate the reactor and prevent energy losses by heat dissipation. The reactor was installed inside a model HTF55122A Lindberg/Blue M single zone tube furnace with a temperature range 0 – 1000 °C. A Thermo Fisher Scientific UP150 programmable controller was used to manually set the temperature inside the furnace. Liquid feed and hydrogen co-feed lines merge before they enter the top of the reactor. The flow in the reactor is vertical down flow – from top to bottom.

The product stream that emerged from the reactor at a high temperature was passed through a co-current flow heat exchanger (HX-1) that was 39 cm long with an outer tube diameter of 1.27 cm and inner tube diameter of 0.64 cm. Water, used as a cooling fluid, was passed through the outer tube and the product stream flowed through the inner tube. Water was continuously circulated at 5 °C at a rate of 17 L/min by a Fisher Scientific Isotemp refrigerated/heated bath circulator. The condensed product stream entered a product tank (PR-1) at ambient temperature and pressure conditions after passing through the back-pressure regulator. The product temperature and pressure were monitored by a thermocouple T5 (similar in model to T1) and pressure gauge P5. The product tank was made of a Swagelok 316 stainless steel vessel of 1L capacity. Liquid product from the tank could be collected periodically by operating a ball valve and a needle valve at the outlet. The needle valve was installed as a safety measure to regulate the rate of draining liquid and thereby reduce the escape of hydrogen gas in the product tank into the atmosphere.

A gas product line emerging from the top of the liquid line passed through a gas flowmeter (GF-1) before being released into the fume hood. The Ritter Drum-type TG-05 model #5 PVC volumetric gas meter was calibrated to precisely measure the outlet gas stream, as explained in section 3.2.9. The measuring range of the device was 0-60 L/h. Since the gas stream was rich in flammable compounds such as hydrogen, the gas flowmeter was connected to an explosion proof

pulse generator V2.0 Ex, which enabled reading the measured gas volume and flowrate values on the computer. The HPLC pump, Brooks mass flow controller, thermocouples and Ritter's drum flowmeter were connected to a LabView program. The LabView interface was used to enter input parameters such as liquid and hydrogen gas flow rates and to monitor temperature and flowrates of inlet and outlet streams.

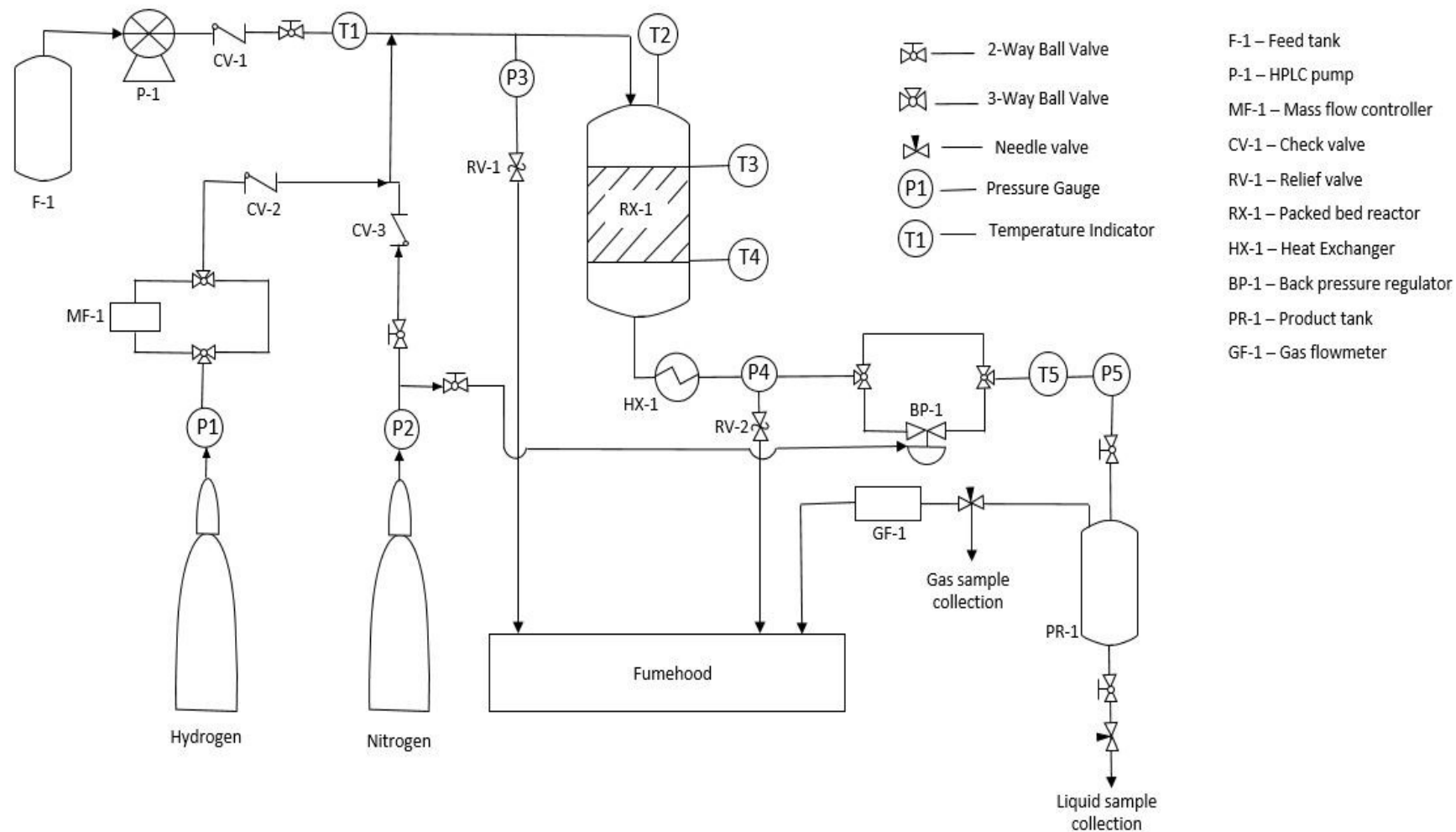


Figure 3.2 Process flow diagram of the reactor used for hydrogenation reactions

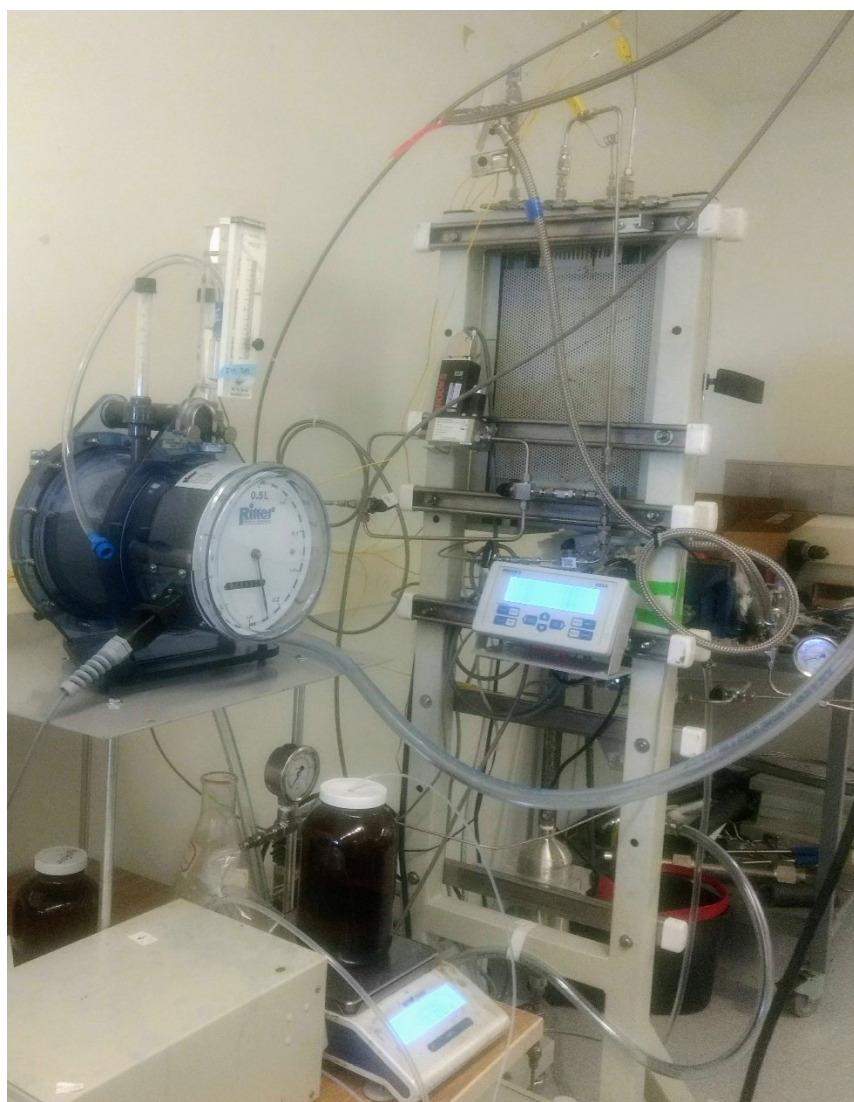


Figure 3.3 Images of the continuous flow reactor designed for hydrogenation reactions

3.2.6 Reactor operation

Hydrogenation reactions in the continuous reactor were performed using the following procedure. The operation conditions are listed in Table 3.2. The phase compositions of the reaction system were calculated for the various operating conditions, with the aid of VMG Symmetry software. The thermodynamic model that was used for simulation was Soave-Redlich-Kwong model. It was found that all the components in the reactor were in the vapor phase at all reaction conditions.

Feed mixture containing 1-hexene (10 wt %), toluene (5 wt %) and *n*-octane (85 wt %) was prepared. Feed was spiked with DMDS (0.5 wt %) for reactions over sulfided Ni catalyst. The back-pressure regulator was set to 1 MPa using nitrogen gas. The system was then pressurized by supplying hydrogen gas. The system pressure and back pressure were monitored using pressure gauges. Hydrogen gas was supplied at the required flow rate through the mass flow controller. Air from the liquid feed line was removed with a syringe to prevent cavitation. Model feed mixture was supplied through the feed line by setting the required flow rate in the HPLC pump. The furnace was heated to the required temperature with the help of the programmable controller. The temperatures and flow rates of inlet and outlet streams were monitored on the LabView interface. When the average temperature in the reactor reached the desired reaction temperature, the temperature was regulated by manually operating the temperature setting of the furnace, to minimize temperature fluctuations, until it reached steady state. Mass balance was commenced about one hour after the system reached steady state. The product tank was drained before starting the mass balance. The weight of the supplied liquid feed was measured using a Mettler Toledo Model ML 3002E electronic weighing balance with a measuring range of 0-3200 g and a precision of 0.01 g. The volume of inlet and outlet gas streams were monitored on the LabView interface. Liquid product was collected from the product tank as soon as the mass balance period ended. The weight of the liquid product was measured with a Mettler Toledo Model ME 204E electronic weighing balance with a measuring range of 0-220 g and a precision of 0.0001 g. A sample of the product gas stream was collected by connecting a gas bag to the gas sampling port. It was immediately injected into a Gas-GC column for analysis. The procedure was repeated, and reactions were performed at different temperatures. After all reactions were finished and samples were collected, the furnace was turned off. The supply of liquid feed was stopped while hydrogen gas was continuously supplied until the reactor temperature reached 80 °C. The system was depressurized when the system cooled down to room temperature.

Table 3.2 Operating conditions for hydrogenation reactions

Catalyst	Temperature (°C)	WHSV (h ⁻¹)	Gauge Pressure (MPa)
Reduced Ni/ γ - Al ₂ O ₃	80	0.5	1
	120	0.5	1
	160	0.5	1
Sulfided Ni/ γ - Al ₂ O ₃	80	0.5	1
	120	0.5	1
	160	0.5	1
	200	0.5	1
	240	0.5	1
	280	0.5	1

3.2.7 Analyses

The gas chromatograph coupled with mass spectrometer (GC-MS) was used to identify the compounds present in the model feed and liquid products. The device used was an Agilent 7820A gas chromatograph with a 5977E mass selective detector and a HP PONA capillary column with dimensions of 50 m x 0.2 mm x 0.5 μ m. The raw data was processed by the Agilent MassHunter software. Samples for the GC analysis were prepared in a 10 mL volumetric flask with 2 mL of product in *n*-octane. Instrument method conditions were set to automatically inject 0.1 μ L of sample through the inlet. The sample inlet cell was maintained at 250 °C. The split ratio was 1:100. Column carrier gas helium flowed through the column at 1 mL/min. The oven was kept at 35 °C for 30 min, then 2 °C/min to 100 °C for 0 min, then 10 °C/min to 300 °C for 7.5 min. The total run time for each sample was 90 min. The detector was programmed to turn off between 32.5 to 37 minutes, to avoid solvent saturation.

Gas chromatography with flame ionization detector (GC-FID) was used for quantitative analysis of the model feed and the liquid products of hydrogenation. The device used for analysis was an Agilent 7890A GC-FID/NPD equipped with a HP PONA column (50 m x 0.2 mm x 0.5 μ m). Raw data was processed by the Agilent ChemStation software. 0.1 μ L of sample was automatically

injected through a split/splitless injector at 250 °C. The sample was carried through the GC column by helium which flowed at 1 mL/min. The temperature program of the oven was: 35 °C for 30 min, then 2 °C/min to 100 °C for 0 min, then 10 °C/min to 300 °C for 7.5 min. The total run time for each sample was 90 min. The heater for FID was maintained at 250 °C with hydrogen gas flow of 40 mL/min and air flow of 400 mL/min. Blank run using octane as a solvent was performed between each sample run. For blank runs, helium gas flowed through the column at 0.72 mL/min, with the oven at 300 °C for 15 min. The determination of GC-FID relative response factors for various compounds has been explained in Appendix A. Quantification of various compounds present in the samples have been done using the following formula.

$$\text{Weight of compound} = \frac{\text{Area of compound} \times \text{Weight of internal standard}}{\text{Area of internal standard} \times \text{RRF of compound or compound class}} \quad (1)$$

The reaction products consisted of many species such as isomers of 1-hexene and addition products containing sulfur. Determination of response factors for all the compounds was impractical due to the costs and time constraints related to purchase of calibration standards and analyses. Consequently, some of these compounds were quantified by using the average response factor for the corresponding compound class. Table 3.3 shows the response factors of compounds and compound classes that were used.

Table 3.3 Average response factors relative to cyclohexane for GC-FID

Compound/Compound class	RRF
<i>n</i> -hexane	1.02
1-hexene	1.05
Paraffins	0.99
Olefins	1.01
Aromatics	1.06
Naphthenes	1.01
S-compounds	0.74

Cyclohexane was used as an internal standard for preparation of liquid samples. The samples were carefully prepared in a 10 mL volumetric flask by adding 2 mL of product and 0.1 mL of cyclohexane in *n*-octane. The volumes of product and internal standard were precisely measured

with Thermo Scientific fixed volume single channel micropipettes having a measurement range of 1-1000 μL for the product and measurement range of 2-200 μL for the internal standard. The flask was then filled with *n*-octane up to the 10 mL mark using a glass pipette. The weights of product and internal standard that was added in the sample were measured using a Mettler Toledo Model ME 204E electronic weighing balance with a measuring range of 0-220 g and a precision of 0.0001 g.

The gas products of hydrogenation reactions were analyzed via manual injection of the collected sample into an Agilent 7890A gas chromatographic device equipped with thermal conductivity detector (TCD) and flame ionization detector (FID). Raw data processing was done by Agilent ChemStation software. The samples were injected through a purged packed inlet which were carried into an Agilent HayeSep R column before entering the TCD followed by FID. Carrier gas helium flowed through the column at 28 mL/min. Temperature program of the oven was 70 $^{\circ}\text{C}$ for 7 min, then 10 $^{\circ}\text{C}/\text{min}$ to 250 $^{\circ}\text{C}$ for 0 min, then -30 $^{\circ}\text{C}/\text{min}$ to 70 $^{\circ}\text{C}$ for 8 min. Total run time for analysis was 41 min. The heater for FID was maintained at 250 $^{\circ}\text{C}$ with hydrogen gas flowing at 40 mL/min and air flowing at 400 mL/min. The heater for TCD was maintained at 200 $^{\circ}\text{C}$ with hydrogen gas flowing at 35 mL/min.

Thermogravimetric Analysis (TGA) of fresh and used catalysts was done using a Mettler Toledo TGA/DSC1 Star^c System. About 20 mg of sample was accurately weighed and placed in a crucible. The samples were heated in nitrogen environment from 25 $^{\circ}\text{C}$ to 600 $^{\circ}\text{C}$, followed by heating in air from 600 $^{\circ}\text{C}$ to 700 $^{\circ}\text{C}$. The gases were flowing at 50 mL/min. The flowrate of gases was monitored using a Mettler Toledo GC10 Gas Controller. The temperature program of the furnace was set from 25 $^{\circ}\text{C}$ to 600 $^{\circ}\text{C}$ at 10 $^{\circ}\text{C}/\text{min}$, then kept constant at 600 $^{\circ}\text{C}$ for 20 minutes and then increased from 600 $^{\circ}\text{C}$ to 700 $^{\circ}\text{C}$ at 10 $^{\circ}\text{C}/\text{min}$.

The presence of acidic sites on fresh and spent catalysts was studied by Diffuse Reflectance Fourier Transform Infrared Spectroscopy (DRIFTS). The device used was an ABB MB3000 FTIR Spectrometer with a Pike DiffusIR attachment. 5 mg of finely crushed catalyst particles was mixed with 5 mg of KBr and pressed into a ceramic cup. The cup was then loaded into the furnace and subjected to a constant stream of nitrogen. The cell was then heated to 450 $^{\circ}\text{C}$ and allowed to soak at that temperature for 60 minutes, then cooled to 420 $^{\circ}\text{C}$ and allowed to soak at that temperature for 10 minutes, then cooled to 150 $^{\circ}\text{C}$ and allowed to soak for 110 min. When the cell temperature

reached 150 °C, a reference spectrum was obtained. This was followed by saturation of the nitrogen stream with pyridine vapors for 40 minutes. After the pyridine flow was turned off, absorbance spectra were recorded once in every 10 minutes for 60 minutes as the average of 120 scans, while the cell remained at 150 °C.

3.2.8 Calculations

The reactants were passing through the hydrogenation plant had a weight hourly space velocity (WHSV) of 0.5 h⁻¹. The mass flow rate of the model liquid feed mixture was determined using the formula:

$$\text{Mass flow rate of feed} = \text{WHSV} \times \text{Total mass of catalyst bed} \quad (2)$$

Conversion of a compound is measured as % conversion using the formula:

$$\% \text{ Conversion} = \frac{\text{Moles of reactant reacted}}{\text{Moles of reactant in feed}} \times 100 \quad (3)$$

where,

$$\begin{aligned} \text{Moles of reactant reacted} \\ = \text{Moles of reactant in feed} - \text{Moles of reactant in product} \end{aligned}$$

Consider a reaction system that has several reactions occurring simultaneously.



The hydrogenation reactions resulted in the formation of various product species such as internal isomers, skeletal isomers and in some cases, thiols and thioethers. The selectivity of formation of product species A is defined by the following equation:

$$\text{Selectivity of A} = \frac{\text{Moles of R reacted to form product species A}}{\text{Moles of R reacted to form product species A+B+C}} \quad (4)$$

Mole balance was performed based on the concentrations of feed and product mixtures, according to the following equation:

$$\text{Mole balance (\%)} = \frac{\text{Moles of species R reacted} + \text{Moles of species R unreacted}}{\text{Moles of species R in feed}} \quad (5)$$

3.2.9 Calibration

The HPLC pump that was used to pump the liquid feed into the reactor was calibrated using *n*-octane. A feed bottle containing *n*-octane was placed on a Mettler Toledo Model ML 3002E electronic weighing balance with a measuring range of 0-3200 g and a precision of 0.01 g. The pump was set to operate at a specific flowrate. The mass of octane that was pumped was measured for a known period of time. The volumetric flowrate of the liquid was determined by using the density of *n*-octane. The procedure was repeated for various set points in the range of 1 mL/min to 8 mL/min to obtain the calibration curve of the HPLC pump. The calibration curve that was obtained is charted in Figure 3.4.

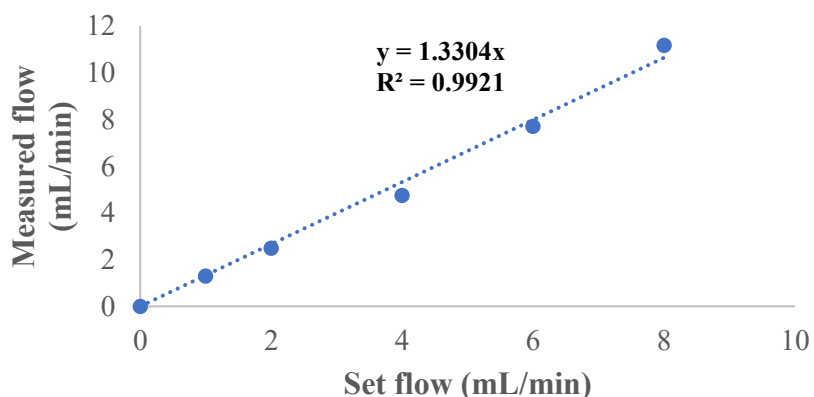


Figure 3.4 Calibration curve of the HPLC pump for *n*-octane

The Ritter Drum-type gas flowmeter was calibrated against the Brooks mass flow controller (MFC) with hydrogen gas. The MFC supplied hydrogen gas at a specific set flow rate. The volume of gas passing through the drum flowmeter for a known period of time was noted at 20 °C and atmospheric pressure (93.27 kPa). The measured flow rate was calculated by dividing the volume of gas that passed through the drum flowmeter by the time. The procedure was repeated for hydrogen flow rates in the range of 0 – 1000 mL/min. The values of set flow rate vs measured flow rates were plotted to obtain a calibration curve for the drum flowmeter₁.

₁ - The MFC was calibrated to provide flow in normal mL/min, i.e., flow at 273.15 K and 101.325 kPa absolute, whereas the flow rate of drum flowmeter was measured at 293 K and 93.27 kPa absolute.

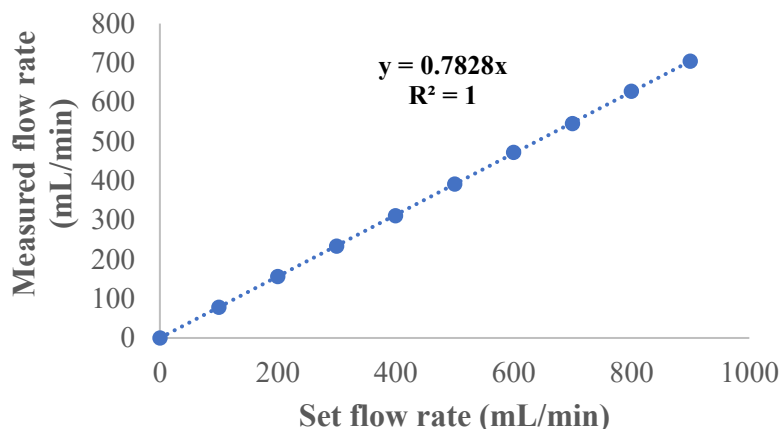


Figure 3.5 Calibration curve of the drum-type gas flowmeter for hydrogen gas at 293 K and 93.27 kPa absolute

3.3 Results

Hydrogenation reactions in the continuous reactor took place as described in section 3.2.6. The liquid-phase model feeds and products of hydrogenation were characterized by GC-MS as well as GC-FID. The gas-phase products were characterized by gas-phase GC-FID/TCD. Fresh and spent catalysts were analyzed using TGA. The analyses were done in two phases; the feed and products for hydrogenation over unsulfided catalyst followed by feed and products for reactions over sulfided catalyst.

3.3.1 GC-MS identification of reaction products

3.3.1.1 Unsulfided model feed hydrogenation

The solvent used for the feed had trace impurities such as heptane, but they did not take part in the hydrogenation reactions. 1-hexene was hydrogenated into *n*-hexane and toluene converted to methylcyclohexane. No other side reactions were found to occur.

Figure 3.6 shows the chromatogram (up to 40 min) for the model feed used for hydrogenation over unsulfided Ni/Al₂O₃ catalyst. Table 3.4 lists the compounds identified using the MS detector for the peaks in Figure 3.6. A typical chromatogram of GC-MS analysis of liquid-phase products after hydrogenation over unsulfided Ni/Al₂O₃ catalyst is shown in Figure 3.7. Table 3.5 lists the compounds identified by the MS detector for the peaks in Figure 3.7. All the peaks that were seen beyond retention time of 25 minutes were present as impurities in the solvent. No peaks were

observed for retention times greater than 40 mins. The solvent peak for *n*-octane was not seen as the detector was turned off from 32.5 to 37 min.

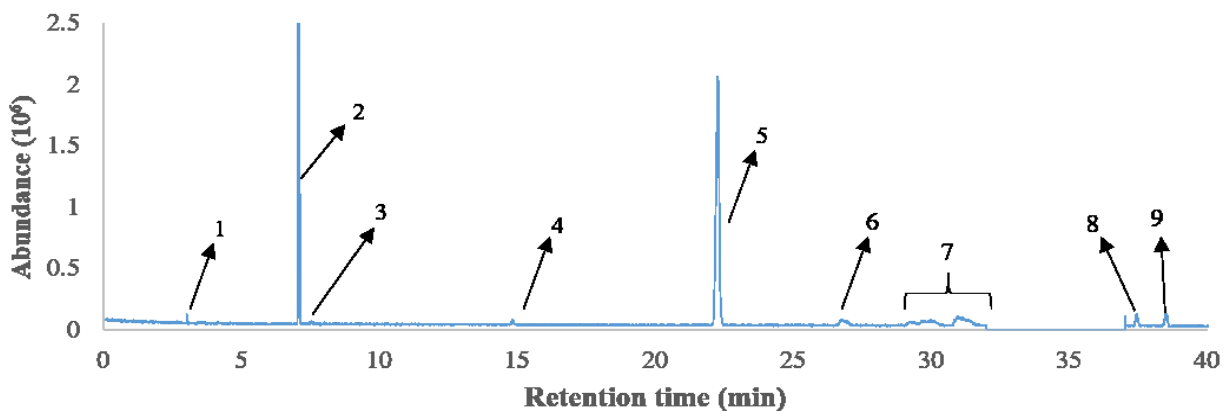


Figure 3.6 Chromatogram for GC-MS analysis of unsulfided model feed

Table 3.4 Compounds in unsulfided feed for hydrogenation reactions

Peak	Retention time (min)	Compound	Structure
1 ^a	3.03	nitrogen	$\text{N}\equiv\text{N}$
2	7.12	1-hexene	<chem>CCCCC=C</chem>
3 ^b	7.57	<i>n</i> -hexane	<chem>CCCCCC</chem>
4 ^b	14.84	heptane	<chem>CCCCCCC</chem>
5	22.51	toluene	<chem>Cc1ccccc1</chem>
6 ^b	26.79	$\text{C}_{10}\text{H}_{22}$	-
7 ^b	29.25 – 31.35 ^c	- ^d	-

Peak	Retention time (min)	Compound	Structure
8 ^b	37.46	C ₈ H ₁₇	-
9 ^b	39.16	C ₈ H ₁₈	

a - Peak does not indicate sample composition. May be dissolved in the sample as a contaminant.
b – Peaks present as impurities in the solvent acquired from supplier. Compound identity could not be verified.

c – Representative of various peaks grouped together.

d – Unidentified mass spectra of respective retention times shown in Appendix D.

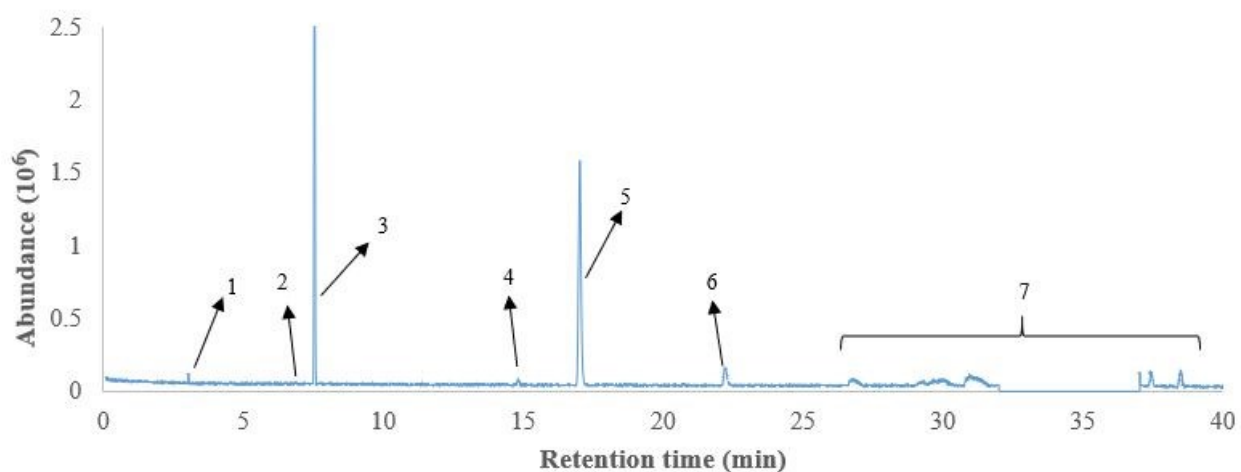
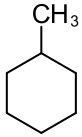
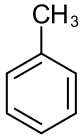


Figure 3.7 Chromatogram for GC-MS analysis of hydrogenated product over unsulfided catalyst at 120 °C

Table 3.5 Compounds in hydrogenated product over unsulfided catalyst

Peak	Retention time (min)	Compound	Structure
1 ^a	3.03	nitrogen	N≡N
2	7.13	1-hexene	<chem>H2C=CCCCC</chem>
3	7.57	<i>n</i> -hexane	<chem>CCCCCC</chem>
4 ^b	14.84	heptane	<chem>CCCCCCC</chem>

Peak	Retention time (min)	Compound	Structure
5 ^c	17.36	methyl-cyclohexane	
6	22.52	toluene	
7 ^b	26.79 – 39.16 ^d	- ^e	-

a – Peak does not indicate sample composition. May be dissolved in the sample as a contaminant.

b – Peaks present as impurities in the solvent acquired from supplier.

c – Peak verified with pure compound from supplier.

d – Representative of various peaks grouped together.

e – Identity of impurities were not verified, as mentioned in Table 3.4.

3.1.1.2 Sulfided model feed hydrogenation

Figure 3.8 shows the chromatogram (up to 40 min) for the model feed used for hydrogenation over sulfided Ni/Al₂O₃ catalyst. No peaks were observed for retention times greater than 40 mins. Table 3.6 lists the compounds identified using GC-MS analysis for the peaks in Figure 3.8.

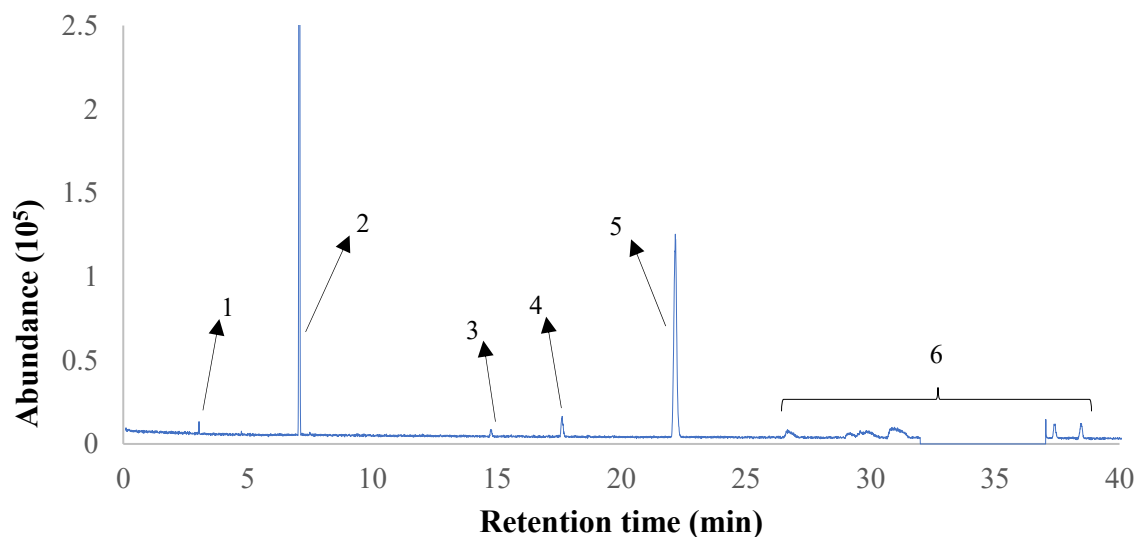
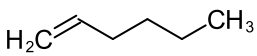
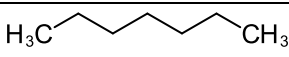
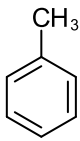


Figure 3.8 Chromatogram for GC-MS analysis of sulfided model feed

Table 3.6 Compounds in sulfided feed for hydrogenation reactions

Peak	Retention time (min)	Compound	Structure
1 ^a	3.03	nitrogen	$\text{N}\equiv\text{N}$
2	7.12	1-hexene	
3 ^b	14.84	heptane	
4	17.90	dimethyl disulfide	$\text{H}_3\text{C}-\text{S}-\text{S}-\text{CH}_3$
5	22.52	toluene	
6 ^b	26.79 – 39.16 ^c	- ^d	-

a – Peak does not indicate sample composition. May be dissolved in the sample as a contaminant.

b – Peaks present as impurities in the solvent acquired from supplier. Compound identity assigned based on MS library suggestion.

c – Representative of various peaks grouped together.

d – Identity of impurities were not verified, as mentioned in Table 3.4.

A typical chromatogram of GC-MS analysis of liquid-phase products after hydrogenation over sulfided Ni/Al₂O₃ catalyst is shown in Figure 3.9. Table 3.7 lists the compounds identified using the MS detector for the peaks in Figure 3.9. The solvent peak (*n*-octane) for the samples was not seen as the detector was turned off from 32.5 to 37 min.

Hydrogenation reactions with a sulfided model feed resulted in hydrogenation of 1-hexene but toluene remained unreacted in the current operating temperature range of 80 – 280 °C. The products were also found to have internal isomers of hexene such as *cis*-3-hexene, which were not part of the model feed mixture. The identity of the internal isomers namely, *cis*-2-hexene, *trans*-2-hexene, *cis*-3-hexene and *trans*-3-hexene (see peaks 4 to 7 in Figure 3.9) were verified with authentic compounds. In the case of peak 8, the mass spectrum indicated that the compound had the molecular formula C₆H₁₂. Since all the internal isomers of 1-hexene were already identified, this compound could have been a cycloparaffin, i.e., cyclohexane or methyl-cyclopentane, or a

skeletal isomer of *n*-hexene. Cycloparaffins were ruled out by spiking the liquid product with methylcyclopentane and cyclohexane. The spiked sample was analyzed using GC-FID with the same temperature program. The resulting chromatogram (shown in Appendix D), showed corresponding peaks for methylcyclopentane and cyclohexane at higher retention times than that of the unidentified peak 8. Thus, it was deduced that peak 8 represented a skeletal isomer of 1-hexene. The specific identity, i.e., 3-methyl-2-pentene was tentatively assigned based on the MS Library suggestion and was not verified with an authentic compound.

The addition of DMDS to the feed mixture resulted in the formation of H₂S addition products such as hexanethiol. The identity of these compounds (see peaks 12 to 17 in Figure 3.9) were not verified with pure compounds. Instead, the identities were assigned by evaluating the mass spectra and deducing the chemistry that was likely to occur over the given catalyst.

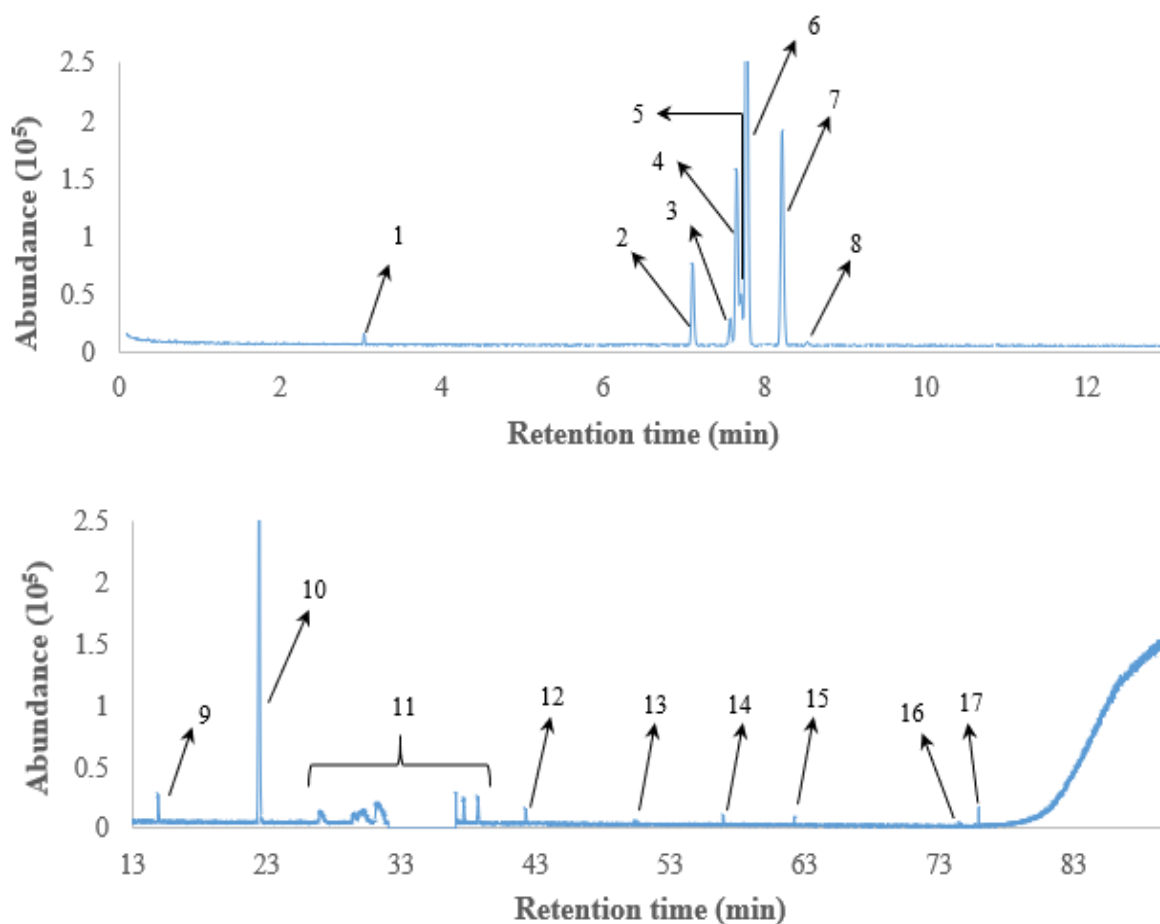
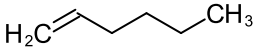
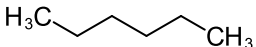
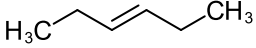
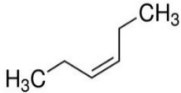
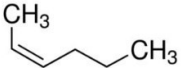
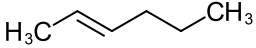
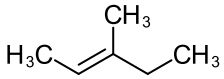
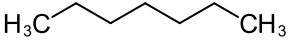
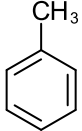
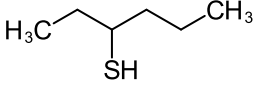
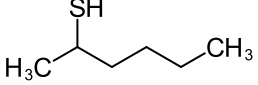
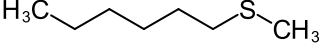
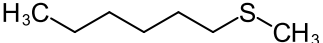
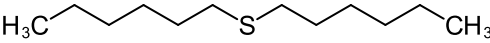


Figure 3.9 Chromatogram for GC-MS analysis of hydrogenated product over sulfided catalyst at 200 °C

Table 3.7 Compounds in hydrogenated product over sulfided catalyst

Peak	Retention time (min)	Compound	Structure
1 ^a	3.03	nitrogen	$\text{N}\equiv\text{N}$
2	7.12	1-hexene	
3	7.57	<i>n</i> -hexane	
4 ^b	7.66	<i>trans</i> -3-hexene	
5 ^b	7.71	<i>cis</i> -3-hexene	
6 ^b	7.78	<i>cis</i> -2-hexene	
7 ^b	8.22	<i>trans</i> -2-hexene	
8	8.56	3-methyl-2-pentene	
9	15.09	heptane	
10	22.59	toluene	

Peak	Retention time (min)	Compound	Structure
11 ^c	26.79 – 39.16 ^e	- ^e	-
12	42.24	3-hexanethiol	
13	50.39	2-hexanethiol	
14	56.92	1-(methylthio)-hexane	
15	62.20	2-heptanethiol	
16	74.51	- ^f	-
17	75.92	1-(hexylthio)-hexane	

a – Peak does not indicate sample composition. May be dissolved in the sample as a contaminant.

b – Peak verified with pure compound from supplier. Compound identity assigned based on MS library suggestion.

c – Peaks present as impurities in the solvent acquired from supplier.

d – Representative of various peaks grouped together.

e – Identity of impurities were not verified, as mentioned in Table 3.4.

f – Unidentified mass spectrum shown in Appendix D.

3.3.2 Conversion of 1-hexene and toluene into hydrogenated products

3.3.2.1 Reactions over unsulfided Ni/Al₂O₃

Mass balances were obtained by measuring the weight or volumes of inlet and outlet streams, as explained in Appendix C. Table 3.8 shows a summary of mass balances for reactions over unsulfided catalyst.

Table 3.8 Mass balances of hydrogenation reactions over unsulfided catalyst

Reaction temperature (° C)	Liquid inlet (g)	Liquid outlet (g)	Liquid phase mass recovery (%)	Gas inlet (g)	Gas outlet (g)	Overall mass recovery (%)
80	16.96	15.48	91.27	2.16	2.73	95.28
120	16.96	15.86	93.51	2.16	2.66	96.92
160	16.96	15.19	89.56	2.16	3.34	96.94

The concentration of hydrogenated liquid products was analyzed using GC-FID as described in section 3.7. Detailed calculations are shown in Appendix B. Table 3.9 shows the composition of feed and hydrogenated products in the liquid phase for reactions over unsulfided Ni/Al₂O₃. A portion of volatile compounds such as *n*-hexane, unreacted 1-hexene and unreacted toluene, that could not be recovered by the gas trap, escaped in the gas stream. This resulted in an apparent increase in the concentration of solvent *n*-octane in the product liquid phase. The unsaturated compounds in the feed, namely, 1-hexene and toluene were hydrogenated into *n*-hexane and methyl-cyclohexane respectively.

Table 3.9 GC-FID results for composition of unsulfided feed and hydrogenated products

Compound	Model feed (wt %)	Hydrogenation product (wt %)		
		80° C	120° C	160° C
1-hexene	9.91	0.13	0.00	0.00
Toluene	5.35	4.37	2.72	0.00
<i>n</i> -hexane	0.01	4.42	4.35	4.54
Methylcyclohexane	0.00	0.33	2.01	4.15
<i>n</i> -octane	84.77	90.80	90.95	90.20

The composition of the reaction products that were present in the gas phase could not be analyzed accurately by the Gas GC equipment due to limitations of the separation column. Instead, the conditions of the product tank for the various reaction temperatures were simulated on VMG Symmetry (v2018) software, using the Soave-Redlich-Kwong model, to estimate the equilibrium phase composition of the hydrotreated product. The composition of compounds in the gas phase,

listed in table 3.10 were considered while determining the mole balances and conversions of the various species in the reaction mixture.

Table 3.10 Equilibrium vapor-phase compositions of reaction products over unsulfided catalyst at various reaction temperatures

Compound	mol %		
	80 °C	120 °C	160 °C
octane	0.50	0.50	0.50
1-hexene	0.03	0.00	0.00
hexane	1.20	1.20	1.20
toluene	0.20	0.08	0.00
methylcyclohexane	0.02	0.12	0.32
hydrogen	98.10	98.10	98.10

Mole balances were performed as per equation (5). Table 3.11 shows the mole balances for the species of interest that took part in reactions over unsulfided Ni/Al₂O₃ catalyst at various temperatures. Molar balances of 1-hexene, toluene and octane were almost 100%, indicating that the concentrations measured by GC-FID and simulation of equilibrium conditions were reliable. However, the lower values obtained for hydrogen are most likely due to an overestimation of the moles of hydrogen supplied by the MFC at the inlet of the continuous packed bed reactor.

Table 3.11 Molar balance of species for reactions over unsulfided catalyst

Reaction temperature (° C)	Mole balance (%)			
	1-hexene	toluene	octane	hydrogen
80	99.38	101.63	101.70	91.55
120	99.20	100.56	102.23	91.93
160	100.80	100.60	102.28	92.07

Conversions for 1-hexene and toluene were calculated according to equation (3). As seen in Table 3.12, 1-hexene and toluene achieved complete conversion at reaction temperature of 180 °C.

Table 3.12 Conversion of 1-hexene and toluene on hydrogenation over unsulfided catalyst

Sample	1-hexene		toluene	
	mmol	Conversion	mmol	Conversion
Feed	20	--	10.0	--
Product at 80° C	0.2	0.99	9.0	0.10
Product at 120° C	0.0	1.00	6.0	0.40
Product at 160° C	0.0	1.00	0.0	1.00

3.3.2.2 Reactions over sulfided Ni/Al₂O₃

Mass balances for hydrogenation reactions over sulfided catalyst are summarized in Table 3.13. The non-closure of mass balance indicated that a certain proportion of products could not be recovered after the reaction.

Table 3.13 Mass balances of hydrogenation reactions over sulfided catalyst

Reaction temperature (° C)	Liquid inlet (g)	Liquid outlet (g)	Liquid phase mass recovery (%)	Gas inlet (g)	Gas outlet (g)	Overall mass recovery (%)
80	16.98	14.72	86.69	2.16	3.42	94.77
120	16.98	14.85	87.46	2.16	3.45	95.65
160	16.98	14.81	87.22	2.16	3.23	94.26
200	16.98	14.73	86.75	2.16	3.32	94.29
240	16.98	14.65	86.28	2.16	3.67	95.73
280	16.98	14.54	85.63	2.16	3.57	94.63

The nature and concentration of the products of hydrogenation over sulfided catalyst varied with temperature. Internal isomers of 1-hexene were dominant until 200 °C, but the onset of skeletal isomerization products was observed at temperatures above 240 °C. The hydrogenation of 1-hexene to *n*-hexane became significant at 160 °C and increased in concentration at higher temperatures. DMDS in the liquid feed reacted to form addition products such as thiols and thioethers at temperatures below 200 °C. Table 3.14 shows the GC-FID quantification results for model feed and liquid products of hydrogenation reactions over sulfided Ni/Al₂O₃ catalyst. A

portion of the reaction products including *n*-hexane, unreacted 1-hexene and unreacted toluene, that could not be recovered by the gas trap, escaped in the gas stream. This resulted in an apparent increase in the concentration of solvent *n*-octane in the product liquid phase.

Table 3.14 GC-FID results for composition of sulfided feed and hydrogenated products

Compound	Model feed (wt%)	Hydrogenation product (wt%)					
		80 °C	120 °C	160 °C	200 °C	240 °C	280 °C
1-hexene	9.34	3.71	3.27	1.45	0.30	0.16	0.16
<i>n</i> -hexane	0.00	0.00	0.00	0.04	0.32	0.35	0.86
DMDS	0.50	0.00	0.00	0.00	0.00	0.00	0.00
Toluene	5.80	4.17	5.01	4.98	4.83	4.43	5.02
2/3-hexene ^a	0.00	0.20	0.37	2.07	3.88	3.30	2.73
S species ^b	0.00	0.32	0.34	0.41	0.32	0.00	0.00
hexene skeletal isomer	0.00	0.00	0.00	0.00	0.00	0.00	0.12
octane	84.36	91.60	91.01	91.06	90.34	91.76	91.17

a – Representative of all internal isomers namely *cis*-3-hexene, *trans*-3-hexene, *cis*-2-hexene and *trans*-2-hexene

b – Representative of thiols and thioethers that were identified in Table 3.7

As mentioned earlier, the compositions of gas-phase products could not be obtained by analytical means. Instead, the equilibrium vapor-phase compositions of the product streams at various reaction temperatures were obtained by simulation and listed in Table 3.15.

Table 3.15 Equilibrium vapor-phase compositions of reaction products over sulfided catalyst at various reaction temperatures

Compound	mol %					
	80 °C	120 °C	160 °C	200 °C	240 °C	280 °C
1-hexene	1.04	0.91	0.40	0.07	0.05	0.04
hexane	0.00	0.00	0.01	0.07	0.08	0.25
toluene	0.21	0.24	0.24	0.22	0.23	0.23
2/3-hexene ^a	0.05	0.07	0.71	0.81	0.76	0.56
hexene skeletal isomer	0.00	0.00	0.00	0.00	0.00	0.06

Compound	mol %					
	80 °C	120 °C	160 °C	200 °C	240 °C	280 °C
octane	1.34	1.34	1.32	1.33	1.34	1.34
methane	0.00	0.00	0.00	0.02	0.03	0.04
hydrogen sulfide	0.00	0.00	0.00	0.04	0.04	0.04
hydrogen	97.37	97.44	97.32	97.44	97.47	97.45

a – Representative of all internal isomers namely *cis*-3-hexene, *trans*-3-hexene, *cis*-2-hexene and *trans*-2-hexene

Table 3.16 shows the molar balances for the species of interest that took part in reactions over sulfided Ni/Al₂O₃ catalyst at various temperatures. Compared to hydrogenation over unsulfided catalyst, reactions over sulfided catalyst resulted in many side reactions. As a result, the product mixture had many species as indicated in Table 3.7. The non-closure of mole balances for 1-hexene, toluene and octane indicated that the concentrations measured by GC-FID and simulation of equilibrium conditions were not accurate but an educated estimate. As discussed earlier, the lower values obtained for hydrogen are most likely due to an overestimation of the moles of hydrogen supplied by the MFC during the continuous reaction over the catalyst bed.

Table 3.16 Molar balance of species for reactions over sulfided catalyst

Reaction temperature (° C)	Mole balance (%)			
	1-hexene	toluene	octane	hydrogen
80	97.20	95.39	105.40	92.32
120	99.97	98.42	105.26	92.39
160	97.04	97.55	104.86	92.27
200	95.49	93.50	103.72	92.88
240	98.81	96.97	104.14	92.88
280	96.55	95.29	103.40	93.05

Conversions and molar selectivity of formation of *n*-hexane for hydrogenation over sulfided catalyst at various reaction temperatures were calculated according to equations (3) and (4) respectively and listed in table 3.17.

It was seen that the conversion of 1-hexene increased with increase in reaction temperature. The reaction selectivity showed that formation of *n*-hexane was also favored at higher temperatures.

Table 3.17 Conversion of 1-hexene and selectivity towards *n*-hexane on hydrogenation over sulfided catalyst

Sample	1-hexene (mmol)	Conversion (%)	<i>n</i> -hexane (mmol)	Side products (mmol)	Selectivity towards <i>n</i> -hexane
Feed	18.88				
Product 80° C	17.11	9.41	0.00	1.25	0.00
Product 120° C	16.90	10.50	0.00	1.98	0.00
Product 160° C	6.65	64.76	0.16	11.51	0.01
Product 200° C	1.30	93.11	1.24	15.49	0.07
Product 240° C	0.81	95.71	4.27	13.58	0.24
Product 280° C	0.66	96.52	6.30	11.28	0.36

3.3.3 Spent catalyst analysis

The percentage weight loss of fresh catalyst and spent catalysts were measured as a function of temperature. The TGA analysis was repeated for triplicate samples using the conditions described in section 3.2.7. It was seen that the weight loss profile of the spent reduced catalyst was like that of the fresh catalyst. This indicated that there was no significant coke formation after reactions, suggesting that for reduced Ni/Al₂O₃ catalyst, there was loss in activity due to coking. The weight loss profile for the spent sulfided catalyst varied from that of the fresh catalyst. It exhibited relatively lesser weight loss when heated in inert atmosphere under 600 °C and steep weight loss up to 2 wt% when heated in air from 600 °C to 700 °C. The chemistry of the species that decomposed was not analyzed. Table 3.15 shows the weight loss that was recorded for catalyst samples. The weight loss profile as a function of sample temperature is shown in Figure 3.10.

Table 3.18 TGA results for catalyst samples

Sample	Weight loss after heating (%)	
	In N ₂	In air
Fresh catalyst	6.65±0.06	0.19±0.02
Spent reduced catalyst	6.46±0.09	0.21±0.02
Spent sulfided catalyst	5.07±0.08	1.93±0.06

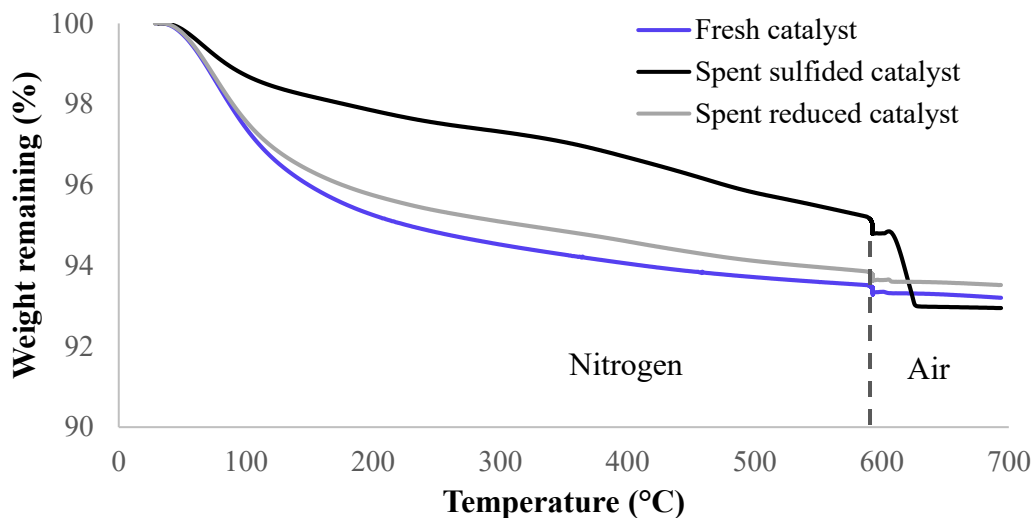


Figure 3.10 TGA weight loss profiles of Ni/Al₂O₃ catalysts

The carbon, hydrogen and sulfur composition of fresh and used catalyst samples were estimated by elemental analysis. The results are tabulated in Table 3.19. Here, the *fresh catalyst* refers to NiO/Al₂O₃, prepared by incipient wet impregnation. Since the pretreatment processes namely, reduction and sulfiding were conducted in-situ and immediately followed by reaction studies, the corresponding unspent catalysts could not be analyzed. Hydrogen was likely present as H₂O due to the absorption of ambient moisture on the catalyst surface. The relatively high values for carbon and sulfur content in the spent sulfided catalyst indicate the accumulation of carbonaceous deposits and sulfur species.

Table 3.19 Elemental analysis of catalyst samples

Sample	C (wt %)	H (wt %)	S (wt %)
Fresh catalyst	0.03	0.72	0.00
Spent reduced	0.26	0.67	0.00
Spent sulfided	3.39	0.97	0.54

An attempt was made to determine the presence of acid sites by FTIR analysis as described in Section 3.2.7. Brønsted acid sites could be the active centers for the formation of a product identified as a skeletal isomer. The spectrum of fresh alumina and that of spent sulfided Ni/Al₂O₃ were recorded and compared, as shown in Figure 3.11. After pyridine absorption, the absorbance

spectrum of a material containing Brønsted acid sites is expected to exhibit a definitive peak at 1540 cm^{-1} . However, the Brønsted acidity of the sulfided catalyst could not be confirmed. The FTIR analysis was inconclusive.

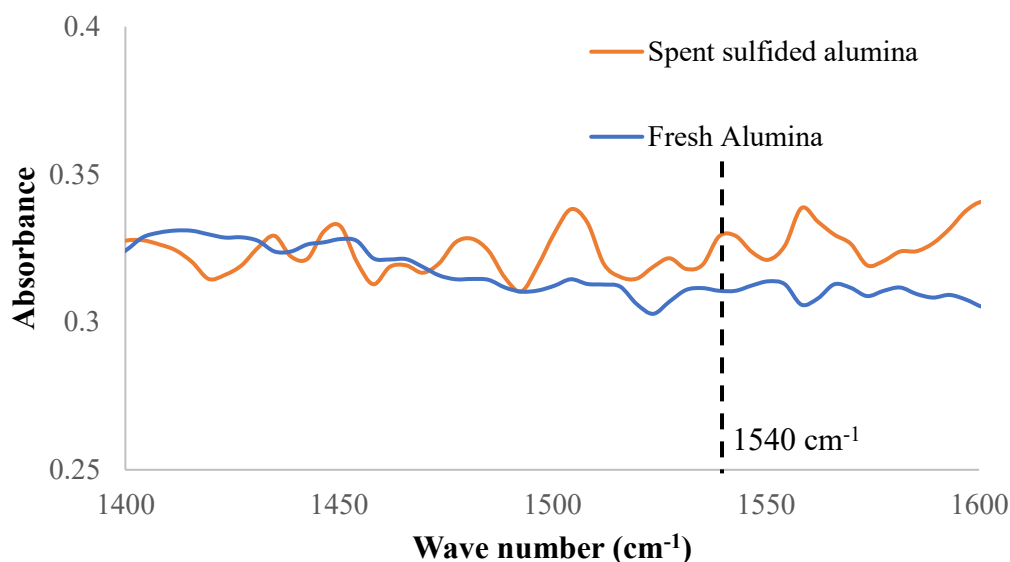


Figure 3.11 FTIR Spectra of pyridine treated catalysts in the 1400 to 1600 cm^{-1} region

3.4 Discussion

3.4.1 Equilibrium of olefin and aromatic hydrogenation reactions

Hydrogenation of olefins is an exothermic reaction. The catalysts that enable hydrogen addition to olefins sometimes also catalyze isomerization and double bond shift reactions.⁸ In such cases, a comparison of the equilibrium constants (K) at a constant temperature is useful to understand the thermodynamic favorability and the extent to which the competing reactions could potentially occur.

The equilibrium constants for the conversion of 1-hexene into various compounds is given in Table 3.20. At the temperatures that are relevant for the current study ($<300\text{ }^{\circ}\text{C}$), the high value of K for the addition of hydrogen indicates that if the reaction is not kinetically hindered, then the resulting equilibrium mixture will consist almost entirely of n -hexane.

With regards to the formation of internal and skeletal isomers, the positive values of K indicate that the reactions are driven forward at equilibrium for the listed temperatures. Yet, the relatively

low values of K indicate that these reactions are highly reversible with equilibrium mixtures expected to contain the reactant and the product species.

Table 3.20 Equilibrium constants for formation of compounds from 1-hexene at various temperatures⁹

Compound	Equilibrium constant [K]		
	127 °C	227 °C	337 °C
<i>cis</i> -2-hexene	7.53	4.58	3.16
<i>trans</i> -2-hexene	17.4	8.9	5.59
<i>cis</i> -3-hexene	3.29	1.93	1.32
<i>trans</i> -3-hexene	8.87	4.43	2.81
2-methyl-1-pentene	58.4	23.4	12.6
2-methyl-2-pentene	210	53.2	20.8
<i>cis</i> -3-methyl-2-pentene	94	28	12.2
<i>trans</i> -3-methyl-2-pentene	141	42	18.3
<i>n</i> -hexane	3.6x10 ⁹	1.67x10 ⁶	9.3x10 ³

Addition of hydrogen to aromatic compounds is more difficult than that of olefins, due to resonance stabilization of the π -electrons in the aromatic ring. These reactions are highly exothermic, with the amount of heat released per mole of aromatic compound increasing proportionately with the moles of hydrogen consumed.¹⁰ The equilibrium concentration of aromatic compounds decreases with increasing temperatures. The equilibrium constants for hydrogenation of toluene into methylcyclohexane at various temperatures are listed in Table 3.21. Based on the negative K values, the dynamic equilibrium for hydrogenation of toluene will be shifted backwards at temperatures exceeding 300 °C.

Table 3.21 Equilibrium constants for hydrogenation of toluene into methylcyclohexane¹⁰

Temperature (°C)	Equilibrium constant [K]
200	3.54
300	-0.19
400	-2.71

3.4.1 Hydrogenation of olefins over reduced Ni/Al₂O₃ catalyst

Activation of supported metal catalysts such as Ni/Al₂O₃ in a stream of hydrogen gas enables the formation of reduced metal (Ni) on the catalyst surface which act as active catalytic centers for hydrogenation reactions.¹¹ Various kinetic studies of metal catalyzed olefin hydrogenation have revealed that the reaction occurs through the formation of a catalyst-alkyl intermediate followed by addition of each hydrogen atom in a sequential manner, which results in hydrogen exchange and double bond migration, as well as addition of hydrogen to saturate the olefinic species.¹²⁻¹⁴ The catalyst-alkyl intermediates that can be formed during hydrogenation of 1-butene over Ni catalyst were illustrated in Figure 2.5. The rate determining step is the addition of the second hydrogen atom to the 2-butyl intermediate, resulting in desorption of the saturated compound from the active surface of the catalyst.

The reduced Ni catalyst used in the current study was found to be highly active for olefin hydrogenation, resulting in near complete conversion of 1-hexene to *n*-hexane at a relatively low temperature of 80 °C. The swift conversion of the hexyl intermediate on the catalyst into *n*-hexane masked observation of double bond shift reactions.

It must be noted, however that the high hydrogenation activity of reduced Ni was seen in the absence of sulfur compounds in the feed. When reduced Ni is exposed to sulfur, it poisons the surface of the catalyst. Studies have shown that H₂S and other sulfur compounds adsorb on the active surface of the metal immediately and irreversibly at high coverages, thus preventing the adsorption of H₂ and olefins for reactions.¹⁵

3.4.2 Hydrogenation of olefins over sulfided Ni/Al₂O₃ catalyst

Presulfiding of the Ni/Al₂O₃ lowered the activity of the catalytic surface and compared to reaction at the same temperature, resulted in lower conversion by hydrogenation of 1-hexene. The low activity of the sulfide catalyst significantly reduced the rate of hydrogenation of 1-hexene to *n*-hexane. Instead, 1-hexene predominantly formed internal isomers caused by double bond shift, at temperatures below 200 °C. Considering the large equilibrium constant of hydrogenation to *n*-hexane at <200 °C (Table 3.20), it appears unlikely that double bond isomerization took place due to dehydrogenation of *n*-hexane. Formation of the addition product *n*-hexane was seen above 200

°C due to acceleration in the rate of the hydrogenation reaction caused by increasing the temperature.

At temperatures above 240 °C, olefin hydrogenation products included a skeletal isomer, (tentatively identified as 3-methyl-2-pentene). The possibility that this C₆H₁₂ species was either cyclohexane or methylcyclopentane was ruled out (Appendix D). Sulfide catalysts are known to exhibit polyfunctional behavior due to the participation of the carriers in the catalytic process, especially at high temperatures (typically above 400 °C).¹⁶ However, acid-catalyzed skeletal isomerization is catalyzed by Brønsted acid sites. The current study could not confirm the presence of such sites on the surface of the catalyst. Another likely reason for the acid catalytic activity could be the incomplete reduction of the NiO/Al₂O₃ catalyst pellets leading to the formation of spinel structure (NiAl₂O₄) at the high temperatures that were employed during the sulfiding process.¹⁷ This hypothesis, however, was not further investigated.

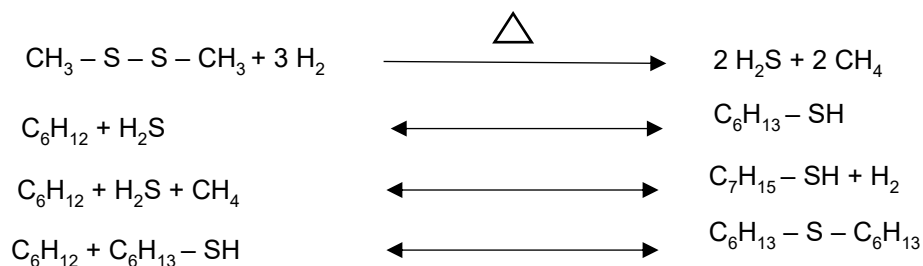
3.4.3 Effect of catalyst pretreatment on hydrogenation of aromatic compounds

Aromatic compounds are stabilized by resonance bonds and hence require higher activation energy to undergo hydrogen addition reactions. A kinetic study of gas-phase hydrogenation of toluene to methylcyclohexane over Ni/Al₂O₃ catalyst found that the reaction is of the order 0.5-2 with respect to hydrogen and the order was found to increase with increase in temperature.¹⁸ It can be reasonably assumed that the same kinetic parameters hold for the current reactions over unsulfided Ni/Al₂O₃. The rate of formation of methylcyclohexane increased with an increase in temperature, with conversion attaining near completion at 160 °C. At this temperature the equilibrium constant is positive (Table 3.21).

Sulfided Ni/Al₂O₃, however, was not sufficiently active for aromatic hydrogenation at mild temperatures, i.e., below 280 °C. Equilibrium for aromatic hydrogenation at higher temperatures is limited by thermodynamics (Table 3.21) and conversion of aromatics to cycloparaffins requires high hydrogen partial pressure. Thus, hydrogenation of feed containing aromatics over sulfided Ni/Al₂O₃ at 1MPa H₂ pressure resulted in selective hydrogenation of olefins.

3.4.4 Reactions of sulfur compounds in the feed

DMDS was added in the feed to keep the catalyst in the sulfided state. It decomposed to form methane and hydrogen sulfide, which were found to take part in addition reactions leading to the formation of thiols and thioethers. The reactions are shown below:



Two isomers of hexanethiol were identified by GC-MS. They are expected to be 2-hexanethiol and 3-hexanethiol, since their formation is favored according to Markovnikov's rule of addition to olefins. The addition of hydrogen sulfide to olefins is an exothermic reaction and the reaction equilibrium is shifted backwards at higher temperatures.¹⁹ In the current study, thiols and thioether species in the product were detected only at temperatures below 200 °C. The presence of H₂S and CH₄ were detected in the product stream at higher temperatures, because addition reactions of sulfur-containing species to olefins are thermodynamically not favored above 200 °C.

3.5 Conclusions

Catalytic hydrogenation of model feed mixture containing olefinic and aromatic compounds was studied using a continuous flow packed bed reactor. Reaction conditions were designed to evaluate the effect of *temperature* and *catalyst sulfiding* on the conversion and selectivity of olefin and aromatic hydrogenation. The conclusions of the study are as follows:

- Reduced Ni/Al₂O₃ is very active for olefin and aromatic hydrogenation in the absence of sulfur containing compounds. Reaction mixtures with model compounds attained near complete conversion of 1-hexene to *n*-hexane at 80 °C and toluene to methylcyclohexane at 160 °C.
- In situ presulfiding of Ni/Al₂O₃ catalyst significantly lowers the catalytic activity and modifies reaction selectivity for olefin hydrogenation. Sulfided Ni/Al₂O₃ does not catalyze aromatic hydrogenation at temperatures below 280 °C.

- c) For reactions over sulfided Ni/Al₂O₃, the selectivity of formation of the paraffin increases at temperatures above 200 °C. About 5 mol% of the terminal olefin converted into a skeletal isomer at 280 °C.
- d) Hydrotreatment of cracked naphtha over the same sulfided Ni/Al₂O₃ catalytic reactor system at 280 °C is expected to decrease the concentration of olefins and increase the concentration of saturated products.

3.6 References

- (1) Raseev, S. *Thermal and Catalytic Processes in Petroleum Refining*; Marcel Dekker: New York, 2003.
- (2) De Klerk, A. *Annual Report 2016-2017 (Year 1), Progress Report on Industrial Research Chair Program*; Edmonton, 2017.
- (3) Le Page, J. F. *Applied Heterogeneous Catalysis*; Technip: Paris, 1987.
- (4) Bond, G. C. *Metal-Catalysed Reactions of Hydrocarbons*, 1st ed.; Springer US, 2005.
- (5) Riya. Reaction Pathways of Binuclear Aromatics Containing 5-Membered Rings - MSc Thesis, University of Alberta, 2018.
- (6) Criterion Catalysts. *Hydrotreating Catalyst In-Situ Presulphiding Guidelines - Liquid Phase (Preferred Method) - Gas Phase (Alternative Method)*; Calgary, 2005.
- (7) Municipal district of Greenview No. 16. Code of Practice Hydrogen Sulfide <http://mdgreenview.ab.ca/wp-content/uploads/2013/12/3007-01-Code-of-Practice-Hydrogen-Sulfide-H2S.pdf> (accessed Aug 23, 2019).
- (8) Germain, J. E. *Catalytic Conversion of Hydrocarbons*; Academic Press Inc: New York, 1969.
- (9) Kilpatrick, J. E.; Prosen, E. J.; Pitzer, K. S.; Rossini, F. D. Heats, Equilibrium Constants, and Free Energies of Formation of the Monoolefin Hydrocarbons. *J. Res. Natl. Bur. Stand. (1934)*. **1946**, 36, 559–612.

- (10) Ali, S. A. Thermodynamic Aspects of Aromatic Hydrogenation. *Pet. Sci. Technol.* **2007**, 25 (10), 1293–1304.
- (11) Pernicone, N.; Traina, F. Catalyst Activation by Reduction. *Stud. Surf. Sci. Catal.* **1979**, 3, 321–351.
- (12) Bond, G. C. *Catalysis by Metals*; London Academic Press: London, 1962.
- (13) Hirota, K.; Teratani, S.; Yoshida, N.; Kitayama, T. On the Hyperfine Reaction Deuterium with Distribution Deuterium of the Catalytic Powders of Propene on Copper. *J. Catal.* **1969**, 13 (3), 306–315.
- (14) Twigg, G. H.; Wood, W. A. The Catalytic Isomerization of Butene-1. In *Proceedings of the Royal Society A*; 1941; pp 106–117.
- (15) Bartholomew, C. H. Mechanisms of Nickel Catalyst Poisoning. In *Catalyst Deactivation*; Delmon, B., Froment, G. F., Eds.; Elsevier Science Publishers B.V.: Amsterdam, 1987; pp 81–104.
- (16) Weisser, O.; Landa, S. *Sulphide Catalysts, Their Properties and Applications*; Academia publishing house: Prague, 1973.
- (17) Sayari, A.; Ghorbel, A. Isobutylene Nitroxidation on Catalysts Containing Nickel Oxide. *React. Kinet. Catal. Lett.* **1980**, 15 (4), 401–406.
- (18) Lindfors, L. P.; Salmi, T. Kinetics of Toluene Hydrogenation on a Supported Ni Catalyst. *Ind. Eng. Chem. Res.* **1993**, 32, 34–42.
- (19) Barr, F.; Keyes, D. B. Equilibria in a Chemical System Hydrogen Sulfide-Propylene—Isopropyl Mercaptan-Propyl Mercaptan. *Ind. Eng. Chem.* **1934**, 26 (10), 1111–1114.

CHAPTER 4: ATMOSPHERIC DISTILLATION OF THERMALLY CRACKED PRODUCT BEFORE AND AFTER HYDROTREATMENT

4.1 Introduction

Distillation is a widely employed unit operation in the petroleum industry. It is used to separate or purify complex mixtures into smaller fractions based on the vapor pressures of the individual components. A fractional distillation column enables a high degree of separation between the components with minimal loss or hold-up of the material.¹ Typical products of petroleum distillation include liquid petroleum gas (-50 – 20 °C), naphtha (20 – 180 °C), distillate (180 – 360 °C), atmospheric residue (360 – 550 °C) and vacuum residue (>550 °C).

For the current study, the material of interest was a light petroleum product in the naphtha and distillate range (15 – 240 °C), henceforth referred as “cracked naphtha”. It was obtained from a bitumen upgrader facility in Long Lake, Alberta. The source of the naphtha was deasphalted oil that had undergone thermal cracking (visbreaking) followed by distillation in an atmospheric distillation unit. As a consequence of thermal cracking, the mixture contained olefins. There are strict regulations that require treatment of olefins in order to make the material suitable for pipeline transport.² A detailed characterization of the nature of olefins and other hydrocarbon species in the cracked naphtha is important to design reaction pathways and operating conditions for the treatment of olefins. As a first step towards this endeavor, the cracked naphtha was further distilled into sub-fractions, using a lab-scale atmospheric distillation column. The cracked naphtha was also subjected to catalytic hydrotreatment over NiS/Al₂O₃ 280 °C and 1 MPa, with an objective of aiding characterization studies by selective conversion of olefins. The hydrotreated product was then distilled into sub-fractions with the same boiling cuts as the cracked naphtha.

The focus of this study was to evaluate the boiling point distribution of the cracked product before and after hydrotreatment and record the yields, densities and refractive indices of the distilled sub-fractions. The distillation profiles were also evaluated by simulated distillation analysis using gas chromatography. The sub-fractions obtained in this study facilitated the olefin identification and characterization studies using gas chromatography, which is discussed in the next chapter.

4.2 Experimental

4.2.1 Materials

The distillation studies employed thermally cracked product (naphtha) obtained from a bitumen upgrader facility in Long Lake, Alberta. The sample was made available by CNOOC International (formerly Nexen ULC) for the purpose of research and analysis.

Another product used for this study was the same thermally cracked naphtha that was subjected to hydrotreatment in the reactor set-up described in Section 3.2.5. The hydrogenation reaction was conducted over sulfided Ni/Al₂O₃ at 280 °C and 1 MPa H₂ pressure. The WHSV of the liquid feed (cracked naphtha) was 0.5 h⁻¹. Hydrogen gas was supplied at a rate of 1000 mL/mL of liquid feed. The purpose of preparing a mildly hydrotreated product was to assist with positive identification of the olefins, which would be reduced by such treatment.

The properties of thermally cracked naphtha and hydrotreated product are listed in Table 4.1. A mixture of acetone and dry ice was used to maintain a cooling bath over the distillation column in order to trap condensate gases. Toluene was used to clean the distillation column before and after each run. Carbon disulfide was used as a solvent for GC Simulated Distillation (SimDis) analysis. The chemicals and gases used are listed in Table 4.2.

Table 4.1 Properties of cracked naphtha and hydrotreated product used for distillation studies

Property	Units	Cracked naphtha	Hydrotreated product
Density @ 20 °C	kg/m ³	745.69	772.63
Refractive Index @ 20 °C	--	1.4193	1.4115
Kinematic Viscosity @ 20 °C	cSt	0.6156	0.8738
API Gravity @ 20 °C	--	57.78	50.53
Bromine number	g Br ₂ /100 g	56.49	42.51
Carbon	wt %	84.21	82.62
Hydrogen	wt %	13.96	15.8
Sulfur	wt %	1.39	0.92
Nitrogen	wt %	<0.1	<0.1

Property	Units	Cracked naphtha	Hydrotreated product
¹ H NMR analysis			
Aliphatic Saturate	mol %	94.17	95.02
Aliphatic Olefin	mol %	3.53	2.38
Aromatic	mol %	2.31	2.60

Table 4.2 Chemicals and gases used for hydrotreatment and distillation

Compound	Formula	CASRN ^a	Mass Fraction Purity ^d	Supplier
<i>Chemicals</i>				
Acetone	C ₃ H ₆ O	67-64-1	>.995	Fisher Chemical
Toluene	C ₇ H ₈	108-88-3	0.999	Fisher Chemical
Carbon disulfide	CS ₂	75-15-0	0.999	Fisher Chemical
<i>Gases</i>				
Dry ice	CO ₂	124-38-9	- ^c	Praxair
Hydrogen	H ₂	1333-74-0	0.99999 ^d	Praxair
Nitrogen	N ₂	7727-37-9	0.99999 ^d	Praxair

^a CASRN = Chemical Abstracts Services Registry Number

^b Purity of the material guaranteed by the supplier; material used without further purification

^c Mass fraction purity not specified

^d Mole fraction purity

4.2.2 Distillation column design

The fractionation of cracked naphtha and hydrotreated naphtha was carried out in a batch distillation column manufactured by B/R Instrument Corporation. The crude oil distillation system is shown in Figure 4.1.

The distillation system consisted of a glass boiling flask of 1L capacity in which the known volume of sample could be charged. A temperature probe was placed in the boiling flask to measure the temperature of the feed. The distillation feed was stirred with a magnetic stirrer to ensure thorough

heat distribution and maintain homogeneity of the feed. The speed of the stirrer was controlled with the aid of a stirring controller device. The glass boiling flask was insulated with a heat jacket to reduce heat energy loss by radiation. The flask was placed on a heating mantle that could heat the flask at a controlled rate. The position of the heating mantle could be adjusted vertically using a lab jack.

The vapors rising from the flask entered a distillation column equipped with spinning band technology to enhance vapor-condensate contact.³ The glass column was 50 cm long with a diameter of 4 cm. The column was coated with silvered mirror to prevent adiabatic heat losses. The spinning band was made up of Monel with separation capacity equivalent to 40 theoretical plates. The vapors eventually rose into the condenser. A temperature probe in the column measured the actual vapor temperature.

A recirculating bath supplied the coolant (tetrafluoroethane) from a Polyscience chiller (Model #AD07R-20-A11B) to maintain the condenser at the desired temperature. A reflux valve directed the condensed fluids into either the fraction collector or back into the distillation column at a predetermined reflux ratio.

A cold trap that was set-up with a (1:1) mixture of acetone and dry ice received the light gases as condensates. The distillate fluid entering the fraction collector was directed into one of the 8 receivers through a funnel. The receivers were glass cylindrical jars (100 mL capacity) with graduated markings at 2 mL intervals to measure the volume of distillate. A stepper motor was used to automatically rotate the fraction collector funnel towards the next receiver at the end of each boiling cut. A vacuum vent maintained the pressure of the fraction collector set-up at the same pressure as the distillation column.

A plug board located above the condenser provided power supply to the vapor/pot temperature probes, reflux valve, vacuum vent and stepper motor. The distillation system was connected to a computer with access to the BR M690 software. The software was used to program the process parameters such as temperatures of boiling cuts, condenser temperature, heating rates and reflux ratio for each run. The software interface also enabled continuous monitoring of process parameters during the runs.



Figure 4.1 BR M690 Distillation system used for fractionation of cracked naphtha

4.2.3 Distillation column operation

Standard operating procedures were followed to obtain the fractions during each run. About 600 mL of sample was accurately weighed on a Mettler Toledo Model ML 3002E electronic weighing balance with a measuring range of 0-3200 g and a precision of 0.01 g. The sample was then charged into the glass boiling flask that was pre-chilled at 5 °C to minimize loss of volatile components in the feed. The flask was carefully affixed to the distillation column and insulated by wrapping the heat jacket around the flask. The position of the heating mantle was adjusted by moving the lab jack while ensuring that there was enough space between the flask and the mantle to allow for thermal expansion of the column.

A cold trap was prepared by adding a (1:1) mixture of dry ice and acetone above the light gas condensate collector. The chiller was connected to the condenser set-up and set to an initial value of -5 °C.

The program for distillation operation was prepared by selecting the reflux ratio, initial and final temperatures, heating rate and condenser temperature for each boiling cut on the BR M690 software. Since only 8 fractions could be obtained for each run, the collection of sub-fractions was done over 3 consecutive runs. The detailed program for each run is shown in Table 4.3. The pot and temperature probes were placed in the respective slots and magnetic stirrer in the boiling flask was turned on. The distillation process was then initiated through the software interface.

The collection of distillate fractions in the receivers commenced when the vapor temperature in the column reached the opening temperature for the respective boiling cuts. When the vapor temperature reached the closing temperature, the funnel in the fraction collector moved towards the next receiver. After collection of distillates was completed, the respective receivers were dismantled from the set-up and the volume of distillate was noted from the graduated markings on the cylinder. Additionally, the weight of each fraction was measured by weighing the receiver on a Mettler Toledo Model ME 204E electronic weighing balance with a measuring range of 0-220 g and a precision of 0.0001 g. The receivers were equipped with a rubber stopper during weight and volume measurements to prevent loss of volatile compounds. The distillate was then carefully transferred into a pre-chilled glass jar and stored in the refrigerator at 2 °C. At the end of each run, the receivers were washed with toluene and dried before being attached to the fraction collector set-up.

The distillation column was cleaned after collection of all sub-fractions from 3 consecutive runs. For this purpose, the flask was charged with 300 mL of toluene and heated to 110 °C. The Monel column and spinning bands were thus cleaned by the rising toluene vapors. The condenser cooled the vapors and directed the distillate into the fraction collector. The fraction collector set-up was rinsed with the distilled toluene as the fluid accumulated in the receivers. At the end of the cleaning run, the leftover toluene in the flask and accumulated fluids in the receivers were discarded and dried the entire set-up was left to dry.

Table 4.3 Process parameters for atmospheric distillation of cracked naphtha and hydrotreated product

	Cut Number	Open temperature ° C	Close temperature ° C	Heating rate %	Condenser temperature ° C	Reflux ratio
Run 1	1	15	25	10	-5	5:1
	2	25	35	10	-5	5:1
	3	35	45	10	-5	5:1
	4	45	55	15	-5	5:1
	5	55	65	15	0	5:1
	6	65	75	15	0	5:1
	7	75	85	15	0	5:1
	8	85	95	18	3	5:1
Run 2	1	90	100	18	20	5:1
	2	100	110	35	20	5:1
	3	110	120	35	20	5:1
	4	120	130	35	20	5:1
	5	130	140	35	20	5:1
	6	140	150	35	20	5:1
	7	150	160	35	20	5:1
	8	160	170	35	20	5:1
Run 3	1	165	175	40	30	5:1
	2	175	185	40	30	5:1
	3	185	195	40	30	5:1

4.2.4 Analyses

The boiling point distribution of cracked naphtha was obtained by simulated distillation (SimDis) analysis. Standard test method ASTM D7169 for High Temperature Simulated Distillation⁴ was used for the analysis. This method was chosen for its ability to analyze samples in the wide boiling

range of 36 – 720 °C and it was of interest to identify the end boiling point of the cracked naphtha before and after hydrotreatment.

The equipment used for this analysis was Agilent 7890B Gas Chromatograph (GC) with DB-HT Simdis column of dimensions 5m x 0.53mm x 0.15µm and the detector used was flame ionization detector (FID). 0.5 µL of sample was automatically injected through the cool-on-column inlet. The injector was initially maintained at 50 °C and gradually heated to 425 °C at the rate of 15 °C/min. The sample was carried through the column by helium gas at 20 mL/min. The oven was initially at -20 °C and heated to 425 °C at 15 °C/min. Liquid nitrogen was used to maintain the oven at below room temperature conditions. The FID detector had hydrogen flowing at 40 mL/min and air at 350 mL/min. The total run time for the sample was 40 minutes. 0.1±0.005g of the sample was weighed and diluted with carbon disulfide to 10ml. Polywax 655 (Agilent Technologies) was used for retention time calibration. The response factor of the FID detector was determined using ASTM® D6352/D7169 Reference Material 5010 (Separation Systems Inc.) as the external standard. OpenLAB GC software was used for operating the GC and data acquisition. Dragon Simdis software was used for calibration and data reprocessing to obtain sample recovery as a function of retention time and temperature.

The densities of distilled fractions cracked naphtha and hydrotreated product were measured at 20 °C using Anton Paar Density meter, Model DMA 4500M. The instrument was calibrated using ultra-pure water provided by Anton Paar at 20 °C. The accuracy of the instrument is 0.00005g/cm³ density and the accuracy is 0.01 °C for temperature. When the cell temperature reached 20 °C, about 2 mL of the sample was injected into the instrument for density measurement. Care was taken to prevent formation of bubbles in the measurement cell. The instrument was cleaned with toluene and dried in between each sample measurement.

The refractive indices of distilled fractions cracked naphtha and hydrotreated product were measured at 20 °C Anton Paar Abbemat 200 refractometer. The range of the instrument is 1.30 to 1.72nD and the accuracy is ± 0.0001nD. The instrument was pre-calibrated by the manufacturer using official standards from the National Metrology Institute of Germany. The glass plate on which samples are placed was cleaned and dried with ethanol in between each sample measurement.

4.2.5 Calculations

The distillation fractional yields were calculated as a percentage of the mass of the feed sample collected for a respective fraction.

$$\text{Distillation fractional yield (wt\%)} = \frac{\text{Mass of distillate in the fraction}}{\text{Total mass of feed sample}} \times 100 \quad (1)$$

In the cases where there was very little sample collected (<2 mL), it was not possible to measure the density using the density meter. Instead, the density was estimated as the ratio of mass to volume of distillate in the respective fractions.

$$\text{Density (g/mL)} = \frac{\text{Mass of distillate (g)}}{\text{Volume of distillate (mL)}} \quad (2)$$

4.3 Results

Cracked naphtha was hydrotreated using the packed-bed reactor system describe in section 3.2.5. Mass balance was obtained by measuring the weight or volume of inlet and outlet streams over periods of 1 hour, as explained in Appendix C. A significant proportion of volatile products that were assumed to be mainly light hydrocarbons in the C₄-C₆ range could not be recovered by the gas trap and were present in the vapor-phase of the product. GC analysis of the product gas stream showed many peaks that could not be accurately identified nor quantified. The vapor phase composition of model naphtha hydrogenation over sulfided catalyst at 280 °C (presented in Table 3.15) was used as reference to estimate the average molecular weight of the hydrotreated naphtha gas product. Table 4.4 shows a summary of mass balance.

Table 4.4 Average mass balance over 1 hour for hydrotreatment of cracked naphtha over sulfided Ni/Al₂O₃

Liquid inlet (g)	Liquid outlet (g)	Liquid phase mass recovery (%)	Gas inlet (g)	Gas outlet (g)	Overall mass recovery (%)
16.98	13.69	80.62	2.16	4.70	95.56

The conditions of the product tank were simulated on VMG Symmetry (v2018) software, using the Soave-Redlich-Kwong model, to estimate the phase composition of the hydrotreated product

at equilibrium. The equilibrium phase compositions of the various boiling fractions, listed in Table 4.5, helped estimate the concentration of the products lost in the gas phase. It was deduced that about 60 wt% of components in the boiling range 0 – 120 °C migrated to the gas phase.

Table 4.5 Equilibrium phase compositions of hydrotreated product in the reaction product tank

Boiling range (°C)	Liquid phase (wt%)	Vapor phase (wt%)
0-10	8	92
10 - 20	11	89
20 - 30	15	85
30 - 40	19	81
40 - 50	24	76
50 - 60	30	70
60 - 70	46	54
70 - 80	60	40
80 -90	69	31
90 - 100	82	18
100 - 110	95	5
110 - 120	97	3
>120	100	0

Atmospheric distillation of cracked naphtha as well as hydrotreated naphtha as described in section 4.2.3 resulted in 19 sub-fractions of each sample. Table 4.6 shows the fractional yields for various boiling fractions of cracked naphtha and hydrotreated naphtha. The mass loss light hydrocarbons eventually resulted in very low distillation yields for boiling cuts below 75 °C for the hydrotreated product.

Table 4.6 Fractional yields of cracked naphtha and hydrotreated product distillation cuts

Cut number	Open temperature	Close temperature	Cracked naphtha ^a	Hydrogenated product ^b
	°C	°C	Yield (wt %)	Yield (wt %)
1	Cold trap (B.P <15 °C)		1.97	0.37
2	15	25	0.47	0.00
3	25	35	1.03	0.09
4	35	45	4.9	0.19
5	45	55	5.49	0.57
6	55	65	3.8	0.79
7	65	75	5.42	1.22
8	75	85	5.88	4.02
9	85	100	7.7	8.46
10	100	110	8.09	7.58
11	110	120	6.58	8.55
12	120	130	5.97	10.08
13	130	140	6.55	7.74
14	140	150	5.17	6.86
15	150	160	4.83	6.37
16	160	175	5.39	7.02
17	175	185	3.73	5.01
18	185	195	3.97	3.94
19	Residue (B.P>195 °C)		9.26	18.91

a – Based on 96.2 wt% recovery in the distillation column

b – Based on 97.8 wt% recovery in the distillation column

Cracked naphtha and the hydrotreated product were subjected to SimDis analysis as explained in section 4.2.4. The results show the boiling point distribution as a function of sample recovery. Figure 4.2 shows the SimDis distillation curve of thermally cracked naphtha. 90 wt% of the sample showed boiling points below 280 °C. Only 94 wt% of the sample was recoverable below 700 °C.

The SimDis distillation curve of the hydrotreated product, depicted in figure 4.3, showed that the end boiling point of the sample was 298 °C, i.e., 100 wt% of the sample was recovered below 300 °C.

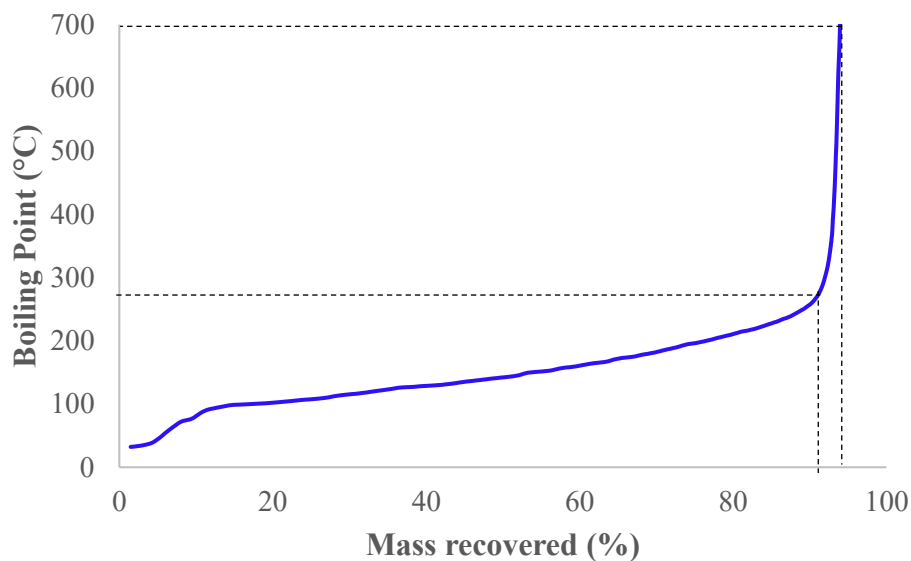


Figure 4.2 Simulated distillation curve of thermally cracked naphtha

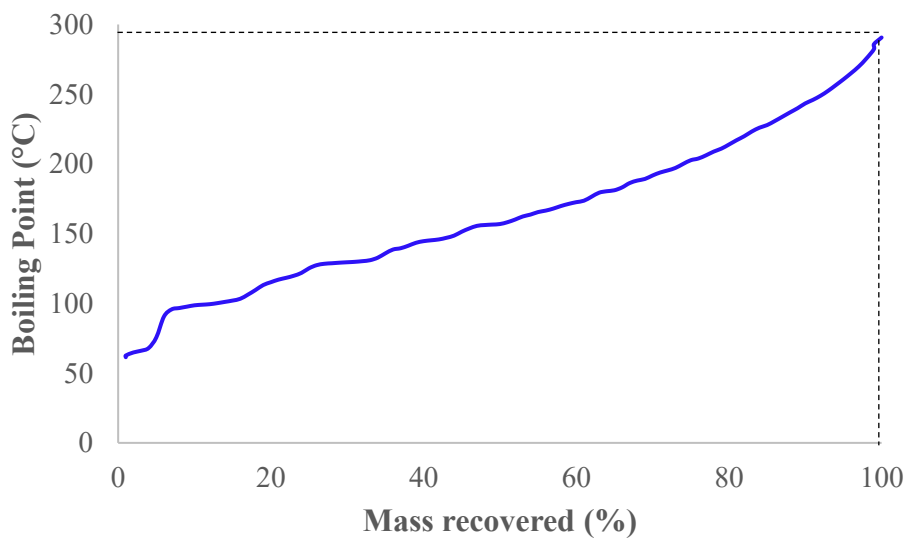


Figure 4.3 Simulated distillation curve of hydrotreated product

The densities and refractive indices of the sub-fractions were measured at 20 °C as described in section 4.2.4. The low-boiling sub-fractions of cracked naphtha (cuts below 45°C) were found to have lost between 5 wt% to 30 wt% of their initial weights due to evaporation over the period

between sample collection and density and refractive index measurements. For such cases, the density of the sub-fraction was calculated theoretically using equation (2). The lower boiling fractions (<65 °C) of the hydrotreated product were not used to measure density and refractive index since the light compounds in these fractions could not be recovered in the liquid product after hydrotreatment. The densities and refractive indices of the remaining sub-fractions are listed in Table 4.7.

Table 4.7 Densities and refractive indices of the distilled sub-fractions at 20 °C

Cut number	Cracked naphtha		Hydrotreated product	
	Density kg/m ³	Refractive index n _D	Density kg/m ³	Refractive index n _D
1	528 ^a	-- ^b	-- ^c	-- ^b
2	533 ^a	-- ^b	-- ^c	-- ^b
3	551 ^a	-- ^b	-- ^c	-- ^b
4	656 ^a	-- ^b	-- ^c	-- ^b
5	666.60	1.3776	598 ^a	-- ^b
6	673.91	1.3845	616 ^a	-- ^b
7	688.43	1.3919	643.42	1.3946
8	701.93	1.3978	668.63	1.3977
9	716.21	1.4043	709.69	1.4035
10	733.36	1.4117	721.97	1.4109
11	743.50	1.4170	729.05	1.4159
12	753.88	1.4223	734.81	1.4210
13	765.30	1.4279	744.86	1.4269
14	775.05	1.4324	756.58	1.4317
15	783.97	1.4369	778.94	1.4357
16	794.11	1.4418	786.94	1.4407
17	806.16	1.4474	800.53	1.4453
18	815.98	1.4516	825.73	1.4491
19	845.40	1.4654	832.72	1.4618

- a – Calculated theoretically using equation (2), based on measured mass and volume of sample
- b – Reliable data could not be collected due to evaporation of volatile compounds during sample collection and preservation.
- c – Density could not be estimated theoretically since the amount of sample obtained in the respective sub-fractions was less than 1 mL.

4.4 Discussions

4.4.1 Boiling point distribution of cracked naphtha – Comparison of simulated distillation and atmospheric distillation

Simulated distillation is an analytical technique that works on the principle of gas chromatography to provide the boiling point distribution of petroleum and heavy oil samples. SimDis analysis uses a small quantity of the oil sample (~0.10 g) and processes the sample in less than 40 minutes. In comparison, physical distillation columns are more cumbersome to operate, require larger sample quantities and take much longer to operate. In this study, the distillation profile of cracked naphtha was obtained through both these methods, as shown in Figure 4.4. The distillation profiles by both these methods exhibited similar trends, but the boiling points in SimDis deviated by 30 °C on average, compared to those obtained by atmospheric distillation.

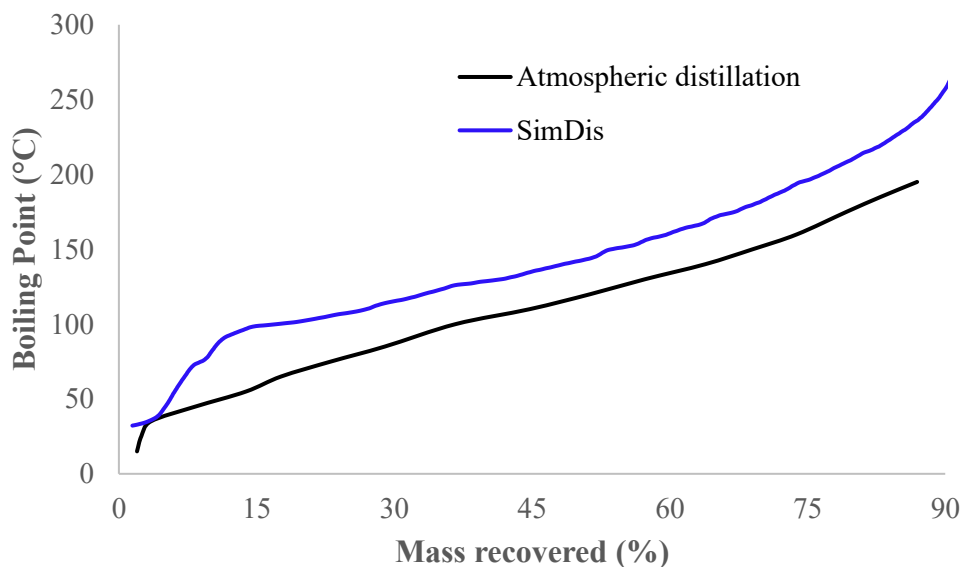


Figure 4.4 Atmospheric and Simulated distillation curves of thermally cracked naphtha

The SimDis analysis was done by following the standard method ASTM D7169-11.⁴ This method for High Temperature Simulated Distillation allowed for boiling point distribution in the temperature range of 36 – 720 °C, thus enabling analysis of samples containing C₅-C₁₂₀ compounds. However, the simulated distillation profile may not be representative of the true boiling points due to the following reasons:

- *Co-elution of light compounds:* The temperature program for gas chromatographic separation, described in section 4.2.4, enables elution of the solvent carbon disulfide at -20 °C. If the sample contains light compounds in the C₁-C₅ range, they co-elute with the solvent. This adversely impacts accurate retention time calibration for these compounds, resulting in a significant bias in boiling point measurement below 36 °C.
- *Deviating behavior of non-normal paraffins on stationary phase:* The retention time calibration for the SimDis analysis was done using Polywax® 655, which is a blend of polyethylene oligomers with a carbon number ranging from C₁₀ to C₁₁₀ in even-number increments.⁵ Thus, a boiling point distribution curve is prepared. Figure 4.5 shows the boiling point distribution based on the calibration standard that was used for the current analysis.

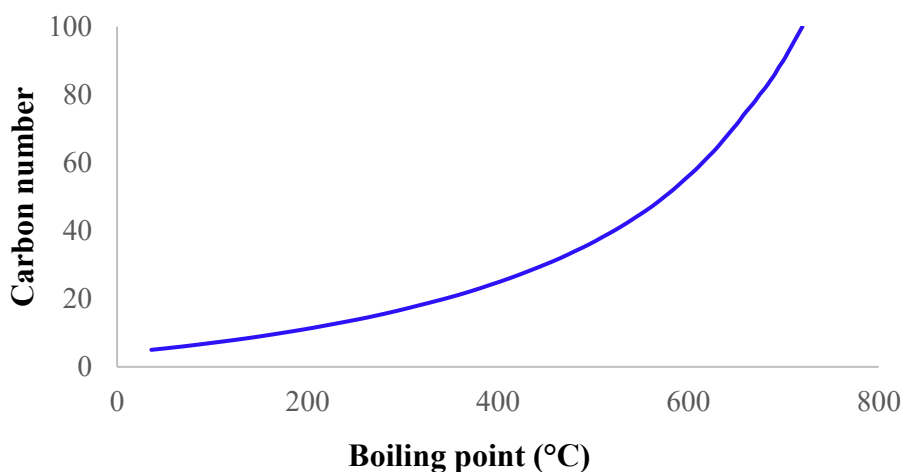


Figure 4.5 Boiling point distribution based on number of carbon atoms

When the sample mixture contains aromatic, heteroatomic and non-normal paraffinic compounds, a significant deviation from the calibration curve is usually observed. The deviation in the true boiling point is also dependent on the stationary phase of the

chromatographic column. Figure 4.6 shows the deviation of non-normal paraffins when the stationary phase is dimethylpolysiloxane, which was the material used for the current study.

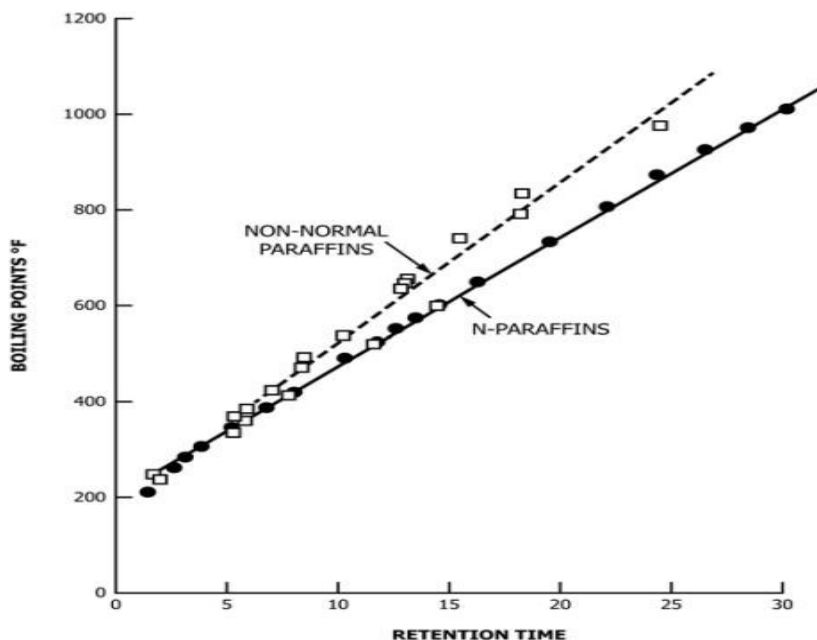


Figure 4.6 Boiling point deviation of non-normal paraffin compounds in methylpolysiloxane stationary phase ⁶

The sample of cracked naphtha used in the current study consisted of a significant proportion of non-paraffins including aromatics, naphthenic, olefinic and sulfur-containing compounds, which could have led to a positive deviation in the true boiling point measurements in the SimDis analysis.

Sub-fractionation of the sample mixture by atmospheric distillation was done using a spinning-band distillation column. The boiling point distribution curve was obtained based on the measured yields for the stipulated boiling cuts that were programmed for the column operation, as described in Table 4.6. Details regarding the composition of each sub-fraction is available in Appendix E. It was observed that each boiling cut had components with normal boiling points that differed widely from those of the distillation program. For instance, GC-MS analysis of the sub-fraction obtained for the boiling cut 75 – 85 °C showed the presence of compounds with normal boiling points in the range of -11°C (isobutane) in the lower end and 110 °C (toluene) in the higher end. This

indicated that the separation efficiency of the distillation column was poor. Some factors that influence separation efficiency of spinning band columns are discussed below:

- *Material of spinning band:* The spinning band column enhances vapor-liquid contact via helical rotation. The material of the spinning band influences separation efficiency. It was found that bands made of Teflon material had a greater efficiency than those made of metal or metal alloys.⁷ However, Teflon spinning bands cannot be used in columns that operate at temperatures above 225 °C due to material instability issues. The spinning band used in the current study was made of monel, a metal alloy, which could have lowered the separation efficiency.
- *Speed of spinning band:* The speed at which the spinning band rotates impacts the efficiency of the distillation operation. The separation efficiency increases on increasing the band speed, up to a critical speed beyond which it remains constant.⁸ In the current study, the speed of the band was a factor that could neither be controlled nor monitored. It is speculated that the spinning speed was not optimized for efficient separation.
- *Operating pressure:* The separation efficiency of the spinning band column decreases with decrease in the operating pressure.⁸ However, this factor is relevant only for operation at near vacuum conditions. Since the current separation was conducted at atmospheric pressure condition, it is not believed to have affected the efficiency.

In summary, the boiling point distribution curves obtained by both high temperature simulated distillation and atmospheric distillation do not show the true boiling points, but the similarity in the trends indicate that these methods can still be used to approximate the boiling nature of the complex mixture.

4.4.2 Effect of hydrotreatment on boiling point distribution of cracked naphtha

Thermally cracked naphtha is a mixture of numerous hydrocarbons including paraffins, aromatics, cycloparaffins, olefins and sulfur containing species. In principal, hydrogenation will result in the saturation of olefins (and saturation of aromatics at severe reaction conditions) as well as hydrodesulfurization. However, based on the behavior of the sulfided catalyst that was studied in chapter 3, it is reasonable to expect side reactions such as isomerization of olefins. A comparison of the properties of cracked naphtha before and after hydrotreatment is discussed below to understand the changes caused by hydrotreatment.

Based on the mass balance for hydrotreatment of cracked naphtha (Table 4.4), it was observed that approximately 19 wt% of the product could not be recovered in the liquid phase. This was because of migration of components in the product tank into the vapor-phase due to the phase equilibrium conditions established by high partial pressure of hydrogen gas. Based on VLE data simulation (Table 4.5), the yield loss mainly corresponded to loss of components from the cracked naphtha in the boiling range 0 – 120 °C. Consequently, the atmospheric distillation yields for lower boiling cuts were low, since the components were not retrieved in the liquid-phase from the product tank.

In order to obtain a distillation profile of the product that could be compared with cracked naphtha, theoretical distillation yields were obtained by considering the mass lost in the vapor-phase for each sub-fraction of the hydrotreated product. Table 4.8 gives the corrected distillation yields after accounting for mass loss.

Table 4.8 Theoretical distillation yields of hydrotreated product by accounting for the liquid yield lost due to migration to vapor-phase

Cut number	Hydrogenated product	
	Measured Yield (wt %)	Theoretical Yield (wt %)
1	0.37	3.54
2	0	0.00
3	0.09	0.63
4	0.19	0.97
5	0.57	2.33
6	0.79	2.57
7	1.22	3.17
8	4.02	6.84
9	8.46	11.03
10	7.58	8.59
11	8.55	8.16
12	10.08	8.30
13	7.74	6.24
14	6.86	5.37

Cut number	Hydrogenated product	
	Measured Yield (wt %)	Theoretical Yield (wt %)
15	6.37	4.98
16	7.02	5.49
17	5.01	3.92
18	3.94	3.08
19	18.91	14.79

The theoretical yields were used to obtain the boiling point distribution curve for the hydrotreated product, shown in Figure 4.7, in comparison with the boiling point distribution of cracked naphtha. By assuming that the separation efficiency of the distillation column was the same for both the distillation runs, it can be deduced that the boiling points of the components did not change by a large margin, post hydrotreatment.

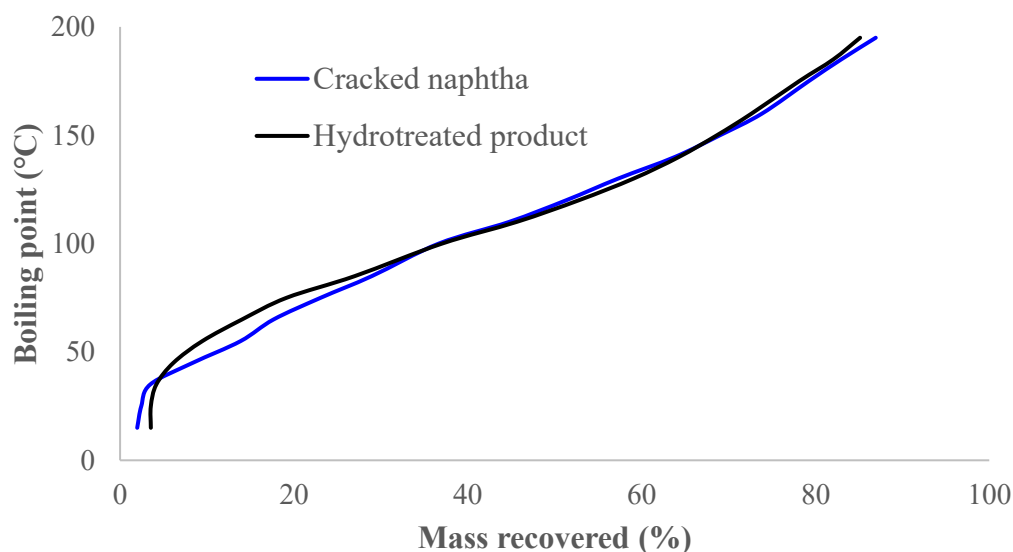


Figure 4.7 Boiling point distribution curves of cracked naphtha and hydrotreated product

4.4.3 Effect of hydrotreatment on density and refractive indices of sub-fractions

The densities and refractive indices of sub-fractions were measured at 20 °C (Refer to Table 4.7). It must be noted that the actual densities and refractive indices of sub-fractions boiling below 120

°C (i.e., fractions below cut number 11) were most likely lower than the measured values since the samples had lost the light components.

The densities and refractive indices of the sub-fractions decreased slightly after hydrotreatment. Density reduction in bitumen derived materials by thermal and chemical processes is most likely due to an increase in the H:C ratio and decrease in the nitrogen and sulfur contents.⁹ This was confirmed by results from elemental analysis of cracked naphtha and the hydrotreated product (Refer to table 4.1). It can thus be concluded that mild hydrotreatment of cracked naphtha resulted in an increase in the H:C ratio and reduction of sulfur. Further investigation on the effect of hydrotreatment on the individual species in cracked naphtha will be reported in the next chapter.

4.5 Conclusions

Cracked naphtha was hydrogenated over NiS/Al₂O₃ catalyst at 280 °C and 1 MPa. Cracked naphtha and the hydrogenated product were then distilled into 19 sub-fractions in a spinning band distillation column. The distillation profile of cracked naphtha by atmospheric distillation was compared with the boiling point distribution curve by SimDis analysis. The boiling distribution curves, densities and refractive indices of the various sub-fractions were used to evaluate the effect of hydrotreatment on the properties of cracked naphtha. The conclusions of the study are as follows:

- a) The conditions used for hydrotreatment of cracked naphtha resulted in about 19% mass loss in the liquid phase due to migration of components into the hydrogen-rich vapor phase. Based on VLE data, it was deduced that roughly 60 wt% of the components with boiling points 120 °C or lower migrated into the gas phase.
- b) The distillation curves of physical and simulated distillation showed similar trends, but the latter curve had an average positive deviation of 30 °C. The distillation profile obtained by both the methods was not reflective of the true boiling points of the compounds in the mixture but can be used to approximate the boiling nature of the complex mixture.
- c) The densities of the sub-fractions (except B.P 185 – 195 °C) decreased after hydrotreatment, indicating an increase in the H:C ratio and decrease in sulfur content of the cracked naphtha. The refractive indices of the sub-fractions also decreased after hydrotreatment.

4.6 References

- (1) Fahim, M. A. Crude Distillation. In *Fundamentals of Petroleum Refining*; Elsevier, 2010; pp 69–93.
- (2) Enbridge. *Enbridge Quality Pooling Specification Package*; Edmonton, 2019.
- (3) B/R Corporation. Comparison of Spinning Band Distillation with Packed Column Distillation http://www.solvent--recycling.com/spinning_band_packed_column.html (accessed Nov 29, 2019).
- (4) ASTM International. *ASTM D7169-11 Standard Test Method for Boiling Point Distribution of Samples with Residues Such as Crude Oils and Atmospheric and Vacuum Residues by High Temperature Gas Chromatography*; West Conshohocken, PA, 2015.
- (5) Subramanian, M.; Deo, M. D.; Hanson, F. V. Compositional Analysis of Bitumen and Bitumen-Derived Products. *J. Chromatogr. Sci.* **1996**, *34* (January), 20–26.
- (6) ASTM International. *ASTM D6352-15 Standard Test Method for Boiling Range Distribution of Petroleum Distillates in Boiling Range from 174 ° C to 700 ° C by Gas Chromatography*; West Conshohocken, PA, 2019.
- (7) Jones, F. S.; Nerheim, A. G. A Macro Spinning Band Distillation Column. *Anal. Chem.* **1959**, *31* (11), 1929.
- (8) King, P. J.; Yates, B. J. Spinning Band Columns. *Chem. Eng. Prog.* **1966**, *47* (5), 214–223.
- (9) Gray, M. R. Fundamentals of Partial Upgrading of Bitumen. *Energy and Fuels* **2019**, *33*, 6843–6856.

CHAPTER 5: CHARACTERIZATION OF CRACKED NAPHTHA TO IDENTIFY AND MEASURE CONCENTRATION OF OLEFINIC SPECIES

Abstract

Thermal cracking processes result in the formation of olefins. These olefins must be treated to improve the storage stability of the cracked product and to meet the regulatory specifications for transportation by pipelines which require the product to contain <1 wt% 1-decene equivalent olefins based on a proton nuclear magnetic resonance (^1H NMR) method of analysis. Determination of the nature and abundance of olefins provides knowledge that is needed to design reaction pathways and processes for treatment of olefins. Light petroleum product (boiling point 15 – 240 °C), i.e., cracked naphtha, from a thermal cracking unit (visbreaker) at a bitumen upgrader facility was characterized to identify and measure olefin concentration. The cracked naphtha was sub-fractionated into smaller boiling cuts and analyzed using gas chromatography with mass spectrometer (GC-MS) and flame ionization detector (GC-FID). The compound identification by GC-MS was verified for selected compounds with representative model compounds and by spiking sub-fractions. Identification of olefinic species was confirmed by subjecting the cracked naphtha to mild hydrotreatment and comparison of chromatograms before and after hydrotreatment. This was necessary because assignment of compound identity based solely on the suggestions of the Mass Spectral Library was unreliable for distinguishing between olefins and cycloparaffins with the same molecular formula. Quantification of species was done by evaluating typical FID response factors for various compound classes. Approximately 74 wt% of the compounds in cracked naphtha were identified out of which 13 wt% consisted of olefins mainly in the C₅-C₇ range. The nature of the olefinic species was also determined – straight chained (~6 wt%), branched olefins (~4 wt%), cyclic olefins (~3 wt%) and diolefins (~0.2 wt%).

5.1 Introduction

The BitumaxTM Process for bitumen partial upgrading employs a thermal cracking unit, i.e., a visbreaker, to aid in the production of a material that meets the viscosity and density specifications for pipeline transport without resorting to hydroprocessing. However, thermal cracking processes result in the formation of olefins (refer to table 1.1).¹ The pipeline specifications also require that the product must contain < 1 wt% 1-decene equivalent olefins based on a proton nuclear magnetic resonance (¹H NMR) method of analysis.² Thus, the cracked product from the visbreaking unit must undergo further treatment wherein the olefins in the lower boiling fraction (naphtha) react with aromatics in the higher boiling fraction (distillate) over an acid catalyst to form alkyl aromatics via a Friedel Crafts alkylation reaction.

Olefin-aromatic alkylation has been conventionally used in the petrochemical industry for production of mono-alkyl aromatics.^{3,4} However, the process feed for the BitumaxTM olefin treatment plant is vastly different from the clean feed that is used for the production of petrochemical alkyl-aromatics. In the case of the BitumaxTM process, the olefin to aromatic ratio of the feed is determined by the thermal cracking operation and cannot be independently controlled. Previous studies have also determined that thermally cracked naphtha sourced from oilsands bitumen contains potential catalyst poisons and inhibitors such as nitrogen bases and dienes.^{5,6} Additionally, there is a knowledge gap regarding the concentration and structure of olefinic species present in the cracked product.

The current study aims to investigate the nature and abundance of olefins that are present in thermally cracked naphtha (boiling point 15 – 240 °C), as a first step to improve the olefin-aromatic alkylation process for bitumen partial upgrading. The characterization studies are conducted using the sub-fractions of cracked naphtha and hydrotreated cracked naphtha, whose distillation profile, densities and refractive indices were detailed in the previous chapter. The compounds in the sub-fractions are separated by high resolution gas chromatography in a capillary column lined with polydimethylsiloxane as the stationary phase. The compounds were then identified by a mass spectroscopic detector, followed by verification of selected species using model compounds as well as hydrotreatment of cracked naphtha. The concentration of the identified species was determined using a flame ionization detector.

5.2 Experimental

5.2.1 Materials

The main materials used for this study were thermally cracked naphtha and hydrotreated product of the same cracked naphtha, whose properties have been listed in Table 4.1. The distilled sub-fractions of cracked naphtha and hydrotreated product were analyzed using GC-MS and GC-FID instruments. Helium was used as a carrier gas in the GC columns. Hydrogen and air were used for the FID detector. Pentane was used as a blank sample between each sample run. Several model compounds were used for retention time verification in GC-MS and for spiking the sub-fractions in GC-FID. All the compounds are listed in Table 5.1.

Table 5.1 Materials used for cracked naphtha characterization study

Compound	Formula	CASRN^a	Mass Fraction Purity^b	Supplier
<i>Chemicals</i>				
Pentane	C ₅ H ₁₂	109-66-0	0.99	Fisher Chemical
2-Methyl-2-butene	C ₅ H ₁₀	513-35-9	0.95	Sigma Aldrich
Cyclopentane	C ₅ H ₁₀	287-92-3	0.98	Acros Organics
1-Hexene	C ₆ H ₁₂	592-41-6	>0.99	Sigma
Thiophene	C ₄ H ₄ S	110-02-1	0.99	Sigma Aldrich
Cyclohexane	C ₆ H ₁₂	110-82-7	>0.99	Sigma Aldrich
1-Heptene	C ₇ H ₁₄	592-76-7	0.97	Sigma
Methyl-cyclohexane	C ₇ H ₁₄	108-87-2	>0.99	Sigma Aldrich
Tetrahydrothiophene	C ₄ H ₈ S	110-01-0	0.99	Sigma Aldrich
Cycloheptane	C ₇ H ₁₄	291-64-5	0.99	Acros Organics
1-Octene	C ₈ H ₁₆	111-66-0	>0.99	Acros Organics
Ethylbenzene	C ₈ H ₁₀	100-41-4	0.99	Alfa Aesar
<i>m</i> -Xylene	C ₈ H ₁₀	108-38-3	0.99	Acros Organics
<i>p</i> -Xylene	C ₈ H ₁₀	106-42-3	>0.99	Sigma
<i>o</i> -Xylene	C ₈ H ₁₀	95-47-6	>0.99	Sigma Aldrich
1-Nonene	C ₉ H ₁₈	124-11-8	Analytical standard	Sigma Aldrich

Compound	Formula	CASRN ^a	Mass Fraction Purity ^b	Supplier
Cyclooctane	C ₈ H ₁₆	292-64-8	>0.99	Alfa Aesar
Propylbenzene	C ₉ H ₁₂	103-65-1	>.99	Sigma Aldrich
1,2,4-Trimethylbenzene	C ₉ H ₁₂	95-63-6	0.98	Sigma Aldrich
2-Methyl-benzothiophene	C ₉ H ₈ S	1195-14-8	0.96	Sigma Aldrich
3-Methyl-benzothiophene	C ₉ H ₈ S	1455-18-1	0.96	Sigma Aldrich
<i>Gases</i>				
Hydrogen	H ₂	1333-74-0	0.99999 ^d	Praxair
Air	-	132259-10-0	- ^c	Praxair
Helium	He	132259-10-0	0.99999 ^d	Praxair

^a CASRN = Chemical Abstracts Services Registry Number

^b Purity of the material guaranteed by the supplier; material used without further purification

^c Mass fraction purity not specified

^d Mole fraction purity

5.2.2 Analyses

The gas chromatograph coupled with mass spectrometer (GC-MS) was used to identify the compounds present in the cracked naphtha sub-fractions. The device used was an Agilent 7820A gas chromatograph with a 5977E mass selective detector and a HP PONA capillary column with dimensions of 50 m x 0.2 mm x 0.5µm. The raw data was processed by the Agilent MassHunter software. Sub-fractions were analyzed without solvent dilution. A blank run using pentane as solvent was performed in between every fraction, in order to clean the column. The instrument method conditions were determined based on the recommended ASTM standard test methods – ASTM D5134-13 and ASTM D6733-01.^{7,8} Specific method conditions are detailed as follows:

- For the analysis of sub-fractions of cracked naphtha and hydrotreated product, instrument conditions were set to automatically inject 0.1 µL of sample through the inlet. The sample inlet cell was maintained at 250 °C. The split ratio was 1:100. Column carrier gas helium flowed through the column at 1 mL/min. The oven was kept at 35 °C for 30 min, then 2

°C/min to 200 °C for 0 min, then 10 °C/min to 300 °C for 7.5 min. The total run time for each sample was 130 min.

- For the blank run using pentane, instrument conditions were set to automatically inject 1 µL of sample through the inlet. The sample inlet cell was maintained at 250 °C. The split ratio was 1:100. Column carrier gas helium flowed through the column at 1 mL/min. The oven was kept at 100 °C for 0 min, then 10 °C/min to 300 °C for 0 min. The total run time for each sample was 20 min.
- Some model compounds were analyzed using GC-MS to verify the results of the NIST mass spectral search program to identify the correct compound. These samples were prepared by diluting 0.1 mL of model compound in 10 mL of pentane. Instrument conditions were set to automatically inject 1 µL of sample through the inlet. The sample inlet cell was maintained at 250 °C. The split ratio was 1:100. Column carrier gas helium flowed through the column at 1 mL/min. The oven was kept at 35 °C for 30 min, then 2 °C/min to 80 °C for 0 min, then 10 °C/min to 300 °C for 5.5 min. The total run time for each sample was 80 min. The detector was programmed to turn off between 4.7 to 5 minutes, to avoid solvent saturation. The analysis was done using a temperature program with a much shorter run time since the main objective was to verify that the suggestions by the NIST mass spectral search program based on the mass spectrum were reliable and consistent for compounds belonging to the various compound classes present in cracked naphtha. Hence, the verification was not based on the retention times but based on the mass spectra.

Gas chromatography with flame ionization detector (GC-FID) was used to quantify the species that were identified in the various sub-fractions of cracked naphtha. The device used for analysis was an Agilent 7890A GC-FID equipped with a HP PONA column (50 m x 0.2 mm x 0.5 µm). Raw data was processed by the Agilent ChemStation software. Sub-fractions were analyzed without solvent dilution. A blank run using pentane as solvent was performed in between every fraction, in order to clean the column. The method conditions for analysis of sub-fractions were like the corresponding method used for GC-MS analysis. Specific details are mentioned below:

- For the analysis of sub-fractions, 0.1 µL of sample was automatically injected through a split/splitless injector at 250 °C. The split ratio was 1:100. The sample was carried through

the GC column by helium which flowed at 1 mL/min. The temperature program of the oven was: 35 °C for 30 min, then 2 °C/min to 200 °C for 0 min, then 10 °C/min to 300 °C for 7.5 min. The total run time for each sample was 130 min. The FID had hydrogen gas flowing at 40 mL/min and air flowing at 400 mL/min. Samples of sub-fractions that were spiked with model compounds were also analyzed using the same method conditions.

- For the blank runs using pentane, 1 µL of sample was automatically injected through a split/splitless injector at 250 °C. The split ratio was 1:100. The sample was carried through the GC column by helium which flowed at 0.72 mL/min. The oven temperature was maintained at 300 °C for 15 min. The total run time for each sample was 15 min. The FID had hydrogen gas flowing at 40 mL/min and air flowing at 400 mL/min.

Quantification of various compounds present in the samples was done by using response factor of the specific compound class relative to *n*-octane (RRF). The determination of GC-FID relative response factors for various compounds has been explained in Appendix A. Table 5.2 lists the relative response factors that were used for this study. The formulae used to measure the concentration of various compounds in cracked naphtha are given below:

$$\text{Conc of compound in sub - fraction (wt\%)} = \frac{\text{Peak area of compound (\%)} \times \text{Conc of octane (wt\%)}}{\text{Area of octane} \times 100 \times \text{RRF}} \quad (1)$$

$$\text{Conc of compound in cracked naphtha (wt\%)} = \text{Conc of compound in sub - fraction (wt\%)} \times \text{Distillation yield of sub - fraction (wt\%)} \quad (2)$$

Table 5.2 Average response factors relative to *n*-octane for GC-FID

Compound class	RRF
Paraffins	0.99
Olefins	1.01
Aromatics	1.06
Cycloparaffins	1.01
S-compounds	0.74

5.3 Results

The results of the characterization study were obtained by analyzing the sub-fractions of cracked naphtha in GC-MS and GC-FID instruments. This section summarizes the important results of the analyses. For the purpose of clarity, the salient observations have been illustrated with a segment of the sub-fraction in the boiling range 85 – 100 °C. The lists of compounds that were identified and quantified in cracked naphtha are provided in Appendix E and Appendix F.

5.3.1 GC-MS compound identification

The sub-fractions of cracked naphtha were analyzed using GC-MS instrument as explained in section 5.2.2. The resulting chromatogram of each sub-fraction had several peaks, as illustrated in figure 5.1a. The mass spectrum for every peak was obtained using the NIST mass spectral search program for the NIST/EPA/NIH mass spectral library, version 2.0. Table 5.3 lists the MS library suggestions for the compounds that eluted between 14.2 to 17.2 minutes in the GC column. The list of all compounds that were assigned to the peaks in each sub-fraction of cracked naphtha is available in Appendix E.

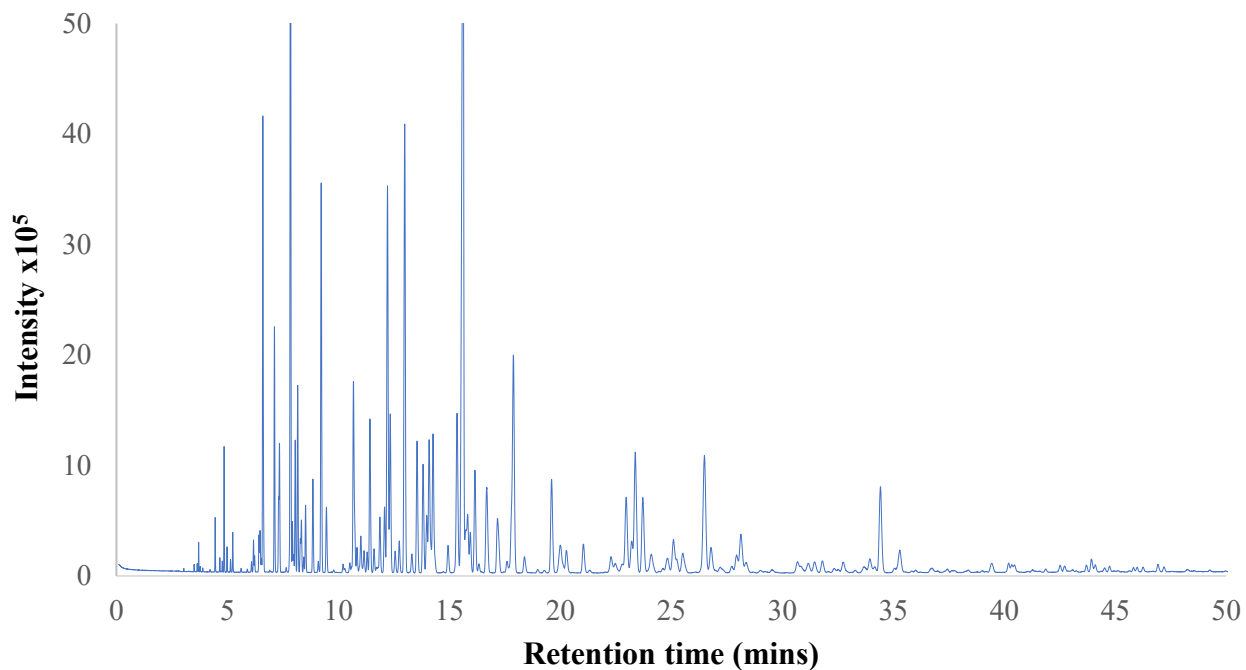


Figure 5.1a GC-MS chromatogram of cracked naphtha fraction (B.P 85 – 100 °C) up to 50 mins

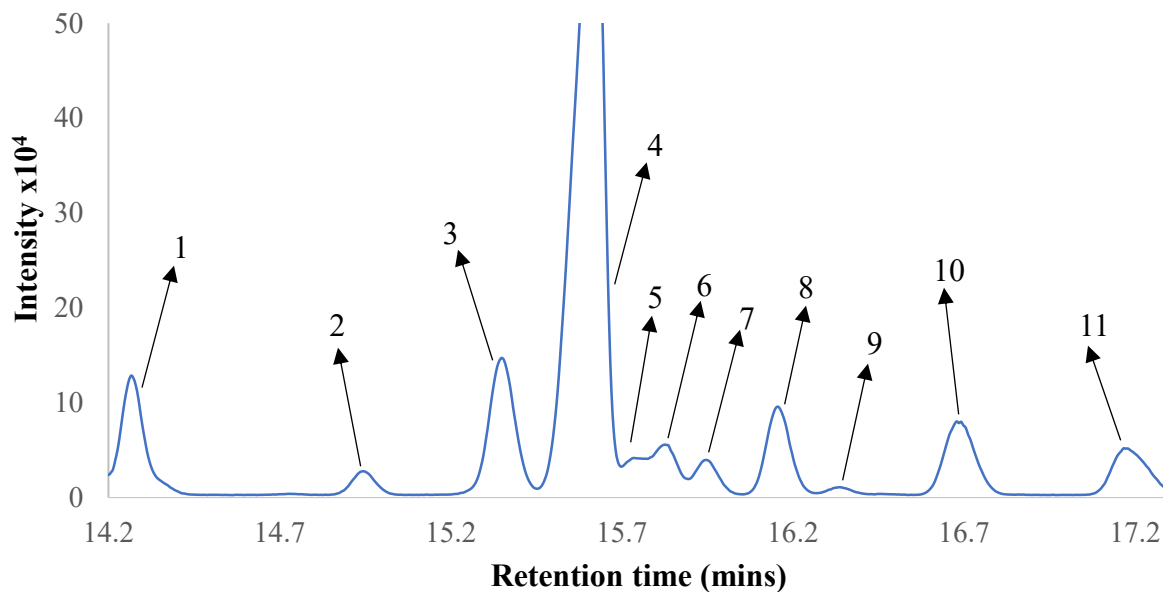


Figure 5.1b A segment of the above-mentioned chromatogram between 14.2 to 17.2 mins

Table 5.3 Compound suggestions given by the MS Library for peaks in figure 5.1b

Peak	Retention time (mins)	Compound suggestion	Probability (%)
1	14.267	1-heptene	28.7
2	14.942	3-methyl-3-hexene	27.4
3	15.343	3,3-dimethyl-1,4-pentadiene	17
4	15.59	<i>n</i> -heptane	70.1
5	15.73	2-heptene	35.6
6	15.831	3-heptene	18.8
7	15.951	3-methyl-3-hexene	17.9
8	16.158	3-heptene	20.3
9	16.24	- ^a	-
10	16.686	2-methyl-1-hexene	9.55
11	17.174	2-methyl-2-hexene	13.6

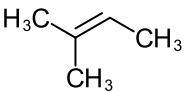
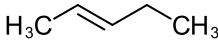


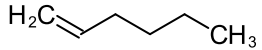
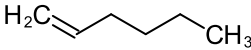
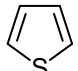
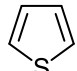
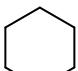
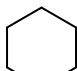
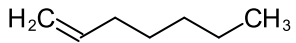
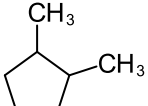
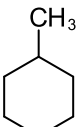
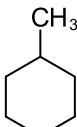


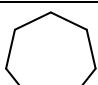
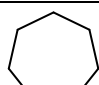
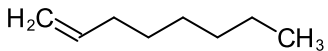
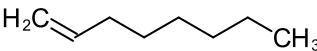
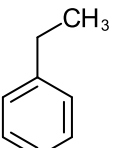
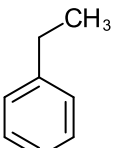
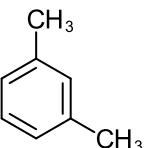
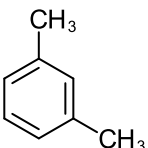
a – Unidentified mass spectrum

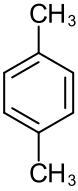
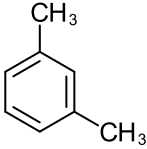
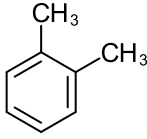
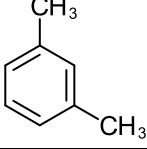
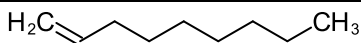
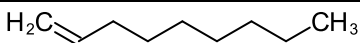
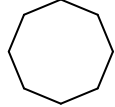
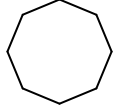
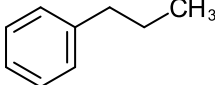
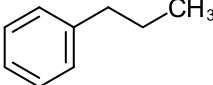
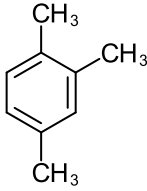
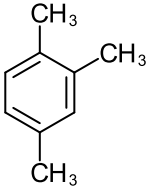
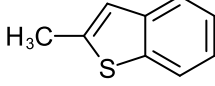
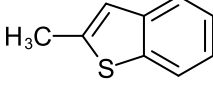
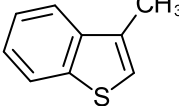
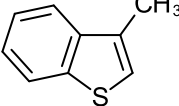
5.3.2 Compound verification with model compounds

The compound identification based on MS Library suggestions could be inaccurate, especially since isomers with the same molecular weight have identical mass spectra. 20 model compounds were chosen to verify the ability of the MS Library software to identify the compound correctly. In this regard, 1 % v/v solutions of various model compounds in pentane were analyzed in the GC-MS instrument as described in section 5.2.2. Outcome of the analysis is listed in Table 5.4.

Among the model compounds, 3 of the 5 olefins were correctly identified, while 2-methyl-2-butene was identified as *trans*-2-pentene and 1-heptene as 1-2-dimethyl-cyclopentane. Aromatics were correctly identified except for *p*-xylene and *o*-xylene. These results indicated that the instrument could not effectively differentiate between structural isomers. However, when the compounds were not identified correctly in the first suggestion, the subsequent suggestions identified the compound with a lower probability. All cycloparaffins and thiophenes were correctly identified. Based on these results, it was evident that the structural identity of olefinic isomers could not be confirmed based solely on the MS Library suggestions.

Table 5.4 Verification of MS Library suggestions with model compounds

Model Compound	MS library suggestion	Probability%
		17.7
		57.7
		23
		98.8
		73.8
		20.9
		72.9
		86.4
		50.8
		17.6
		62.2
		38.4

Model Compound	MS library suggestion	Probability%
		37.6
		34.7
		25.2
		38.4
		75.6
		22.9
		62.7
		29.1

5.3.3 Verification of compounds by hydrotreatment

In order to differentiate between olefins, diolefins and cycloparaffins, the cracked naphtha was subjected to mild hydrotreatment as described in section 4.2.1. The hydrotreated product was analyzed using GC-MS as described in section 5.2.2. All the compounds that were earlier identified as olefins, diolefins and cycloparaffins were compared before and after hydrogenation. The compounds that underwent a change after hydrotreatment exhibited variations in the peak area, due to change in concentration. The peak area of terminal olefins decreased, the areas of internal olefins increased due to isomerization of terminal olefins whereas cycloparaffins did not react. The

compounds in Appendix E were updated based on this verification step. More details about the identification of nature of olefinic species is discussed in section 5.4.1

5.3.4 Verification of compounds by spiking sub-fractions

Sub-fractions were spiked with specific model compounds, as listed in table 5.5, and analyzed using the GC-FID instrument. The analysis was an additional investigation to verify the peak identification of the selected compounds. All the spiked samples showed a noticeable increase in the height and area of the peaks that was assigned to the corresponding model compounds. Figure 5.2 illustrates this by showing a comparison of GC-FID chromatograms for the sub-fraction in the boiling range 85 – 100 °C that was spiked with 1-heptene.

Table 5.5 Model compounds chosen for spiking sub-fractions of cracked naphtha

Sub-fraction	Open temperature °C	Close temperature °C	Model compounds used for spiking
2	15	25	cyclopentane
3	25	35	1-hexene, cyclohexane
4	35	45	methyl-cyclohexane
5	45	55	thiophene
9	85	100	1-heptene
10	100	110	<i>m</i> -xylene, <i>o</i> -xylene, ethyl-benzene
13	130	140	1-nonene
14	140	150	propyl-benzene, 1,2,4-trimethylbenzene

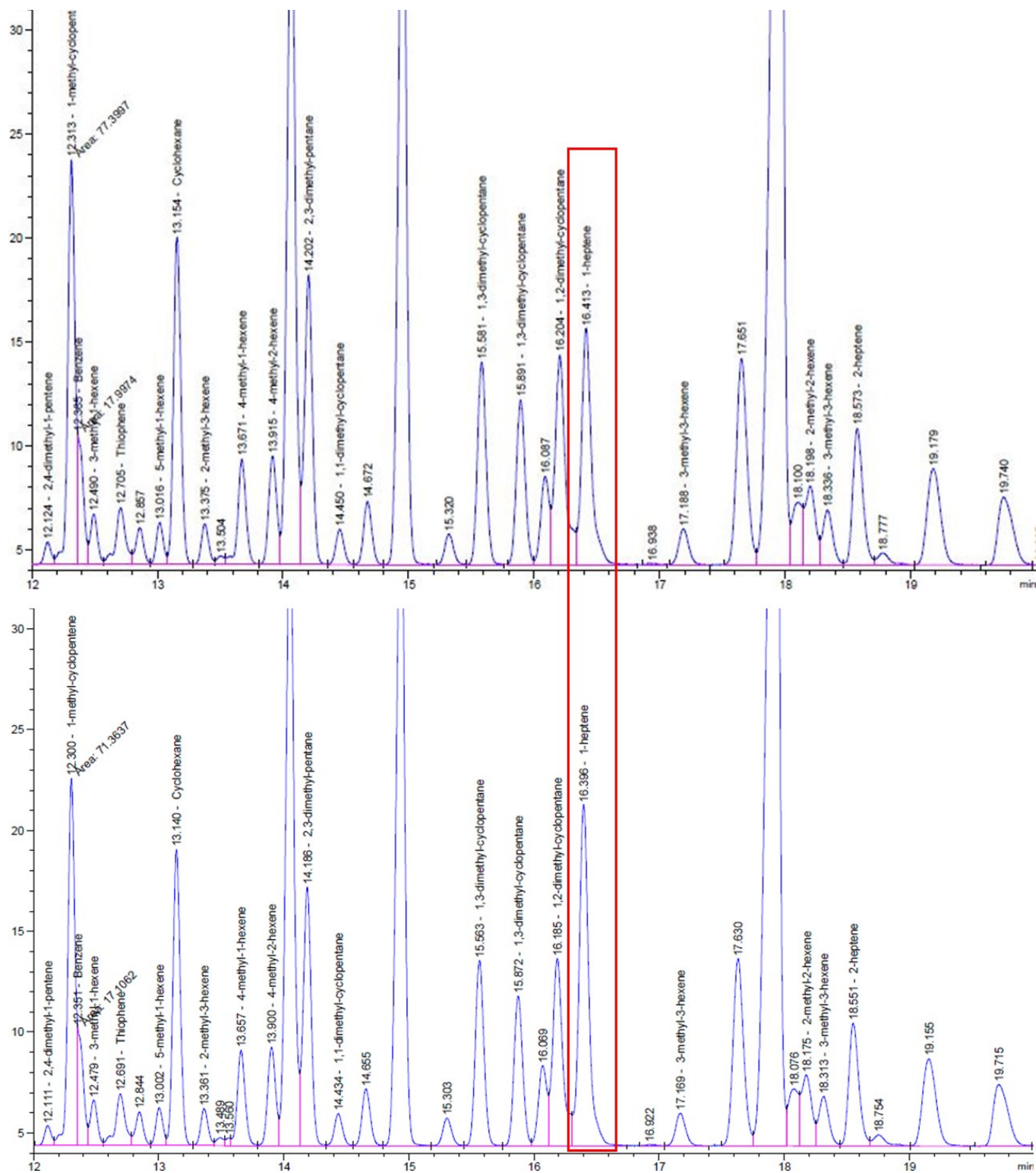


Figure 5.2 GC-FID chromatograms of a sub-fraction showing increase in the peak area after spiking with 1-heptene

5.3.5 Concentration of various compound classes in cracked naphtha

All the compounds that were identified in the sub-fractions were quantified by GC-FID, based on the areas of the peaks and the relative response factors for the respective compound classes shown in Table 5.2. The concentration of each compound was calculated as a fraction in cracked naphtha (wt%), using equations 1 and 2. The complete list of compounds and their concentrations is available in Appendix F. Table 5.6 lists all the olefins that were present in cracked naphtha, with their concentrations expressed as a weight fraction of the total cracked naphtha sample.

Table 5.6 Concentration of olefinic compounds in cracked naphtha

Carbon atoms	Compound	wt%	Compound	wt%
4	2-butene	0.36	2-methyl-1-propene	0.16
	2-pentene	0.99	1-methylidene-cyclobutane	0.46
5	3-methyl-1-butene	0.09	cyclopentene	0.13
	2-methyl-1-butene	0.37		
6	1-hexene	0.68	2-methyl-1-pentene	0.30
	3-hexene	0.27	2-methyl-2-pentene	0.70
	2-hexene	0.76	3-methyl-2-pentene	0.52
	4-methyl-1-pentene	0.25	3-methyl-cyclopentene	0.72
	3-methyl-1-pentene	0.11	ethylidene-cyclobutane	0.11
	4-methyl-2-pentene	0.07		
7	1-heptene	0.58	4-methyl-2-hexene	0.21
	3-heptene	0.58	3-methyl-3-hexene	0.23
	2-heptene	0.40	2-methyl-2-hexene	0.22
	2,3-dimethyl-2-pentene	0.03	3-methyl-2-hexene	0.37
	3-ethyl-2-pentene	0.07	3-ethyl-cyclopentene	0.04
	5-methyl-1-hexene	0.06	ethylidene-cyclopentene	0.20
	2-methyl-3-hexene	0.06	ethyl-methyl-cyclopentene	0.18
	4-methyl-1-hexene	0.18	ethylidene-cyclopentane	0.11
8	1-octene	0.22	1-ethyl-5-methyl-cyclopentene	0.24
	3-octene	0.15	1,3-dimethyl-cyclohexene	0.40
	4-methyl-2-heptene	0.04	3-(1-methylethyl)-cyclohexene	0.07
	6-methyl-2-heptene	0.11		
9	1-nonene	0.34	2,6-dimethyl-1-heptene	0.17
	4-nonene	0.14	2,6-dimethyl-3-heptene	0.14
	2-nonene	0.15		
11	1-undecene	0.09		

Table 5.7 summarizes the concentration of all the compound classes that were identified in cracked naphtha. Of the 74 wt% of species that were identified, 13 wt% of cracked naphtha was found to be made up of olefinic species that require to be treated further in order to meet the pipeline specifications, listed in table 1.1. A significant proportion (~10 wt%) of the compounds that could not be identified were in the sub-fractions with boiling points above 160 °C.

Table 5.7 Summary of various compound classes identified in cracked naphtha

Compound class	wt%
Paraffins	40
Olefins	13
Cycloparaffins	12
Aromatics	4
S compounds	5
Not identified	26

5.4 Discussion

5.4.1 Verification of nature of identified olefins

The identification of compounds using GC-MS is done by generation of an electron impact mass spectrum by the mass spectroscopic detector, followed by assignment of a molecular formula by comparing the mass spectrum to those available in the MS Library software. This method is not highly reliable, mainly due to the identical nature of mass spectra of isomeric compounds. GC-MS analysis of model compounds showed that the MS Library suggestions were particularly unreliable for the identification of olefinic isomers (refer to table 5.2). For the current study, two additional techniques were used to confirm the position and geometry of the double bonds in compounds that were identified as olefins by the GC-MS library in the first pass.

Firstly, the cracked naphtha underwent mild hydrotreatment. The hydrogenation study using model compounds discussed in chapter 3 found that hydrotreatment of terminal olefins over NiS/Al₂O₃ resulted in conversion of terminal olefins to form internal olefins and the corresponding saturated alkane. The comparison of GC chromatograms before and after hydrotreatment of cracked naphtha showed that the GC chromatogram peaks of terminal olefins had diminished. However, the same could not be said with certainty about the other olefinic species.

The internal and branched olefins exhibited little to no change after hydrotreatment, possibly due to the low activity of the sulfided catalyst. The identity of branched olefins was thus assigned by calculating a parameter known as Kováts retention index. The retention index converts the retention times of the eluted peaks into system independent constants, by normalizing the retention time to that of adjacently eluting *n*-alkanes. The isothermal retention index of any organic compound can be measured based on its solubility in the stationary phase and the pure liquid vapor pressure at the given temperature. When the GC is operated with a linear temperature program, the non-isothermal retention index is measured by a formula defined by Van Den Dool and Kratz⁹:

$$I_x = 100 \times \left(n + \frac{(t_x - t_n)}{(t_{n+1} - t_n)} \right) \quad (3)$$

where, I_x – Non-isothermal retention index of compound *x*

t_x – Retention time of compound *x*

t_n – Retention time of reference *n*-alkane eluting immediately before *x*

t_{n+1} – Retention time of reference *n*-alkane eluting immediately after *x*

The database of non-isothermal retention indices for numerous organic compounds eluting in polydimethylsiloxane capillary column (the stationary phase of the current study) have been reported in literature.^{10,11} It must be noted that for a given stationary phase, the absolute values of retention indices reported in literature show slight deviations due to variations in the temperature program used for GC analyses. Yet, the retention indices provide a fair idea about the order of elution of individual compounds in complex organic mixtures.

Figure 5.3 illustrates a section of the GC chromatogram (between 14.2 to 17.2 minutes) of cracked naphtha before and after hydrotreatment. Table 5.8 summarizes the details of each peak including the MS library suggestions and assigned identity. The non-isothermal retention indices were calculated using equation (3) and compared with the values reported in literature. The GC temperature program of the study cited was 30 to 200 °C at 1 °C/min leading to slight deviations in the absolute values of the retention indices obtained in the current study.

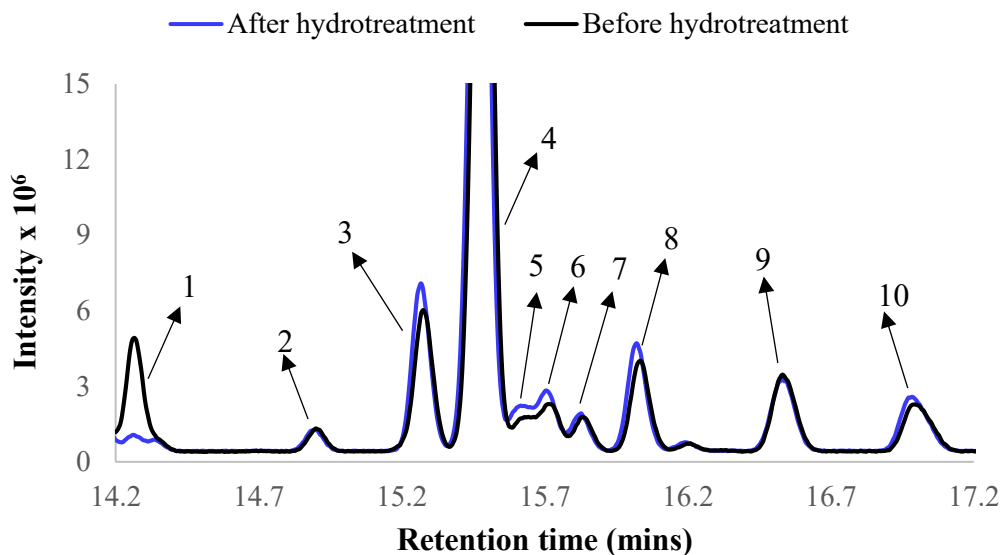


Figure 5.3 GC-MS chromatograms of cracked naphtha before and after hydrotreatment – segments with retention time 14.2 to 17.2 minutes

Table 5.8 Assignment of compounds based on effect of hydrotreatment and retention indices

Peak	MS Library suggestion	Assigned identity	Non – isothermal retention index	
			Measured	Literature ¹⁰
1	1-heptene	1-heptene	683.2	689.3
2	3-methyl-3-hexene	3-methyl-3-hexene	692.0	695.1
3	3,3-dimethyl-1,4-pentadiene	<i>trans</i> -3-heptene	697.0	697.9
4	<i>n</i> -heptane	<i>n</i> -heptane	700.0	700.0
5	2-heptene	<i>cis</i> -3-heptene	700.8	701.6
6	3-heptene	<i>trans</i> -2-heptene	701.3	705.0
7	3-methyl-3-hexene	2,3-dimethyl-2-pentene	701.9	707.6
8	3-heptene	3-ethyl-2-pentene	702.9	709.2
9	2-methyl-2-hexene	3-methyl-2-hexene	705.6	710.9
10	2-methyl-1-hexene	<i>cis</i> -2-heptene	708.3	714.4

The area of the peak 1, initially identified as 1-heptene, diminished after hydrotreatment due to conversion into internal isomers of heptane and *n*-heptane. Thus, the structural identity of peak 1 was assigned as 1-heptene.

There was an apparent increase in the areas of peaks 3,5,6,8 and 10 after hydrotreatment. 4 of these peaks are potential internal isomers of heptene. The structural identity of these peaks was assigned by comparison of measured non-isothermal retention indices with those of various C₇ olefins reported in literature.

Peaks 2,7 and 9 did not change after hydrotreatment. Based on the electron impact mass spectrum of these peaks, all the compounds had molecular formula C₇H₁₄. The structural identity of these peaks was assigned by comparison of measured retention indices with those of olefins and cycloparaffins having this molecular formula reported in literature.

5.4.2 Implications for BitumaxTM partial upgrading process

The current study estimated that about 13 wt% of cracked naphtha was made up of olefinic compounds. Table 5.9 gives a breakdown of the nature and abundance of the olefinic species. It was seen that most of the olefins were in the C₅-C₇ range. With regards to the structure, the distribution was straight-chained olefins > branched olefins > cyclic olefins.

Table 5.9 Nature and concentration of olefinic species identified in cracked naphtha

Carbon atoms	Type of olefin (wt%)			Total
	Straight	Branched	Cyclic	
C ₄	0.36	0.16	-	0.51
C ₅	0.99	0.46	0.59	2.05
C ₆	1.71	1.95	0.83	4.48
C ₇	1.56	1.40	0.53	3.50
C ₈	0.37	0.16	0.72	1.24
C ₉	0.63	0.31	-	0.94
C ₁₁	0.09	-	-	0.09
Total (wt%)	5.71	4.43	2.67	12.82

The olefin treatment unit aims to employ Friedel-Crafts olefin aromatic alkylation to convert the olefins in cracked naphtha into alkyl aromatic species. This reaction, catalyzed by an acid catalyst, occurs via formation of a carbonium ion intermediate by the protonation of the olefinic double bond.¹² The reactive intermediate then interacts with the aromatic species in the distillate fraction

from the thermal cracker. Apart from the mole ratios of the reacting species, the overall conversions and product distribution of the alkylation reaction are influenced by the reactivity of the alkylating species and the nature of substituents on the aromatic compounds.

Terminal olefins in the cracked naphtha are expected to undergo a hydride shift to form secondary arylalkanes, like alkylation products of internal *n*-olefins. Branched olefins are more reactive than straight chained olefins since they can form more stable tertiary carbonium ion intermediates, leading to addition of *t*-alkyl substituents to the aromatic rings. However, unlike the case of alkylation with short chained *n*-olefins, steric considerations play a huge role in determining the alkylation ability of branched olefins.¹² If the aromatic compounds in the cracked feedstock are heavily substituted prior to alkylation, the resulting steric hindrances would adversely affect the alkylation of branched olefins and cyclic olefins. It is thus important to investigate the nature and concentration of aromatic species in the distillation fraction in order to decide the severity of reaction conditions needed to achieve conversion of olefins to meet the pipeline specifications (refer to table 1.1).

5.5 Conclusions

The current study aimed to characterize the nature and concentration of olefins in thermally cracked naphtha sourced from a bitumen upgrader facility in Alberta, Canada. Sub-fractions of the cracked naphtha sample as well as hydrotreated product of the same cracked naphtha were used for the analyses using GC-MS and GC-FID. The conclusions of the study are as follows:

- a) Identification of species in cracked naphtha was done using GC-MS analyses. The nature of the identified olefinic species was determined by comparison of chromatograms before and after mild hydrotreatment coupled with comparison of non-isothermal retention indices with the values reported in literature, when such data was available.
- b) The concentration of the species was calculated by evaluating average FID response factors for various compound classes identified in the cracked naphtha sample. Approximately 74 wt% of compounds in cracked naphtha were identified. The concentration of various compound classes was estimated – 40 wt% paraffins, 13 wt%

olefins, 12 wt% cycloparaffins, 4 wt% aromatic compounds and 5 wt% sulfur compounds.

- c) Most of the identified olefins were in the C₅-C₇ range. The nature of the identified olefins was: straight chained (~6 wt%), branched olefins (~4 wt%), cyclic olefins (~3 wt%) and diolefins (~0.2 wt%).

5.6 References

- (1) Raseev, S. *Thermal and Catalytic Processes in Petroleum Refining*; Marcel Dekker, Inc: New York, 2003.
- (2) Enbridge. *Enbridge Quality Pooling Specification Package*; Edmonton, 2019.
- (3) Ingallina, P.; Perego, C. Recent Advances in the Industrial Alkylation of Aromatics: New Catalysts and New Processes. *Catal. Today* **2002**, *73*, 3–22.
- (4) Degnan, T. F.; Smith, C. M.; Venkat, C. R. Alkylation of Aromatics with Ethylene and Propylene: Recent Developments in Commercial Processes. *Appl. Catal. A Gen.* **2001**, *221*, 283–294.
- (5) Rao, Y.; De Klerk, A. Characterization of Heteroatom-Containing Compounds in Thermally Cracked Naphtha from Oilsands Bitumen. *Energy and Fuels* **2017**, *31* (9), 9247–9254.
- (6) Paez Cardenas, Y. Identification, Conversion and Reactivity of Diolefins in Thermally Cracked Naphtha, MSc Thesis, University of Alberta, 2016.
- (7) ASTM International. *ASTM D5134-13 Standard Test Method for Detailed Analysis of Petroleum Naphthas through n-Nonane by Capillary Gas Chromatography*; West Conshohocken, PA, 2017.
- (8) ASTM International. *ASTM D6733-01(2016), Standard Test Method for Determination of*

Individual Components in Spark Ignition Engine Fuels by 50-Metre Capillary High Resolution Gas Chromatography; West Conshohocken, PA, 2016.

- (9) Van Den Dool, H.; Kratz, P. D. A Generalization of the Retention Index System Including Linear Temperature Programmed Gas-Liquid Partition Chromatography. *J. Chromatogr.* **1963**, No. 2, 463–471.
- (10) Soják, L.; Addová, G.; Kubinec, R.; Kraus, A.; Hu, G. Gas Chromatographic-Mass Spectrometric Characterization of All Acyclic C5-C7 Alkenes from Fluid Catalytic Cracked Gasoline Using Polydimethylsiloxane and Squalane Stationary Phases. *J. Chromatogr. A* **2002**, 947 (1), 103–117.
- (11) White, C. M.; Hackett, J.; Anderson, R. R.; Kail, S.; Spock, P. S. Linear Temperature Programmed Retention Indices of Gasoline Range Hydrocarbons and Chlorinated Hydrocarbons on Cross-linked Polydimethylsiloxane. *J. High Resolut. Chromatogr.* **1992**, 15 (2), 105–120.
- (12) Patinkin, S. H.; Friedman, B. S. Alkylation of Aromatics with Alkenes and Alkanes. In *Friedel-Crafts and Related Reactions; Volume 2; Part 1*; Olah, G. A., Ed.; Interscience Publishers: New York, 1963; pp 30–31.

CHAPTER 6 – CONCLUSIONS

6.1 Conclusions

The first goal of this thesis project was to determine the nature of the olefins (such as number of carbon-atoms, position of the double-bonds and skeletal structure i.e., linear, branched or cyclic) and the concentration of olefins (in wt%) in thermally cracked naphtha, in order to better understand the feed of the olefin treatment unit for bitumen partial upgrading. Characterization studies were done using gas chromatographic analyses, aided by sub-fractionation and hydrotreatment of the cracked naphtha.

The second objective was to gain a better understanding of the effect of reaction temperature and catalyst sulfiding on olefin conversions and reaction selectivity in a Ni/Al₂O₃ catalytic system. The results from the lab-scale catalytic study complemented the characterization of olefins in cracked naphtha by helping to establish the reaction conditions for hydrotreatment of cracked naphtha.

The main conclusions drawn from the current research are listed below:

- a) Reduced Ni/Al₂O₃ catalyst was very active for hydrogenation of olefins and aromatic compounds in the absence of sulfur compounds in the feed. Near complete conversions were seen for 1-hexene to *n*-hexane at 80 °C and for toluene to methylcyclohexane at 160 °C.
- b) Reaction studies over sulfided Ni/Al₂O₃ revealed that to achieve better than 20% conversion of 1-hexene to *n*-hexane required temperatures above 200 °C, indicating that the hydrogenation activity of the sulfided catalyst was decreased after sulfidation. The reaction products at lower temperatures predominantly consisted of internal isomers of 1-hexene and less than 15% of *n*-hexane. Selectivity towards formation of *n*-hexane increased with increasing the reaction temperature, with the onset of skeletal isomerization of 1-hexene detected at temperatures above 240 °C. Hydrogenation of toluene was not detected even at 280 °C.
- c) Identification of species in cracked naphtha was done via GC-MS analyses. The identification of olefinic species was checked by comparison of chromatograms before and after mild hydrotreatment coupled with comparison of non-isothermal retention indices with the values reported in literature, when such data was available. The concentration of

the species was calculated by evaluating average FID response factors for various compound classes identified in the cracked naphtha sample. Approximately 74 wt% of compounds in cracked naphtha were identified. The concentration of various compound classes was estimated – 40 wt% paraffins, 13 wt% olefins, 12 wt% cycloparaffins, 4 wt% aromatic compounds and 5 wt% sulfur compounds.

- d) Most of the identified olefins were in the C₅-C₇ range. The nature of the identified olefins was: straight chained (~6 wt%), branched olefins (~4 wt%), cyclic olefins (~3 wt%) and diolefins (~0.2 wt%). Process conditions and catalysts for olefin treatment at bitumen partial upgrading technologies (such as BituMax™ olefin-aromatic alkylation process) should be selected enable conversion of these olefins to meet the olefin pipeline specifications.
- e) The current study estimated the nature and abundance of olefins in the naphtha fraction (Boiling Point 15 °C – 240 °C) of thermally cracked material that was obtained from bitumen. About 26 wt% of compounds in the cracked mixture could not be identified due to analytical limitations.

6.2 Future work

It would be of use to conduct a similar characterization study to estimate the nature and abundance of aromatic species in the higher boiling distillate fraction (Boiling Point 180 °C – 350 °C). Establishing the nature of olefinic and aromatic species in the complex feed mixture would help conduct reaction and catalyst deactivation studies using model compounds. Such studies will help develop a provide a better fundamental understanding of the olefin-aromatic alkylation over amorphous silica-alumina that have specific application and value in the olefins treating unit of the BituMax™ process.

BIBLIOGRAPHY

- Agilent Technologies Inc. Application specific GC-columns - HP-PONA Columns <https://www.agilent.com/en/product/gc-columns/application-specific-gc-columns/hp-pona-columns> (accessed Dec 15, 2019).
- Ali, S. A. Thermodynamic Aspects of Aromatic Hydrogenation. *Pet. Sci. Technol.* **2007**, *25* (10), 1293–1304.
- Anderson, J.; McAllsiter, S. H.; Derr, E. L.; Peterson, W. H. Diolefins in Alkylation Feedstocks - Conversion to Monoolefins by Selective Hydrogenation. *Ind. Eng. Chem.* **1948**, *40*, 2295–2301.
- ASTM International. *ASTM D5134-13 Standard Test Method for Detailed Analysis of Petroleum Naphthas through n-Nonane by Capillary Gas Chromatography*; West Conshohocken, PA, 2017.
- ASTM International. *ASTM D6733-01(2016), Standard Test Method for Determination of Individual Components in Spark Ignition Engine Fuels by 50-Metre Capillary High-Resolution Gas Chromatography*; West Conshohocken, PA, 2016.
- ASTM International. *ASTM D6352-15 Standard Test Method for Boiling Range Distribution of Petroleum Distillates in Boiling Range from 174 ° C to 700 ° C by Gas Chromatography*; West Conshohocken, PA, 2019.
- ASTM International. *ASTM D7169-11 Standard Test Method for Boiling Point Distribution of Samples with Residues Such as Crude Oils and Atmospheric and Vacuum Residues by High Temperature Gas Chromatography*; West Conshohocken, PA, 2015.
- B/R Corporation. Comparison of Spinning Band Distillation with Packed Column Distillation http://www.solvent--recycling.com/spinning_band_packed_column.html (accessed Nov 29, 2019).
- Barr, F.; Keyes, D. B. Equilibria in a Chemical System Hydrogen Sulfide-Propylene—Isopropyl Mercaptan-Propyl Mercaptan. *Ind. Eng. Chem.* **1934**, *26* (10), 1111–1114.
- Bartholomew, C. H. Mechanisms of Nickel Catalyst Poisoning. In *Catalyst Deactivation*; Delmon, B., Froment, G. F., Eds.; Elsevier Science Publishers B.V.: Amsterdam, 1987; pp 81–104.
- Bond, G. C. *Catalysis by Metals*; London Academic Press: London, 1962.
- Bond, G. C. *Metal-Catalysed Reactions of Hydrocarbons*, 1st ed.; Springer US, 2005.

- Cady, W. E.; Marschner, R. F.; Cropper, W. P. Composition of Virgin, Thermal, and Catalytic Naphthas from Mid-Continent Petroleum. *Ind. Eng. Chem.* **1952**, *44* (8), 1859–1864.
- Criterion Catalysts. *Hydrotreating Catalyst In-Situ Presulphiding Guidelines - Liquid Phase (Preferred Method) - Gas Phase (Alternative Method)*; Calgary, 2005.
- De Klerk, A. *Annual Report 2016-2017 (Year 1), Progress Report on Industrial Research Chair Program Issued to NSERC, Nexen Energy ULC, and Alberta Innovates*; Edmonton, 2017.
- De Klerk, A.; Zerpa Reques, N.; Xia, Y.; Omer, A. A. Integrated Central Processing Facility (CFU) in Oil Field Upgrading (OFU). Canada Patent 20140138287, 2014.
- Degnan, T. F.; Smith, C. M.; Venkat, C. R. Alkylation of Aromatics with Ethylene and Propylene: Recent Developments in Commercial Processes. *Appl. Catal. A Gen.* **2001**, *221*, 283–294.
- Eberhardt, N. A.; Guan, H. Nickel Hydride Complexes. *Chem. Rev.* **2016**, *116* (15), 8373–8426.
- Enbridge. *Enbridge Quality Pooling Specification Package*; Edmonton, 2019.
- Fahim, M. A. Crude Distillation. In *Fundamentals of Petroleum Refining*; Elsevier, 2010; pp 69–93.
- Garner, F. R.; Iverson, R. L. How Ethylbenzene Is Made. 1. By the High-Pressure Process. *Oil Gas J.* **1954**, *53* (25), 86–88.
- Gieseman, J.; Keesom, W. *Bitumen Partial Upgrading 2018 Whitepaper AM0401A*; Calgary, 2018.
- Gray, M. R. Fundamentals of Partial Upgrading of Bitumen. *Energy and Fuels* **2019**, *33*, 6843–6856.
- Gray, M. R. *Upgrading Oilsands Bitumen and Heavy Oil*; Pica Pica Press: Edmonton, 2015.
- Gray, M. R.; Mccaffrey, W. C. Role of Chain Reactions and Olefin Formation in Cracking, Hydroconversion, and Coking of Petroleum and Bitumen Fractions. **2002**, *16* (7), 756–766.
- Green, K. P.; Jackson, T. Pipelines are the safest way to transport oil and gas <https://www.fraserinstitute.org/article/pipelines-are-safest-way-transport-oil-and-gas> (accessed Dec 15, 2019).
- Hirota, K.; Teratani, S.; Yoshida, N.; Kitayama, T. On the Hyperfine Reaction Deuterium with Distribution Deuterium of the Catalytic Powders of Propene on Copper. *J. Catal.* **1969**, *13* (3), 306–315.

- Ingallina, P.; Perego, C. Recent Advances in the Industrial Alkylation of Aromatics: New Catalysts and New Processes. *Catal. Today* **2002**, *73*, 3–22.
- Ipatieff, V. N.; Grosse, A. V. Alkylation of Aromatic Compounds with Olefins in the Presence of Boron Fluoride. *J. Am. Chem. Soc.* **1936**, *58*, 233–239.
- Ipatieff, V. N.; Schmerling, L. Ethylation of Benzene in the Presence of Solid Phosphoric Acid. *Ind. Eng. Chem.* **1946**, *38*, 400–402.
- Jones, F. S.; Nerheim, A. G. A Macro Spinning Band Distillation Column. *Anal. Chem.* **1959**, *31* (11), 1929.
- Joshi, J. B.; Pandit, A. B.; Kataria, K. L.; Kulkarni, R. P.; Sawarkar, A. N.; Tandon, D.; Ram, Y.; Kumar, M. M. Petroleum Residue Upgrading via Visbreaking: A Review. *Ind. Eng. Chem. Res.* **2008**, *47*, 8960–8988.
- Kasperik, A. S.; Fuchs, H. A. Selective Hydrogenation of Butadienes and Ethyl-Acetylene. France Patent 1493227, 1967.
- Keesom, B.; Gieseman, J. *Bitumen Partial Upgrading 2018 Whitepaper*; Edmonton, 2018.
- Kilpatrick, J. E.; Prosen, E. J.; Pitzer, K. S.; Rossini, F. D. Heats, Equilibrium Constants, and Free Energies of Formation of the Monoolefin Hydrocarbons. *J. Res. Natl. Bur. Stand. (1934)*. **1946**, *36*, 559–612.
- King, P. J.; Yates, B. J. Spinning Band Columns. *Chem. Eng. Prog.* **1966**, *47* (5), 214–223.
- Le Page, J. F. *Applied Heterogeneous Catalysis*; Technip: Paris, 1987.
- Littlewood, A. B. *Gas Chromatography - Principles, Techniques and Applications*, 1st ed.; Academic Press Inc: New York, 1962.
- Meerbot, W. K.; Hinds, G. P. Reaction Studies with Mixtures of Pure Compounds. *Ind. Eng. Chem.* **1955**, *47* (April), 749–752.
- Monteiro-Gezork, A. C.; Effendi, A.; Winterbottom, J. M. Hydrogenation of Naphthaene on NiMo and Ni/Al₂O₃ Catalysts: Pretreatment and Deactivation. *Catal. Today* **2007**, *128*, 63–73.
- Municipal district of Greenview No. 16. Code of Practice Hydrogen Sulfide [http://mdgreenview.ab.ca/wp-content/uploads/2013/12/3007-01-Code-of-Practice-Hydrogen-Sulfide-H₂S.pdf](http://mdgreenview.ab.ca/wp-content/uploads/2013/12/3007-01-Code-of-Practice-Hydrogen-Sulfide-H2S.pdf) (accessed Aug 23, 2019).

- Nagpal, J. M.; Joshi, G. C.; Singh, J.; Rastogi, S. N.; Joshi, G. C.; Singh, J.; Rastogi, S. Gum Forming Olefinic Precursors in Motor Gasoline, A Model Compound Study. *Fuel Sci. Technol. Int.* **2007**, *12* (6), 873–894.
- O’Kelly, A. A.; Kellett, J.; Plucker, J. Monoalkylbenzenes by Vapor-Phase Alkylation with Silica-Alumina Catalyst. *Ind. Eng. Chem.* **1947**, *39*, 154–158.
- Paez Cardenas, Y. Identification, Conversion and Reactivity of Diolefins in Thermally Cracked Naphtha, MSc Thesis, University of Alberta, 2016.
- Patinkin, S. H.; Friedman, B. S. Alkylation of Aromatics with Alkenes and Alkanes. In *Friedel-Crafts and Related Reactions; Volume 2; Part 1*; Olah, G. A., Ed.; Interscience Publishers: New York, 1963; pp 30–31.
- Pernicone, N.; Traina, F. Catalyst Activation by Reduction. *Stud. Surf. Sci. Catal.* **1979**, *3*, 321–351.
- Ramnas, O.; Ostermark, U.; Petersson, G. Characterization of Sixty Alkenes in a Cat-Cracked Gasoline Naphtha by Gas Chromatography. *Chromatographia* **1994**, *38* (3/4), 222–226.
- Rao, Y.; De Klerk, A. Characterization of Heteroatom-Containing Compounds in Thermally Cracked Naphtha from Oilsands Bitumen. *Energy and Fuels* **2017**, *31* (9), 9247–9254.
- Raseev, S. *Thermal and Catalytic Processes in Petroleum Refining*; Marcel Dekker: New York, 2003.
- Riya. Reaction Pathways of Binuclear Aromatics Containing 5-Membered Rings, MSc Thesis, University of Alberta, 2018.
- Rome, K.; McIntyre, A.; Astra Zeneca. Intelligent Use of Relative Response Factors in Gas Chromatography-Flame Ionisation Detection. *Chromatography Today*. Macclesfield 2012, pp 52–56.
- Silverstein, R. M.; Bassler, G. C.; Morill, T. C. *Spectrometric Identification of Organic Compounds*, 4th ed.; John Wiley & Sons, Inc: New York, 1981.
- Soják, L.; Addová, G.; Kubinec, R.; Kraus, A.; Hu, G. Gas Chromatographic-Mass Spectrometric Characterization of All Acyclic C5-C7 Alkenes from Fluid Catalytic Cracked Gasoline Using Polydimethylsiloxane and Squalane Stationary Phases. *J. Chromatogr. A* **2002**, *947* (1), 103–117.
- Speight, J. G. Visbreaking: A Technology of the Past and the Future. *Sci. Iran.* **2012**, *19* (3), 569–573.

- Speight, J. G.; Ozum, B. *Petroleum Refining Processes*; Marcel Dekker, Inc: New York, 2002.
- Subramanian, M.; Deo, M. D.; Hanson, F. V. Compositional Analysis of Bitumen and Bitumen-Derived Products. *J. Chromatogr. Sci.* **1996**, *34* (January), 20–26.
- Twigg, G. H.; Wood, W. A. The Catalytic Isomerization of Butene-1. In *Proceedings of the Royal Society A*; 1941; pp 106–117.
- Van Den Dool, H.; Kratz, P. A Generalization of the Retention Index System Including Linear Temperature Programmed Gas-Liquid Partition Chromatography. *J. Chromatogr.* **1963**, No. 2, 463–471.
- Weisser, O.; Landa, S. *Sulphide Catalysts, Their Properties and Applications*; Academia publishing house: Prague, 1973.
- White, C. M.; Hackett, J.; Anderson, R. R.; Kail, S.; Spock, P. S. Linear Temperature Programmed Retention Indices of Gasoline Range Hydrocarbons and Chlorinated Hydrocarbons on Cross-linked Polydimethylsiloxane. *J. High Resolut. Chromatogr.* **1992**, *15* (2), 105–120.
- Xin, Q.; Alvarez-Majmutov, A.; Dettman, H. D.; Chen, J. Hydrogenation of Olefins in Bitumen-Derived Naphtha over a Commercial Hydrotreating Catalyst. *Energy Fuels* **2018**, *32* (5), 6167–6175.
- Xia, Y. Acid Catalyzed Aromatic Alkylation in the Presence of Nitrogen Bases, MSc Thesis, University of Alberta, 2012.

APPENDIX A: Determination of Average Response Factors for Compound Classes

The average response factors (relative to *n*-octane) for FID detector was calculated based on the ASTM D4626-95 – Standard Practice for Calculation of Gas Chromatographic Response Factors. Relative response factors (RRF) were obtained for paraffins, olefins, aromatics, cycloparaffins and thiophenes through the following procedure.

Standard solutions were prepared with known quantities of 5 compounds each dissolved in a paraffinic solvent (*n*-heptane or *n*-pentane). The compounds were chosen such that each standard solution contained one compound representing each compound class whose response factor was to be determined. The compounds that were used to prepare the standards are listed in Table A.1.

Table A.1 Compounds used for preparation of standard solutions

Standard 1		Mass fraction purity^a	Supplier
Compound 1	<i>n</i> -pentane	1	Fisher
Compound 2	1-octene	0.98	Sigma Aldrich
Compound 3	Cyclopentane	1	Sigma Aldrich
Compound 4	Benzene	0.99	Alfa Aesar
Compound 5	<i>n</i> -octane	0.98	Sigma Aldrich
Solvent	<i>n</i> -heptane	0.999	Fisher
Standard 2		Mass fraction purity^a	Supplier
Compound 1	<i>n</i> -hexane	0.99	Acros Organics
Compound 2	2-methyl-2-butene	0.95	Sigma Aldrich
Compound 3	Cyclohexane	0.999	Sigma Aldrich
Compound 4	Ethylbenzene	0.99	Sigma Aldrich
Compound 5	<i>n</i> -octane	0.98	Sigma Aldrich
Solvent	<i>n</i> -heptane	0.999	Fisher
Standard 3		Mass fraction purity^a	Supplier
Compound 1	<i>n</i> -heptane	0.999	Fisher

Compound 2	1-hexene	0.975	Sigma
Compound 3	Methylcyclohexane	0.995	Sigma Aldrich
Compound 4	m-xylene	0.99	Sigma Aldrich
Compound 5	<i>n</i> -octane	0.98	Sigma Aldrich
Solvent	<i>n</i> -pentane	1	Fisher
Standard 4		Mass fraction purity ^a	Supplier
Compound 1	<i>n</i> -nonane	0.99	Acros Organics
Compound 2	1-heptene	0.97	Sigma
Compound 3	Cycloheptane	0.99	Acros Organics
Compound 4	Propylbenzene	0.98	Aldrich
Compound 5	<i>n</i> -octane	0.98	Sigma Aldrich
Solvent	<i>n</i> -heptane	0.999	Fisher
Standard 5		Mass fraction purity ^a	Supplier
Compound 1	<i>n</i> -decane	0.99	Sigma Aldrich
Compound 2	1-nonene	1	Sigma Aldrich
Compound 3	Cyclooctane	0.99	Alfa Aesar
Compound 4	1,2,4-trimethylbenzene	0.98	Aldrich
Compound 5	<i>n</i> -octane	0.98	Sigma Aldrich
Solvent	<i>n</i> -heptane	0.999	Fisher
Standard 6		Mass fraction purity ^a	Supplier
Compound 1	Thiophene	0.99	Sigma
Compound 2	1-decene	0.94	Aldrich
Compound 3	3-methylbenzothiophene	0.96	Sigma Aldrich
Compound 4	Mesitylene	0.98	Sigma Aldrich
Compound 5	<i>n</i> -octane	0.98	Sigma Aldrich
Solvent	<i>n</i> -heptane	0.999	Fisher

a – Purity of the material guaranteed by supplier and was not further purified.

Each of the standard solutions were injected into the GC-FID instrument in triplicates. 0.1 μL of each sample was automatically injected and entered the column with a split ratio of 1:100. The oven was set at 35 $^{\circ}\text{C}$ for 30 min, then 2 $^{\circ}\text{C}/\text{min}$ to 160 $^{\circ}\text{C}$ for 0 min, then 10 $^{\circ}\text{C}/\text{min}$ to 300 $^{\circ}\text{C}$ for 0.5 min. The FID detector had hydrogen gas flowing at 40 mL/min and air flowing at 400 mL/min.

Agilent ChemStation software was used to obtain the area under the curve for each component and used to calculate response factor (RF) according to the formula:

$$\frac{1}{\text{Response Factor (RF)}} = \frac{\text{wt\% of compound in sample}}{\text{Area of compound in chromatogram}} \quad (1)$$

The response factors were then converted to relative response factors (RRF) with respect to *n*-octane. Table A.2 shows the RRF of all the compound classes.

$$\text{Relative Response Factor (RRF)} = \frac{\text{RF of compound}}{\text{RF of octane}} \quad (2)$$

Table A.2 Average relative response factors of various compound classes for FID

Compound	wt%	Area	RF	RRF
Pentane	1.44	48.63	33.7708	0.98
Hexane	1.53	53.85	35.1961	1.02
Heptane	1.63	55.04	33.7669	0.98
Octane	1.52	52.525	34.5559	1.00
Nonane	1.46	49.18	33.6849	0.97
Decane	1.62	55.87	34.4877	1.00
Average RRF paraffins				0.99
2-Methyl-2-butene	1.41	52.55	37.2695	1.08
Hexene	1.53	55.34	36.1699	1.05
Heptene	1.37	46.66	34.0584	0.99
Octene	1.61	54.15	33.6335	0.97
Nonene	1.52	50.15	32.9934	0.95
Decene	1.51	51.97	34.4172	1.00
Average RRF olefins				1.01
Benzene	1.42	52.06	36.6620	1.06

m-Xylene	1.73	59.94	34.6474	1.00
Ethylbenzene	1.36	56.49	41.5368	1.20
1,2,4-Trimethylbenzene	1.75	61.53	35.1600	1.02
Mesitylene	1.45	51.63	35.6069	1.03
Propylbenzene	1.68	61.11	36.3750	1.05
Average RRF aromatics				1.06
Cyclohexane	3.2	110.38	34.4938	1.00
Cycloheptane	1.44	51.82	35.9861	1.04
Methylcyclohexane	1.36	49.66	36.5147	1.06
Cyclooctane	1.6	51.75	32.3438	0.94
Average RRF cycloparaffins				1.01
Thiophene	1.4	32.62	23.3000	0.67
3-Methylbenzothiophene	1.62	45.37	28.0062	0.81
Average RRF S-compounds				0.74

APPENDIX B: Quantification of hydrogenation reaction products using GC-FID

The components of model feed and hydrogenation products were analyzed using GC-FID as explained in Section 3.2.7. The area of the curve for each compound and the respective response factor were used to calculate the weight percentage of the compound in the sample according to the formula:

$$wt\% \text{ of compound} = \frac{\text{Area of compound} \times wt\% \text{ of internal std}}{\text{Area of internal std} \times RRF \text{ of compound or compound class}} \quad (1)$$

Response factors for each compound were calculated relative to the internal standard (cyclohexane). RRF values from *Appendix A* were used as follows:

$$RRF \text{ relative to cyclohexane} = \frac{RRF \text{ of compound or class relative to octane}}{RRF \text{ of cyclohexane relative to octane}} \quad (2)$$

Table B.1 Average response factors relative to cyclohexane for GC-FID

Compound/Compound class	RRF
<i>n</i> -hexane	1.02
1-hexene	1.05
Cyclohexane	1.00
Paraffins	0.99
Olefins	1.01
Aromatics	1.06
Naphthenes	1.01
S-compounds	0.74

The samples used for GC-FID analysis were diluted 5 times with solvent (*n*-octane). The quantity of a given compound calculated from equation (1) was multiplied with the dilution factor to obtain the amount of the compound in the product.

$$wt\% \text{ in reaction product} = wt\% \text{ of compound in FID sample} \times \text{Dilution factor} \quad (3)$$

The original reaction products did not contain the internal standard, cyclohexane. Since a known amount of cyclohexane was added, it was subtracted to obtain a normalized weight percentage of each compound in the reaction product.

$$\text{Normalized wt\%} = \frac{\text{wt\% of compound in product \{from equation (3)\}}}{100 - \text{wt\% of cyclohexane}} \times 100 \quad (4)$$

The bulk of the GC-FID samples consisted of *n*-octane. This component was quantified as follows:

$$\text{wt\% of octane} = 100 - \sum \text{wt\% of reaction products}$$

Table B.2 Quantification of reaction products of hydrogenation over sulfided catalyst at 200 °C.

Ret time	Compound	Area	Area ratio	RRF	Normalized wt %
8.09	1-hexene	16.63	0.05	1.05	0.30
8.61	Hexane	17.16	0.06	1.02	0.32
8.83	3-hexene	203.96	0.67	1.01	3.88
12.37	Cyclohexane	303.07	1.00	1	0.00
24.96	Toluene	266.10	0.88	1.06	4.83
44.30	2-hexanethiol	12.31	0.04	0.74	0.32
	Octane				90.34

APPENDIX C: Model mass balance calculations for hydrogenation reactions

The catalytic hydrogenation reactor was operated in continuous mode. The mass balance of inlet and outlet streams was evaluated for the reactions at all reaction temperatures, in order to ascertain that the pilot plant was operating efficiently. For this purpose, the flow rates of liquid and gas streams were recorded for a period of 1 hour. The following section shows the mass balance calculations for hydrogenation of model feed over sulfided catalyst at 200 °C.

The overall mass balance equation is given by:

$$\text{Mass of inlet streams (liquid + gas)} = \text{Mass of outlet streams (liquid + gas)} \quad (1)$$

i. Mass of inlet liquid stream:

The feed was pumped into the reactor by a HPLC pump at a predefined flowrate.

$$\text{Flowrate of liquid feed} = 0.4 \text{ mL/min}$$

$$\text{Feed density} = 0.7076 \text{ g/mL}$$

$$\begin{aligned} \text{Mass of liquid feed} &= \text{Flowrate (mL/min)} \times \text{Density (g/ml)} \times \text{Time (min)} \quad (2) \\ &= 0.4(\text{mL/min}) \times 0.7076(\text{g/ml}) \times 60(\text{min}) \end{aligned}$$

$$\text{Mass of liquid feed} = 16.98 \text{ g}$$

ii. Mass of inlet gas stream:

Hydrogen gas was introduced into a reactor at a controlled rate by a mass flow controller. A constant volumetric flowrate was maintained for the reaction.

$$\text{Flowrate of gas feed} = 400 \text{ mL/min}$$

$$\text{Feed density} = 8.9 \times 10^{-5} \text{ g/mL}$$

$$\begin{aligned} \text{Mass of gas feed} &= \text{Flowrate} \left(\frac{\text{mL}}{\text{min}} \right) \times \text{Density} \left(\frac{\text{g}}{\text{ml}} \right) \times \text{Time (min)} \quad (3) \\ &= 400(\text{mL/min}) \times 8.9 \times 10^{-5}(\text{g/ml}) \times 60(\text{min}) \end{aligned}$$

$$\text{Mass of gas feed} = 2.16 \text{ g}$$

iii. Mass of outlet liquid stream:

The liquid phase products of the reaction were collected in a product tank. The product was collected after 60 minutes and the weight was measured with a weighing balance.

$$\text{Mass of liquid product collected in 60 min} = 14.73 \text{ g}$$

iv. Mass of outlet gas stream:

The volume of gas exiting the reactor was measured precisely by a drum flowmeter. A sample of the gas was collected in a gas bag and its composition was analyzed using a Gas-GC as explained in Section 3.2.7. The results of the analysis was used to estimate the mass of the gas as shown below:

Table C.1 Composition of outlet gas stream for sulfided hydrogenation at 200 °C

Compound	M.W	mol%
Methane	16	0.06
n-hexane	86	0.31
Argon	40	0.08
Nitrogen	14	0.83
Hydrogen	2	98.33
Hydrogen sulfide	34	0.04
1-hexene	84	0.35

$$\begin{aligned} \text{Average molecular weight of gas} &= \frac{\sum_{\text{compounds}} (\text{Molecular weight} \times \text{mol}\%) }{100} \quad (4) \\ &= 3.24 \text{ g/mol} \end{aligned}$$

$$\text{Volume of gas measured at outlet} = 24.63 \times 10^{-3} \text{ m}^3$$

Assuming that the gas mixture is an ideal gas,

$$\begin{aligned} \text{Moles of gas} = n &= \frac{P \left(\frac{\text{J}}{\text{m}^3} \right) \times V(\text{m}^3)}{R \left(\frac{\text{J}}{\text{molK}} \right) \times T(\text{K})} \\ &= \frac{101.3 \times 10^3 \times 24.63 \times 10^{-3}}{8.314 \times 293} = 1.02 \text{ mol} \end{aligned}$$

$$\text{Mass of gas product} = n \times \text{Average molecular weight}$$

$$= 1.02 \text{ (mol)} \times 3.24 \left(\frac{\text{g}}{\text{mol}} \right) = 3.32 \text{ g} \quad (5)$$

Table C.2 Summary of mass balance for sulfided hydrogenation at 200 °C

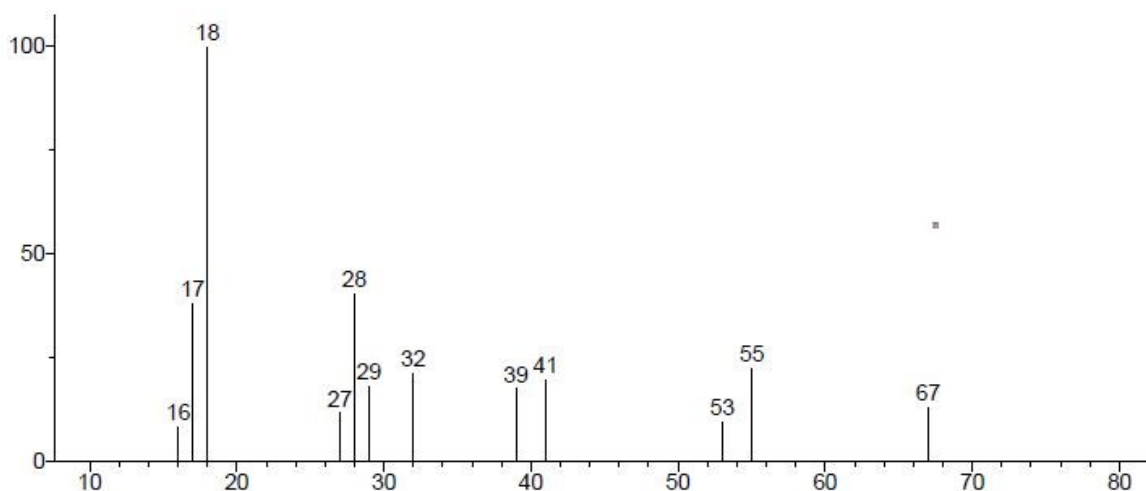
Mass of liquid feed	16.98 g
Mass of gas feed	2.16 g
Total feed	19.14 g
Mass of liquid product	14.73 g
Mass of gas product	3.32 g
Total product	18.05 g
Mass recovery	94.29%

APPENDIX D: Supplementary information for identification of unknown peaks

Chapter 3

Retention time: 29.25 mins

Unknown; InLib=-1589



(Text File) Scan 4364 (29.248 min): Model feed_unsulfided.D\data.ms

Name: Scan 4364 (29.248 min): Model feed_unsulfided.D\data.ms

MW: N/A ID#: 47815 DB: Text File

Comment: Model feed_unsulfided

10 largest peaks:

18 999 | 28 405 | 17 383 | 55 226 | 32 214 | 41 200 | 29 184 | 39 178 | 67 132 | 27 120 |

12 m/z Values and Intensities:

16 86 | 17 383 | 18 999 | 27 120 | 28 405 | 29 184 | 32 214 | 39 178 | 41 200 | 53 98 |

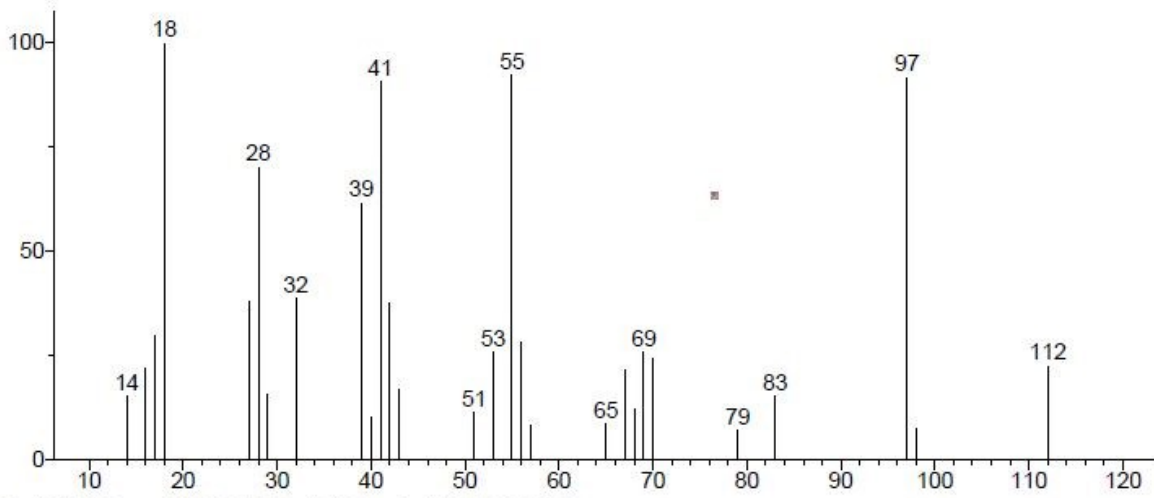
55 226 | 67 132 |

Synonyms:

no synonyms.

Retention time: 31.35 mins

Unknown; InLib=-371



(Text File) Scan 4679 (31.353 min): Product1_200C.D\data.ms

Name: Scan 4679 (31.353 min): Product1_200C.D\data.ms

MW: N/A ID#: 47868 DB: Text File

Comment: Product1_200C

10 largest peaks:

18 999	55 923	97 917	41 907	28 703	39 616	32 387	27 377	42 374	17 297
--------	--------	--------	--------	--------	--------	--------	--------	--------	--------

28 m/z Values and Intensities:

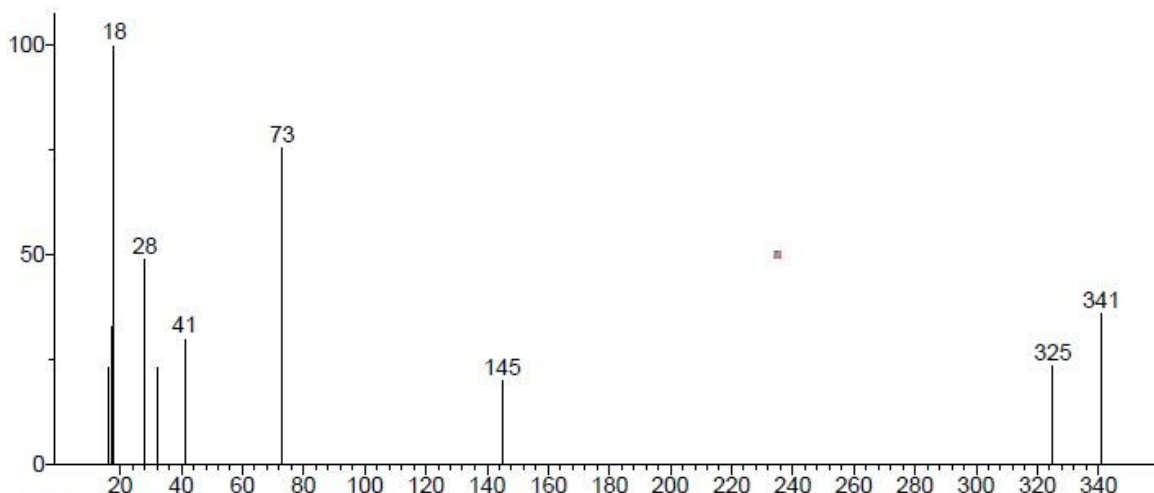
14 155	16 218	17 297	18 999	27 377	28 703	29 156	32 387	39 616	40 99
41 907	42 374	43 167	51 116	53 259	55 923	56 280	57 80	65 88	67 213
68 121	69 260	70 242	79 73	83 155	97 917	98 72	112 227		

Synonyms:

no synonyms.

Retention time: 74.51 mins

Unknown; InLib=-1176



(Text File) Scan 11138 (74.513 min): Product1_200C.D\data.ms

Name: Scan 11138 (74.513 min): Product1_200C.D\data.ms

MW: N/A ID#: 47888 DB: Text File

Comment: Product1_200C

10 largest peaks:

18 999 | 73 754 | 28 489 | 341 360 | 17 327 | 41 301 | 325 237 | 16 230 | 32 228 | 145 202 |

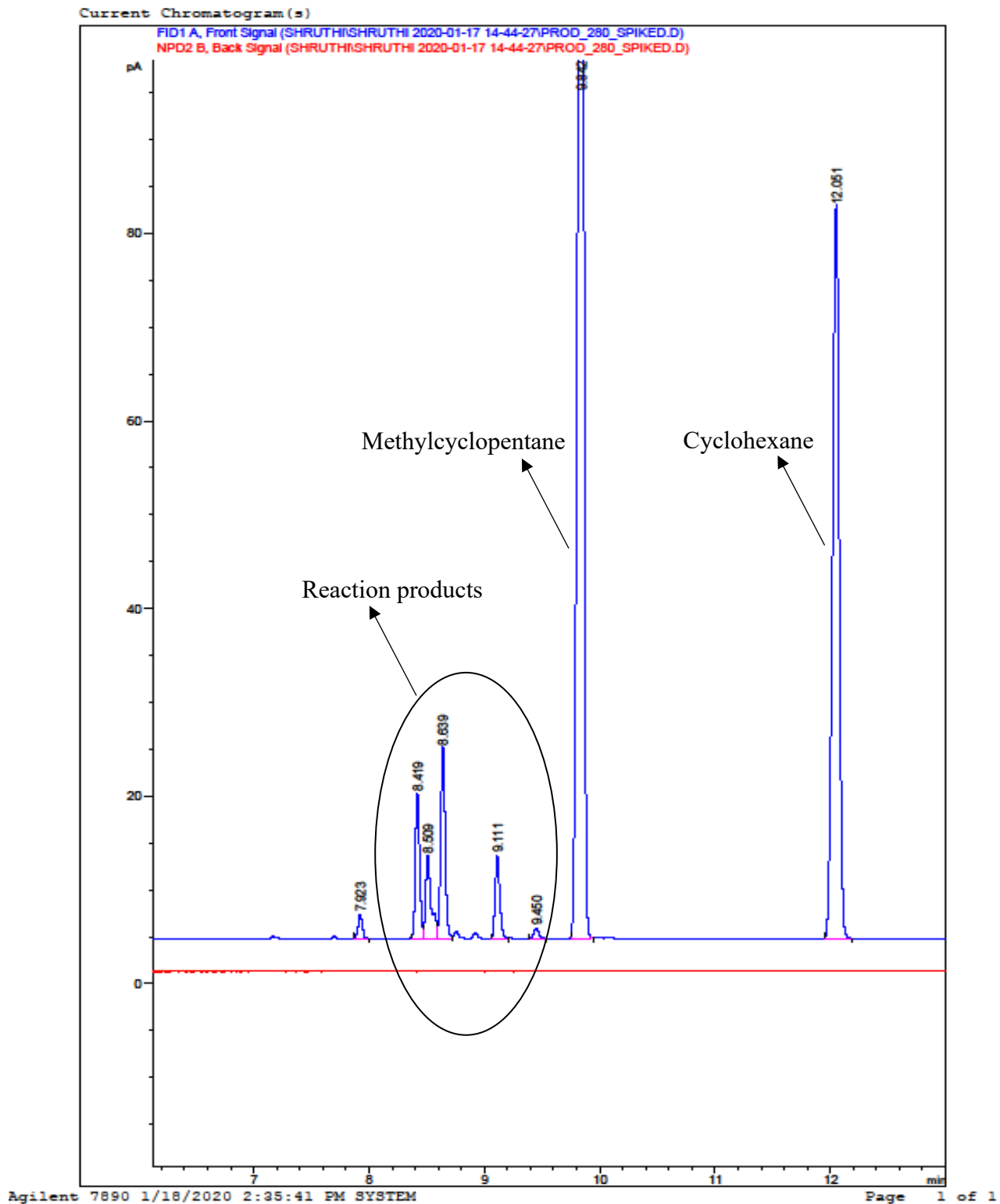
10 m/z Values and Intensities:

16 230 | 17 327 | 18 999 | 28 489 | 32 228 | 41 301 | 73 754 | 145 202 | 325 237 | 341 360 |

Synonyms:

no synonyms.

The liquid-phase product of hydrogenation over sulfided Ni/Al₂O₃ catalyst at 280 °C was spiked with 0.1 mL of cyclohexane and 0.2 mL of methylcyclohexane. The GC-FID analysis of this sample was done using the same method conditions and temperature program as described in section 3.2.7. The resulting chromatogram shown below, indicates separate peaks for methylcyclohexane and cyclohexane respectively. Thus, it can be confirmed that these products were not present in the reaction product.



APPENDIX E: List of compounds identified in cracked naphtha

Cold trap

Retention		Probability	Frequency
time (mins)	Name		
3.509	isobutane	55.6	4
3.649	2-butene	47.1	1
3.709	butane	79.6	3
3.783	2-butene	53.2	2
3.896	2-butene	40.3	1
4.224	3-methyl-1-butene	40.0	1
4.458	2-methyl-butane	84.0	3
4.738	ethanethiol	50.0	3
4.865	pentane	84.4	4
4.992	2-pentene	20.9	2
5.253	3-methyl-1-butene	21.8	1
6.436	cyclopentane	32.0	2
6.609	2-methyl-pentane	42.1	2
7.859	n-hexane	58.8	3
9.249	methyl-cyclopentane	35.1	2

Naphtha_Cut 1_15 - 25 °C

Retention		Probability	Frequency
time (mins)	Name		
3.509	isobutane	76.0	4
3.642	2-methyl-1-propene	31.2	1
3.716	butane	81.3	3
3.783	2-butene	24.2	2
3.896	2-butene (cis-butene)	22.4	1
4.224	2-methyl-1-butene	18.8	2

Naphtha_Cut 1_15 - 25 °C

Retention time (mins)	Name	Probability	Frequency
4.458	2-methyl-butane	85.5	3
4.665	ethyl-cyclopropane	20.2	2
4.738	ethanethiol	93.0	4
4.772	2-methyl-1-butene	20.1	2
4.859	pentane	81.4	4
4.985	trans-2-pentene	21.2	3
5.246	trans-2-pentene	19.1	1
5.62	2,2-dimethyl-butane	45.4	4
5.901	2-propanethiol	91.4	4
6.095	cyclopentene	37.8	3
6.182	4-methyl-1-pentene	56.5	3
6.235	3-methyl-1-pentene	20.6	1
6.429	cyclopentane	50.9	2
6.476	2,3-dimethyl-butane	83.5	4
6.549	4-methyl-2-pentene	20.6	3
6.623	2-methyl-pentane	41.5	2
7.124	3-methyl-pentane	48.1	3
7.318	2-methyl-1-pentene	36.5	3
7.351	1-hexene	30.0	2
7.665	propyl mercaptan	91.1	4
7.845	n-hexane	86.5	3
7.939	3-hexene	19.5	3
8.066	2-hexene	19.3	2
8.3	3-methyl-cyclopentene	27.0	1
8.34	3-methyl-2-pentene	22.7	4
8.534	3-hexene	18.3	2
9.242	methyl-cyclopentane	69.5	3
10.71	3-methyl-cyclopentene	18.2	1

Naphtha_Cut 1_15 - 25 °C

Retention time (mins)	Name	Probability	Frequency
10.75	benzene	75.2	4
11.04	Thiophene	84.1	4
11.45	Cyclohexane	53.5	4
12.11	2-methyl-2-hexene	27.2	2
12.24	2-methyl-hexane	49.5	3
12.36	2,3-dimethyl-pentane	37.1	4
13.01	3-methyl-hexane	39.0	3
13.59	1,3-dimethyl-cyclopentane	31.6	3
15.6	heptane	59.6	3
17.94	methyl-cyclohexane	42.4	4
23.5	toluene	64.5	4

Naphtha_Cut 2_25 - 35 °C

Retention time (mins)	Name	Probability	Frequency
3.509	isobutane	76.5	4
3.642	2-methyl-1-propene	34.0	1
3.709	butane	82.1	3
3.776	2-butene	49.1	4
3.896	2-butene	40.0	2
4.224	3-methyl-1-butene	45.5	2
4.451	2-methyl-butane	82.6	3
4.732	ethanethiol	89.1	4
4.852	pentane	84.8	4
4.979	2-pentene	18.3	2
5.139	2-pentene	18.0	3

Naphtha_Cut 2_25 - 35 °C

Retention time (mins)	Name	Probability	Frequency
5.239	1,2-dimethyl-cyclopropane	22.9	2
5.894	2-propanethiol	75.5	4
6.081	cyclopentene	29.0	3
6.168	4-methyl-1-pentene	49.8	3
6.222	3-methyl-1-pentene	17.0	1
6.415	cyclopentane	29.6	2
6.469	2,3-dimethyl-butane	60.4	4
6.529	4-methyl-2-pentene	18.9	2
6.596	2-methyl-pentane	51.6	2
7.117	3-methyl-pentane	51.8	3
7.304	2-methyl-1-pentene	29.2	3
7.338	1-hexene	20.2	2
7.645	propyl mercaptan	69.9	4
7.832	n-hexane	85.5	3
7.919	3-hexene	17.7	2
8.046	3-hexene	24.1	3
8.326	3-methyl-2-pentene	23.1	4
8.848	3-methyl-2-pentene	18.5	4
9.222	methyl-cyclopentane	71.5	3
10.74	benzene	64.4	4
11.03	thiophene	30.6	3
11.43	cyclohexane	54.6	4
23.43	toluene	33.1	4

Naphtha_Cut 3_35 - 45 °C

Retention time (mins)	Name	Probability	Frequency
3.509	isobutane	80.4	4
3.642	2-methyl-1-propene	32.4	1
3.709	butane	85.7	3
3.783	2-butene	23.6	2
3.896	2-butene	25.4	4
4.224	3-methyl-1-butene	18.6	1
4.451	2-methyl-butane	85.2	3
4.732	ethanethiol	88.0	4
4.772	2-methyl-1-butene	22.0	2
4.852	pentane	87.2	4
4.992	2-pentene	22.4	4
5.139	2-pentene	22.0	1
5.246	1,2-dimethyl-cyclopropane	18.3	2
5.62	2,2-dimethyl-butane	36.2	4
5.901	2-propanethiol	89.6	4
6.095	cyclopentene	37.7	4
6.182	4-methyl-1-pentene	56.7	3
6.235	3-methyl-2-pentene	18.8	1
6.429	cyclopentane	53.2	2
6.482	2,3-dimethyl-butane	74.2	4
6.536	4-methyl-2-pentene	24.4	2
6.603	2-methyl-pentane	70.5	2
7.124	3-methyl-pentane	50.7	3
7.318	2-methyl-1-pentene	29.2	3
7.351	1-hexene	29.6	2
7.658	propyl mercaptan	86.9	4
7.845	n-hexane	87.9	3
7.939	3-hexene	23.0	2

Naphtha_Cut 3_35 - 45 °C

Retention time (mins)	Name	Probability	Frequency
8.066	3-hexene	18.3	2
8.3	3-methyl-cyclopentene	18.2	3
8.534	3-hexene	20.4	2
9.108	2,2-dimethyl-pentane	27.7	1
9.242	methyl-cyclopentane	66.7	3
10.7	3-methyl-cyclopentene	19.6	1
10.75	benzene	75.9	4
11.03	thiophene	70.7	4
11.45	cyclohexane	62.3	4
12.23	2-methyl-hexane	51.6	3
12.36	2,3-dimethyl-pentane	45.4	4
13	3-methyl-hexane	47.9	3
13.57	1,3-dimethyl-cyclopentane	22.2	3
13.85	1,3-dimethyl-cyclopentane	40.4	3
14.12	1,2-dimethyl-cyclopentane	19.4	3
15.58	heptane	62.3	3
17.94	methyl-cyclohexane	49.7	4
23.46	toluene	46.0	4

Naphtha_Cut 4_45 - 55 °C

Retention time (mins)	Name	Probability	Frequency
3.502	isobutane	84.3	4
3.642	2-methyl-1-propene	35.2	1
3.702	butane	85.7	3
3.776	2-butene	24.7	2

Naphtha_Cut 4_45 - 55 °C

Retention time (mins)	Name	Probability	Frequency
3.89	2-butene	24.2	2
4.217	3-methyl-1-butene	20.4	1
4.444	2-methyl-butane	85.9	3
4.658	ethyl-cyclopropane	18.9	2
4.725	ethanethiol	93.0	4
4.765	2-methyl-1-butene	21.2	1
4.845	pentane	84.6	4
4.979	2-pentene	20.2	4
5.133	2-pentene	17.2	2
5.607	2,2-dimethyl-butane	44.1	4
5.888	2-propanethiol	90.0	4
6.075	cyclopentene	27.0	2
6.168	4-methyl-1-pentene	60.6	3
6.215	3-methylene-pentane	20.2	2
6.415	cyclopentane	58.0	2
6.456	2,3-dimethyl-butane	84.8	4
6.522	4-methyl-2-pentene	17.9	3
6.589	2-methyl-pentane	59.6	2
7.104	3-methyl-pentane	48.1	3
7.298	2-methyl-1-pentene	36.1	3
7.331	1-hexene	35.4	2
7.638	propyl mercaptan	88.1	4
7.832	n-hexane	86.0	3
7.912	3-hexene	23.6	2
7.972	3-hexene	24.8	3
8.039	3-hexene	19.0	2
8.153	2-methyl-2-pentene	20.6	1
8.273	3-methyl-cyclopentene	17.3	1

Naphtha_Cut 4_45 - 55 °C

Retention time (mins)	Name	Probability	Frequency
8.32	3-methyl-2-pentene	18.0	4
8.507	3-hexene	19.0	2
8.841	3-methyl-2-pentene	17.1	4
9.075	2,2-dimethyl-pentane	45.1	4
9.215	methyl-cyclopentane	62.3	3
10.67	3-methyl-cyclopentene	21.5	1
10.73	benzene	81.1	4
11.01	thiophene	88.2	4
11.41	ciclohexane	70.8	4
12.07	4-methyl-2-hexene	21.6	1
12.2	2-methyl-hexane	57.1	3
12.32	2,3-dimethyl-pentane	58.4	4
12.74	ethylidenecyclobutane	34.2	1
12.96	3-methyl-hexane	59.3	3
13.54	1,2-dimethyl-cyclopentane	27.4	2
13.81	1,3-dimethyl-cyclopentane	19.9	2
14.08	1,2-dimethyl-cyclopentane	22.9	3
14.94	2-methyl-3-hexene	23.3	1
15.55	heptane	65.4	3
17.89	methyl-cyclohexane	58.2	4
23.4	toluene	30.1	3

Naphtha_Cut 5_55 - 65 °C

Retention time (mins)	Name	Probability	Frequency
3.502	isobutane	70.0	4
3.642	2-methyl-1-propene	29.7	1
3.702	butane	81.4	3
3.776	2-butene	27.7	2
3.896	2-butene	45.4	2
4.224	3-methyl-1-butene	19.9	1
4.451	2-methyl-butane	82.3	3
4.665	ethyl-cyclopropane	21.1	2
4.732	ethanethiol	85.5	4
4.778	2-methyl-1-butene	21.1	2
4.858	pentane	87.6	4
4.985	2-pentene	21.1	4
5.627	2,2-dimethyl-butane	42.8	4
5.901	2-propanethiol	88.8	4
6.095	cyclopentene	34.5	3
6.182	4-methyl-1-pentene	53.6	3
6.235	3-methyl-1-pentene	19.8	1
6.425	cyclopentane	48.6	2
6.482	2,3-dimethyl-butane	79.7	4
6.609	2-methyl-pentane	63.6	2
7.13	3-methyl-pentane	48.1	3
7.317	2-methyl-1-pentene	36.8	3
7.351	1-hexene	23.6	2
7.658	propyl mercaptan	89.6	4
7.852	n-hexane	86.9	3
7.939	3-hexene	23.0	3
7.999	3-hexene	24.3	2
8.066	3-hexene	19.1	2

Naphtha_Cut 5_55 - 65 °C

Retention time (mins)	Name	Probability	Frequency
8.186	2-methyl-2-pentene	22.8	1
8.293	3-methyl-cyclopentene	26.2	1
8.347	3-methyl-2-pentene	18.8	4
8.534	3-hexene	17.8	2
8.868	3-methyl-2-pentene	17.5	4
9.108	2,2-dimethyl-pentane	63.5	4
9.249	methyl-cyclopentane	62.0	3
10.54	2,4-dimethyl-1-pentene	31.4	3
10.69	3-methyl-cyclopentene	24.5	1
10.75	benzene	76.9	4
11.03	thiophene	81.4	4
11.43	ciclohexane	78.7	4
12.22	2-methyl-hexane	53.3	3
12.36	2,3-dimethyl-pentane	61.0	4
13	3-methyl-hexane	52.7	3
13.57	1,3-dimethyl-cyclopentane	25.8	3
13.84	1,3-dimethyl-cyclopentane	24.1	3
14.11	1,2-dimethyl-cyclopentane	21.7	3
14.29	1-heptene	23.0	3
14.96	3-methyl-3-hexene	17.2	2
15.58	heptane	70.5	3
16.18	2-heptene	18.7	3
17.91	methyl-cyclohexane	69.7	4
19.65	ethyl-cyclopentane	50.3	2
23.42	toluene	48.7	4
23.77	3-methyl-thiophene	49.4	4
26.54	2-methyl-heptane	31.9	3

Naphtha_Cut 6_65 - 75 °C

Retention time (mins)	Name	Probability	Frequency
3.502	isobutane	67.8	4
3.636	2-butene	34.1	1
3.703	butane	81.0	3
3.776	2-butene	47.0	4
3.89	2-butene	45.7	2
4.217	3-methyl-1-butene	38.3	1
4.451	2-methyl-butane	84.0	3
4.658	ethyl-cyclopropane	18.1	2
4.725	ethanethiol	74.9	4
4.772	2-methyl-1-butene	20.4	1
4.845	pentane	85.8	4
5.133	2-pentene	17.6	1
5.24	1,2-dimethyl-cyclopropane	20.8	2
5.607	2,2-dimethyl-butane	51.1	4
5.888	2-propanethiol	89.2	4
6.082	cyclopentene	29.7	2
6.168	4-methyl-1-pentene	66.3	3
6.222	3-methylene-pentane	18.7	2
6.416	cyclopentane	54.6	2
6.462	2,3-dimethyl-butane	82.9	4
6.529	4-methyl-2-pentene	19.0	3
6.596	2-methyl-pentane	61.7	2
7.111	3-methyl-pentane	50.9	3
7.298	2-methyl-1-pentene	37.5	3
7.338	1-hexene	29.2	2
7.645	propyl mercaptan	87.7	4

Naphtha_Cut 6_65 - 75 °C

Retention time (mins)	Name	Probability	Frequency
7.846	n-hexane	86.7	3
7.926	3-hexene	24.9	3
7.979	3-hexene	23.1	2
8.046	3-hexene	19.0	2
8.273	3-methyl-cyclopentene	25.4	3
8.514	3-hexene	20.7	2
8.841	3-methyl-2-pentene	18.2	4
9.088	2,2-dimethyl-pentane	59.8	3
9.222	methyl-cyclopentane	59.9	3
10.51	2,4-dimethyl-1-pentene	43.3	3
10.67	1-methyl-cyclopentene	27.3	2
10.73	benzene	84.8	4
11.01	thiophene	87.5	4
11.41	ciclohexane	75.9	4
11.86	5-methyl-1-hexyne	21.2	2
12.08	4-methyl-2-hexene	18.1	2
12.2	2-methyl-hexane	56.5	3
12.32	2,3-dimethyl-pentane	56.5	4
12.98	3-methyl-hexane	58.2	3
13.54	1,3-dimethyl-cyclopentane	30.7	3
13.81	1,3-dimethyl-cyclopentane	26.0	3
14.08	1,2-dimethyl-cyclopentane	27.0	3
14.25	1-heptene	28.1	3
14.94	3-methyl-3-hexene	17.3	1
15.57	heptane	69.0	3
15.8	2-methyl-2-hexene	30.3	1
16.15	2-heptene	17.6	3
17.88	methyl-cyclohexane	70.2	4

Naphtha_Cut 6_65 - 75 °C

Retention time (mins)	Name	Probability	Frequency
19.61	ethyl-cyclopentane	61.5	2
23.38	toluene	57.2	3
23.72	3-methyl-thiophene	52.3	4
26.48	2-methyl-heptane	35.6	3

Naphtha_Cut 7_75 - 85 °C

Retention time (mins)	Name	Probability	Frequency
3.502	isobutane	31.8	3
3.632	2-butene	31.8	1
3.703	butane	83.3	3
3.776	2-butene	46.9	2
3.89	2-butene	33.1	2
4.21	3-methyl-1-butene	46.1	1
4.431	2-methyl-butane	78.8	3
4.645	ethyl-cyclopropane	23.8	1
4.752	3-methyl-1-butene	21.6	1
4.832	pentane	85.3	4
4.966	2-pentene	19.6	3
5.213	1,2-dimethyl-cyclopropane	23.8	2
5.587	2,2-dimethyl-butane	38.6	4
5.861	2-propanethiol	77.2	4
6.048	cyclopentene	24.3	2
6.135	4-methyl-1-pentene	59.1	3
6.182	3-methyl-1-pentene	23.5	3
6.382	cyclopentane	54.8	2

Naphtha_Cut 7_75 - 85 °C

Retention time (mins)	Name	Probability	Frequency
6.422	2,3-dimethyl-butane	83.4	4
6.489	4-methyl-2-pentene	19.3	1
6.549	2-methyl-pentane	64.0	1
7.057	3-methyl-pentane	48.5	3
7.244	2-methyl-1-pentene	33.0	3
7.278	1-hexene	35.4	2
7.578	propyl mercaptan	76.9	4
7.772	n-hexane	86.0	3
7.846	3-hexene	24.2	2
7.906	3-hexene	31.4	3
7.979	2-hexene	19.0	2
8.086	2-methyl-2-pentene	19.9	2
8.2	3-methyl-cyclopentene	23.9	2
8.246	3-methyl-2-pentene	19.6	4
8.434	3-hexene	18.7	3
8.748	3-methyl-2-pentene	20.6	4
8.995	2,2-dimethyl-pentane	52.7	3
9.128	methyl-cyclopentane	59.9	3
10.39	2,4-dimethyl-1-pentene	38.4	3
10.55	1-methyl-cyclopentene	24.3	2
10.6	benzene	77.1	4
10.67	3-methyl-1-hexene	21.6	3
10.88	thiophene	88.5	4
11.15	5-methyl-1-hexene	29.4	2
11.27	ciclohexane	75.7	4
11.45	2-methyl-3-hexene	28.4	3
11.71	4-methyl-1-hexene	21.0	2
12.04	2-methyl-hexane	58.3	3

Naphtha_Cut 7_75 - 85 °C

Retention time (mins)	Name	Probability	Frequency
12.16	2,3-dimethyl-pentane	62.6	4
12.39	1,1-dimethyl-cyclopentane	32.1	2
12.8	3-methyl-hexane	62.5	3
13.35	1,3-dimethyl-cyclopentane	28.9	3
13.62	1,3-dimethyl-cyclopentane	27.2	3
13.89	1,2-dimethyl-cyclopentane	26.4	3
14.05	1-heptene	24.1	3
14.72	3-methyl-3-hexene	19.1	1
15.34	heptane	71.8	3
15.58	2-methyl-2-hexene	25.5	2
15.69	3-methyl-3-hexene	21.1	2
15.9	2-heptene	20.8	2
17.33	3-ethyl-cyclopentene	36.5	2
17.62	methyl-cyclohexane	69.6	4
18.11	1,1,3-trimethyl-cyclopentane	52.9	2
19.31	ethyl-cyclopentane	69.2	2
19.96	2,4-dimethyl-hexane	22.9	3
20.72	1,2,4-trimethyl-cyclopentane	24.6	3
22.85	1-ethylcyclopentene	43.9	3
23.03	toluene	59.1	4
23.36	3-methyl-thiophene	48.4	4
24.72	3-methyl-thiophene	26.1	4
26.07	2-methyl-heptane	48.3	3
26.39	4-methyl-heptane	47.5	3
34.1	2,4-dimethyl-hexane	24.5	2

Naphtha_Cut 8_85 - 100 °C

Retention time (mins)	Name	Probability	Frequency
3.502	isobutane	33.5	3
3.632	2-butene	45.4	1
3.709	butane	76.0	3
3.776	2-butene	57.3	1
3.89	2-butene	40.3	1
4.217	3-methyl-1-butene	38.6	2
4.451	2-methyl-butane	76.3	3
4.772	3-methyl-1-butene	26.9	1
4.859	pentane	80.9	4
4.986	2-pentene	25.7	2
5.139	2-pentene	17.3	1
5.246	1,2-dimethyl-cyclopropane	22.2	2
5.894	2-propanethiol	50.8	4
6.088	cyclopentene	22.4	3
6.175	4-methyl-1-pentene	55.4	3
6.229	3-methyl-2-pentene	17.4	2
6.429	cyclopentane	41.9	2
6.469	2,3-dimethyl-butane	74.0	4
6.536	4-methyl-2-pentene	27.0	4
6.596	2-methyl-pentane	69.9	2
7.117	3-methyl-pentane	52.2	3
7.311	2-methyl-1-pentene	26.0	3
7.344	1-hexene	19.6	2
7.652	propyl mercaptan	73.9	4
7.839	n-hexane	86.7	3
7.932	3-hexene	20.0	2
7.986	3-hexene	26.5	2
8.059	3-hexene	21.1	2

Naphtha_Cut 8_85 - 100 °C

Retention			
time (mins)	Name	Probability	Frequency
8.173	2-methyl-2-pentene	20.2	1
8.287	3-methyl-cyclopentene	24.6	2
8.333	3-methyl-2-pentene	21.8	4
8.52	3-hexene	25.8	2
8.855	3-methyl-2-pentene	16.8	4
9.102	2,2-dimethyl-pentane	62.6	3
9.229	methyl-cyclopentane	59.5	3
10.52	2,4-dimethyl-1-pentene	44.5	3
10.69	1-methyl-cyclopentene	21.1	1
10.73	benzene	48.7	4
10.85	3-methyl-1-hexene	21.8	3
11.01	thiophene	68.8	4
11.29	5-methyl-1-hexene	27.0	2
11.43	ciclohexane	72.4	4
11.61	2-methyl-3-hexene	21.5	3
11.88	4-methyl-1-hexene	29.4	3
12.08	4-methyl-2-hexene	18.7	2
12.22	2-methyl-hexane	60.9	3
12.34	2,3-dimethyl-pentane	70.7	4
12.56	1,1-dimethyl-cyclopentane	32.1	2
12.99	3-methyl-hexane	61.0	3
13.55	1,3-dimethyl-cyclopentane	29.1	3
13.82	1,3-dimethyl-cyclopentane	24.8	3
14.09	1,2-dimethyl-cyclopentane	28.6	3
14.27	1-heptene	28.7	3
14.94	3-methyl-3-hexene	27.4	2
15.34	3,3-dimethyl-1,4-pentadiene	17.0	1
15.59	heptane	70.1	3

Naphtha_Cut 8_85 - 100 °C

Retention			
time (mins)	Name	Probability	Frequency
15.83	2-methyl-2-hexene	18.8	2
15.95	3-methyl-3-hexene	17.9	2
16.16	3-heptene	20.3	2
17.6	3-ethyl-cyclopentene	53.8	1
17.89	methyl-cyclohexane	71.6	4
18.39	1,1,3-trimethyl-cyclopentane	55.1	2
19.61	ethyl-cyclopentane	66.8	2
20.27	2,4-dimethyl-hexane	37.1	3
21.04	1,2,4-trimethyl-cyclopentane	31.3	3
22.97	1-methylethylidene-cyclobutane	31.2	1
23.22	ethylidene-cyclopentene	45.2	1
23.38	toluene	54.9	4
23.72	2-methyl-thiophene	47.7	2
24.83	2,3-dimethyl-1,4-hexadiene	23.3	1
25.1	2-methyl-thiophene	17.6	3
25.25	3-ethyl-2-methyl-pentane	37.0	3
26.5	2-methyl-heptane	60.9	3
26.8	4-methyl-heptane	50.3	4
27.94	1,3-dimethyl-cyclohexane	22.2	3
28.15	3-methyl-heptane	24.3	2
30.69	1-ethyl-3-methyl-cyclopentane	39.5	3
31.18	1-ethyl-3-methyl-cyclopentane	30.6	3
31.46	1-ethyl-3-methyl-cyclopentane	24.3	2
33.96	1,4-dimethyl-cyclohexane	19.0	3
34.42	octane	28.0	3
42.52	ethylbenzene	24.8	2
42.73	3-ethyl-thiophene	41.4	3
43.71	3,4-dimethyl-thiophene	61.1	4

Naphtha_Cut 8_85 - 100 °C

Retention

time (mins)	Name	Probability	Frequency
43.94	p-xylene	29.4	1
44.1	ethinamate	49.0	4
44.75	3,4-dimethyl-thiophene	74.3	2
46.26	3,4-dimethyl-thiophene	62.2	1

Naphtha_Cut 9_100 - 110 °C

Retention

time (mins)	Name	Probability	Frequency
3.642	2-butene	47.5	1
3.703	butane	79.4	3
3.776	2-butene	46.5	1
3.89	2-butene	42.0	1
4.444	2-methyl-butane	70.4	3
4.765	3-methyl-1-butene	31.2	1
4.845	pentane	78.0	4
5.132	3-methyl-1-butene	29.9	1
5.233	1,2-dimethyl-cyclopropane	19.2	1
6.582	2-methyl-pentane	50.9	2
7.097	3-methyl-pentane	38.4	3
7.324	1-hexene	16.0	2
7.819	n-hexane	84.6	3
7.906	3-hexene	19.2	3
8.033	3-hexene	19.8	2
8.26	3-methyl-cyclopentene	18.0	1
8.306	3-methyl-2-pentene	19.2	4
8.494	3-hexene	22.9	3

Naphtha_Cut 9_100 - 110 °C

Retention			
time (mins)	Name	Probability	Frequency
8.821	3-methyl-2-pentene	18.9	4
9.068	2,2-dimethyl-pentane	47.0	4
9.195	methyl-cyclopentane	71.5	3
10.64	3-methyl-cyclopentene	18.2	1
10.81	3-methyl-1-hexene	22.6	3
10.97	2-butanethiol	79.7	2
11.26	5-methyl-1-hexene	16.9	2
11.38	ciclohexane	64.4	4
11.57	2-methyl-3-hexene	19.3	2
11.84	4-methyl-1-hexene	29.5	3
12.04	4-methyl-2-hexene	16.9	2
12.18	2-methyl-hexane	58.1	3
12.3	2,3-dimethyl-pentane	59.6	4
12.52	1,1-dimethyl-cyclopentane	32.5	2
12.94	3-methyl-hexane	60.1	3
13.51	1,3-dimethyl-cyclopentane	29.2	3
13.77	1,3-dimethyl-cyclopentane	32.3	3
14.05	1,2-dimethyl-cyclopentane	26.8	3
14.21	1-heptene	30.0	3
14.9	3-methyl-3-hexene	17.6	1
15.55	heptane	71.5	3
15.9	3-methyl-3-hexene	23.3	3
16.11	2-heptene	21.2	2
17.55	3-ethyl-cyclopentene	46.6	3
17.84	methyl-cyclohexane	71.1	4
18.34	1,1,3-trimethyl-cyclopentane	55.7	2
19.55	ethyl-cyclopentane	73.1	2
19.95	2,5-dimethyl-hexane	20.5	2

Naphtha_Cut 9_100 - 110 °C

Retention			
time (mins)	Name	Probability	Frequency
20.23	2,4-dimethyl-hexane	36.4	3
20.99	1,2,4-trimethyl-cyclopentane	28.8	3
22.24	1,2,3-trimethyl-cyclopentane	23.5	3
22.92	1-methylethylidene-cyclobutane	32.1	1
23.17	ethylidene-cyclopentane	44.9	2
23.33	toluene	60.7	4
23.68	2-methyl-thiophene	53.6	2
24.56	4-methyl-2-heptene	36.1	2
24.77	2,3,3-trimethyl-1,4-pentadiene	14.5	2
25.19	3-ethyl-2-methyl-pentane	26.8	2
26.46	2-methyl-heptane	57.2	3
26.76	4-methyl-heptane	52.3	4
27.15	ethylidene-cyclopentane	20.9	2
27.9	1,3-dimethyl-cyclohexane	32.2	3
28.1	3-methyl-heptane	34.9	2
30.64	1-ethyl-3-methyl-cyclopentane	38.8	3
31.13	1-ethyl-3-methyl-cyclopentane	34.1	3
32.3	1,2-dimethyl-cyclohexane	22.6	4
33.65	1-ethyl-5-methyl-cyclopentene	32.5	2
33.91	1,4-dimethyl-cyclohexane	18.5	4
34.42	octane	31.3	2
39.41	ethyl-cyclohexane	21.4	3
40.17	2,6-dimethyl-heptane	50.8	2
40.32	1,1,3-trimethyl-cyclohexane	49.1	4
40.44	methyl-ethyl-cyclopentene	20.8	2
41.25	2,5-dimethyl-heptane	29.4	4
42.5	ethylbenzene	55.8	3
42.7	2-ethyl-thiophene	45.6	2

Naphtha_Cut 9_100 - 110 °C

Retention time (mins)	Name	Probability	Frequency
43.68	2,5-dimethyl-thiophene	35.8	3
43.92	m-xylene	34.1	2
44.09	ethinamate	43.5	4
44.75	2,4-dimethyl-thiophene	35.6	1
45.81	4-methyl-octane	46.0	2
46.24	2,3-dimethyl-thiophene	32.7	1
47.19	p-xylene	34.0	2
50.84	nonane	34.1	3

Naphtha_Cut 10_110 - 120 °C

Retention time (mins)	Name	Probability	Frequency
3.636	2-butene	47.0	1
3.696	butane	83.0	3
3.763	2-butene	43.4	1
4.391	2-methyl-butane	71.9	3
4.765	pentane	82.8	4
5.126	3-methyl-1-butene	42.8	1
6.389	2-methyl-pentane	32.5	2
6.883	3-methyl-pentane	25.0	3
7.558	n-hexane	81.8	3
7.758	2-hexene	40.2	2
8.901	methyl-cyclopentane	72.7	3
10.28	1-methyl-cyclopentene	17.5	2
11.02	ciclohexane	69.8	4
11.42	4-methyl-1-hexene	28.3	3

Naphtha_Cut 10_110 - 120 °C

Retention			
time (mins)	Name	Probability	Frequency
11.62	4-methyl-2-hexene	20.8	1
11.73	2-methyl-hexane	63.2	3
11.87	2,3-dimethyl-pentane	59.1	4
12.1	1,1-dimethyl-cyclopentane	33.5	2
12.49	3-methyl-hexane	60.8	3
13.04	1,3-dimethyl-cyclopentane	33.6	3
13.31	1,3-dimethyl-cyclopentane	24.5	3
13.57	1,2-dimethyl-cyclopentane	25.7	3
13.71	1-heptene	21.7	3
14.98	heptane	71.7	4
15.32	3-methyl-3-hexene	20.3	3
15.52	2-heptene	16.6	3
16.85	3-ethyl-cyclopentene	40.5	2
17.23	methyl-cyclohexane	71.4	4
17.71	1,1,3-trimethyl-cyclopentane	50.2	2
18.88	ethyl-cyclopentane	70.5	2
19.22	2,5-dimethyl-hexane	35.4	3
19.49	2,4-dimethyl-hexane	32.1	4
20.23	1,2,4-trimethyl-cyclopentane	30.5	3
21.43	1,2,3-trimethyl-cyclopentane	17.5	3
22.07	1-methylethylidene-cyclobutane	30.4	1
22.31	1-ethyl-cyclopentene	47.4	2
22.49	toluene	58.7	4
22.82	2-methyl-thiophene	55.4	2
23.64	4-methyl-2-heptene	46.5	2
23.87	2,3,3-trimethyl-1,4-pentadiene	17.4	2
24.25	3-ethyl-2-methyl-pentane	33.6	3
25.46	2-methyl-heptane	59.9	3

Naphtha_Cut 10_110 - 120 °C

Retention time (mins)	Name	Probability	Frequency
25.74	4-methyl-heptane	53.3	4
26.62	6-methyl-2-heptene	27.2	1
26.9	1,3-dimethyl-cyclohexane	22.1	3
27.04	3-methyl-heptane	45.3	2
28.43	1,1-dimethyl-cyclohexane	51.8	3
29.54	1-ethyl-2-methyl-cyclopentane	33.1	3
30.04	1-ethyl-3-methyl-cyclopentane	28.8	3
30.34	1-ethyl-3-methyl-cyclopentane	17.4	2
31.31	1,2-dimethyl-cyclohexane	24.3	4
32.72	1-ethyl-5-methyl-cyclopentene	21.9	2
33.02	1,4-dimethyl-cyclohexane	20.9	3
33.54	octane	33.7	3
35.18	1-ethyl-5-methyl-cyclopentene	42.8	2
37.67	1,2-dimethyl-cyclohexane	23.2	3
39.56	2,6-dimethyl-heptane	29.6	1
39.72	1,1,3-trimethyl-cyclohexane	56.6	4
39.93	1-ethyl-5-methyl-cyclopentene	19.6	2
40.67	2,5-dimethyl-heptane	39.6	3
41.97	ethylbenzene	53.4	4
42.18	2-ethyl-thiophene	53.2	3
43.2	2,5-dimethyl-thiophene	42.0	3
43.43	p-xylene	34.1	2
43.61	ethinamate	35.0	4
44.26	3,4-dimethyl-thiophene	40.6	2
45.39	4-methyl-octane	52.6	2
45.82	2,3-dimethyl-thiophene	31.6	1
46.3	4-propyl-heptane	24.8	2
46.8	p-xylene	34.6	2

Naphtha_Cut 10_110 - 120 °C

Retention time (mins)	Name	Probability	Frequency
50.53	nonane	39.2	3
54.99	2,6-dimethyl-octane	19.7	2
56.24	1-ethyl-3-methyl-benzene	30.6	2
59.91	mesitylene	18.7	1
62.38	decane	31.0	4

Naphtha_Cut 11_120 - 130 °C

Retention time (mins)	Name	Probability	Frequency
3.703	butane	79.9	3
4.438	2-methyl-butane	63.3	3
4.832	pentane	77.7	4
5.219	3-methyl-1-butene	29.6	1
7.765	n-hexane	57.5	3
9.135	methyl-cyclopentane	68.5	2
11.31	ciclohexane	25.0	3
12.06	2-methyl-hexane	57.8	3
12.19	2,3-dimethyl-pentane	38.6	4
12.82	3-methyl-hexane	47.5	3
13.39	1,3-dimethyl-cyclopentane	24.5	3
13.65	1,3-dimethyl-cyclopentane	22.2	3
13.92	1,2-dimethyl-cyclopentane	23.2	2
15.37	heptane	70.1	4
15.94	2-heptene	16.7	4
17.67	methyl-cyclohexane	69.7	4
18.18	1,1,3-trimethyl-cyclopentane	54.3	2

Naphtha_Cut 11_120 - 130 °C

Retention time (mins)	Name	Probability	Frequency
19.39	ethyl-cyclopentane	64.3	2
19.77	2,5-dimethyl-hexane	37.7	3
20.04	2,4-dimethyl-hexane	37.2	3
20.8	1,2,4-trimethyl-cyclopentane	28.4	3
22.04	1,2,3-trimethyl-cyclopentane	22.2	3
22.73	1-methylethylidene-cyclobutane	30.6	1
22.97	1-ethyl-cyclopentene	43.7	2
23.14	toluene	43.7	4
23.48	2-methyl-thiophene	53.4	2
24.37	4-methyl-2-heptene	32.9	2
25	3-ethyl-2-methyl-pentane	39.5	3
26.27	2-methyl-heptane	61.5	3
26.59	4-methyl-heptane	50.9	4
27.47	6-methyl-2-heptene	28.8	1
27.7	1,3-dimethyl-cyclohexane	31.5	2
27.89	3-methyl-heptane	36.7	2
29.28	1,1-dimethyl-cyclohexane	53.2	3
30.44	1-ethyl-3-methyl-cyclopentane	30.4	3
30.93	1-ethyl-3-methyl-cyclopentane	33.6	3
31.12	1,2-dimethyl-cyclohexane	26.3	4
33.47	1-ethyl-5-methyl-cyclopentene	32.3	2
33.75	1,4-dimethyl-cyclohexane	18.0	4
34.31	octane	29.0	3
40.08	2,6-dimethyl-heptane	25.6	1
40.22	1,1,3-trimethyl-cyclohexane	58.3	4
40.33	1-ethyl-5-methyl-cyclopentene	17.8	2
41.14	2,5-dimethyl-heptane	42.4	3
42.39	ethylbenzene	62.9	3

Naphtha_Cut 11_120 - 130 °C

Retention time (mins)	Name	Probability	Frequency
42.6	2-ethyl-thiophene	57.6	3
43.13	2,6-dimethyl-1-heptene	17.2	3
43.59	2,5-dimethyl-thiophene	53.5	3
43.84	m-xylene	35.7	2
44	ethinamate	31.7	4
44.64	3,4-dimethyl-thiophene	36.3	2
45.73	4-methyl-octane	53.1	2
45.91	2-methyl-octane	17.7	2
46.17	2,3-dimethyl-thiophene	35.0	1
46.86	2,5-dimethyl-heptane	19.9	1
47.11	p-xylene	33.5	2
49.19	1-nonene	18.7	2
50.78	nonane	35.7	3
55.18	2,6-dimethyl-octane	30.7	2
62.47	decane	32.4	4

Naphtha_Cut 12_130 - 140 °C

Retention time (mins)	Name	Probability	Frequency
3.709	butane	62.7	3
4.458	2-methyl-butane	61.7	3
4.859	pentane	78.8	4
7.852	n-hexane	41.3	3
13	3-methyl-hexane	42.6	3
15.57	heptane	70.2	4
17.9	methyl-cyclohexane	74.9	4

Naphtha_Cut 12_130 - 140 °C

Retention time (mins)	Name	Probability	Frequency
19.61	ethyl-cyclopentane	42.1	2
21.05	1,2,4-trimethyl-cyclopentane	24.4	2
23.38	toluene	59.5	3
23.73	2-methyl-thiophene	53.5	2
26.49	2-methyl-heptane	61.1	3
26.79	4-methyl-heptane	51.7	4
27.95	1,3-dimethyl-cyclohexane	33.7	3
28.15	3-methyl-heptane	29.6	2
29.53	1,1-dimethyl-cyclohexane	47.5	3
30.69	1-ethyl-3-methyl-cyclopentane	33.9	3
31.18	1-ethyl-3-methyl-cyclopentane	32.8	3
31.46	1-ethyl-3-methyl-cyclopentane	18.8	2
33.69	1-ethyl-5-methyl-cyclopentene	23.0	2
33.96	1,4-dimethyl-cyclohexane	21.4	3
34.48	octane	34.8	3
40.24	2,6-dimethyl-heptane	30.0	2
40.37	1,1,3-trimethyl-cyclohexane	53.9	4
41.28	2,5-dimethyl-heptane	42.9	4
42.51	ethylbenzene	61.9	3
42.73	2-ethyl-thiophene	48.3	3
43.25	2,6-dimethyl-1-heptene	21.2	3
43.71	2,5-dimethyl-thiophene	52.2	3
43.95	p-xylene	29.6	2
44.11	ethinamate	28.5	4
44.75	3,4-dimethyl-thiophene	36.3	2
45.65	2,6-dimethyl-3-heptene	27.3	2
45.84	4-methyl-octane	58.1	1
46.27	2,3-dimethyl-thiophene	31.8	1

Naphtha_Cut 12_130 - 140 °C

Retention time (mins)	Name	Probability	Frequency
46.72	3-ethyl-heptane	40.5	1
46.96	2,5-dimethyl-heptane	17.2	1
47.2	p-xylene	34.2	2
49.26	1-nonene	19.5	2
49.98	4-nonene	17.9	3
50.88	nonane	34.3	3
54.46	butyl-cyclopentane	36.0	3
55.23	2,6-dimethyl-octane	35.9	2
55.5	propyl-benzene	63.7	3
56.03	3-methyl-2-methyl-heptane	43.7	3
56.17	2-ethyl-5-methyl-thiophene	47.3	1
56.44	1-ethyl-3-methyl-benzene	36.3	1
56.66	1-ethyl-3-methyl-benzene	26.8	1
57.35	1,2,3-trimethyl-benzene	21.1	1
58.44	4-methyl-nonane	32.6	3
20.8	mesitylene	20.8	1
62.51	decane	36.4	4
62.9	1,2,3-trimethyl-benzene	20.2	1

Naphtha_Cut 13_140 - 150 °C

Retention time (mins)	Name	Probability	Frequency
3.702	butane	66.1	3
4.438	2-methyl-butane	47.9	3
4.838	pentane	63.8	4
7.779	n-hexane	61.4	3

Naphtha_Cut 13_140 - 150 °C

Retention time (mins)	Name	Probability	Frequency
15.43	heptane	52.7	4
17.76	methyl-cyclohexane	44.0	4
19.47	ethyl-cyclopentane	48.0	2
23.23	toluene	21.8	4
26.31	2-methyl-heptane	52.3	3
26.62	4-methyl-heptane	44.5	3
27.77	1,3-dimethyl-cyclohexane	23.2	3
27.95	3-methyl-heptane	24.6	2
28.19	1,4-dimethyl-cyclohexane	17.4	3
29.37	1,1-dimethyl-cyclohexane	25.1	3
30.52	1-ethyl-3-methyl-cyclopentane	31.5	3
31.01	1-ethyl-3-methyl-cyclopentane	30.1	3
31.29	1-ethyl-3-methyl-cyclopentane	23.8	3
32.18	1,2-dimethyl-cyclohexane	26.4	3
33.81	1,4-dimethyl-cyclohexane	21.6	3
34.31	octane	43.4	3
35.17	2,3,3-trimethyl-1,4-pentadiene	23.1	2
38.28	1,2-dimethyl-cyclohexane	31.2	3
38.9	2,4-dimethyl-heptane	27.3	3
39.33	ethyl-cyclohexane	19.8	3
40.12	2-methyl-octane	26.4	2
40.27	1,1,3-trimethyl-cyclohexane	56.0	4
41.19	2,5-dimethyl-heptane	30.3	4
42.43	ethylbenzene	59.6	3
42.65	3-ethyl-thiophene	38.6	1
42.81	1,2,4-trimethyl-cyclohexane	32.9	3
43.17	2,6-dimethyl-1-heptene	24.2	3
43.63	2,5-dimethyl-thiophene	55.6	3

Naphtha_Cut 13_140 - 150 °C

Retention			
time (mins)	Name	Probability	Frequency
43.87	p-xylene	31.2	2
44.04	ethinamate	22.5	4
44.46	3-ethyl-hexane	20.7	1
44.68	3,4-dimethyl-thiophene	34.6	2
	1-methyl-3-(1-methyl-ethyl)-		
44.88	cyclopentane	21.8	1
45.26	4-ethyl-heptane	23.2	3
45.58	2,6-dimethyl-3-heptene	23.8	2
45.77	4-methyl-octane	57.6	2
46.2	2,3-dimethyl-thiophene	31.3	1
46.69	3-ethyl-heptane	43.4	2
47.15	p-xylene	31.8	2
49.22	1-nonene	24.0	2
49.92	4-nonene	16.8	4
50.84	nonane	36.5	3
51.37	3-ethyl-2-methyl-1,3-hexadiene	18.4	2
53.38	propyl-cyclohexane	21.0	3
54.43	butyl-cyclopentane	44.5	2
55.21	2,6-dimethyl-octane	24.3	2
55.34	2-propyl-thiophene	32.0	3
55.47	propyl-benzene	56.6	3
56.01	3-methyl-2-methyl-heptane	45.0	4
56.14	2-ethyl-5-methyl-thiophene	39.4	1
56.42	1-ethyl-3-methyl-benzene	38.1	1
56.66	1-ethyl-3-methyl-benzene	27.0	1
57.32	1,2,3-trimethyl-benzene	21.2	1
58.24	5-methyl-nonane	23.7	2
58.42	4-methyl-nonane	38.6	3

Naphtha_Cut 13_140 - 150 °C

Retention time (mins)	Name	Probability	Frequency
60.04	1,2,3-trimethyl-benzene	19.3	1
61.67	2,3,4-trimethyl-thiophene	62.8	1
62.49	decane	38.3	4
62.66	2,5-diethyl-thiophene	36.5	2
62.89	mesytilene	22.1	2
65.89	2-methyl-5-propyl-thiophene	31.1	1
72.11	undecane	19.0	4

Naphtha_Cut 14_150 - 160 °C

Retention time (mins)	Name	Probability	Frequency
4.438	2-methyl-butane	23.8	3
4.839	pentane	61.6	4
7.785	n-hexane	56.1	3
15.45	heptane	38.9	4
26.34	2-methyl-heptane	45.6	3
33.85	1,4-dimethyl-cyclohexane	23.6	4
34.31	octane	28.3	2
38.3	1,2-dimethyl-cyclohexane	24.2	3
38.93	2,4-dimethyl-heptane	17.5	2
40.13	2-methyl-octane	31.2	2
40.27	1,1,3-trimethyl-cyclohexane	56.6	4
41.19	2,5-dimethyl-heptane	42.3	2
42.45	ethylbenzene	61.1	3
42.67	1,3-dimethyl-cyclohexane	20.2	3

Naphtha_Cut 14_150 - 160 °C

Retention			
time (mins)	Name	Probability	Frequency
42.82	1,1,3-trimethyl-cyclohexane	30.7	4
43.19	2,6-dimethyl-1-heptene	27.3	3
43.49	1,2,4-trimethyl-cyclohexane	18.8	3
43.64	2,5-dimethyl-thiophene	39.0	3
43.87	p-xylene	31.5	2
44.04	ethinamate	29.6	4
44.47	3-ethyl-hexane	20.5	1
44.68	3,4-dimethyl-thiophene	35.3	2
44.88	1-methyl-3-(1-methyl-ethyl)- cyclopentane	18.9	1
45.27	4-ethyl-heptane	24.5	3
45.59	2,6-dimethyl-3-heptene	21.1	2
45.78	4-methyl-octane	58.1	3
46.21	2,3-dimethyl-thiophene	31.3	1
46.56	1,2,4-trimethyl-cyclohexane	18.9	1
46.67	3-ethyl-heptane	38.7	2
46.89	2,5-dimethyl-heptane	17.5	1
47.15	p-xylene	28.2	2
47.35	1,2,4-trimethyl-cyclohexane	32.3	4
47.64	3-(1-methylethyl)-cyclohexene	33.0	2
48.99	1,2-diethyl-cyclopentane	32.3	1
50.84	nonane	31.8	3
51.55	2-(1-methylethyl)-thiophene	64.9	1
53.22	3-ethyl-2-methyl-1,3-hexadiene	18.1	1
53.85	propyl-cyclohexane	18.7	3
54.44	butyl-cyclopentane	49.9	3
55.23	2,6-dimethyl-octane	23.9	2
55.35	2-propyl-thiophene	23.9	3

Naphtha_Cut 14_150 - 160 °C

Retention time (mins)	Name	Probability	Frequency
55.48	propyl-benzene	58.1	3
56.02	3-methyl-2-methyl-heptane	47.3	3
56.16	2-(1-methylethyl)-thiophene	44.4	3
56.43	1-ethyl-3-methyl-benzene	35.4	1
56.65	1-ethyl-2-methyl-benzene	27.1	1
57.11	2-(1-methylethyl)-thiophene	57.5	1
57.33	1,2,3-trimethyl-benzene	22.2	1
58.44	4-methyl-nonane	41.6	3
60.06	1,2,3-trimethyl-benzene	24.8	1
60.28	1-isopropyl-3-methyl-cyclohexane	24.7	1
61.68	2,3,4-trimethyl-thiophene	65.9	1
62.51	decane	34.0	4
62.67	2,5-diethyl-thiophene	33.2	2
62.91	mesytilene	20.4	1
65.91	2,5-diethyl-thiophene	26.6	1
66.17	1-methyl-4-propyl-benzene	28.1	1
66.94	2,5-diethyl-thiophene	62.1	1
68.27	5-methyl-decane	17.5	1
72.11	undecane	28.8	4

Naphtha_Cut 15_160 - 175 °C

Retention time (mins)	Name	Probability	Frequency
4.852	pentane	31.0	4
7.839	n-hexane	34.7	3
15.54	heptane	55.5	
34.41	octane	23.4	2

Naphtha_Cut 15_160 - 175 °C

Retention time (mins)	Name	Probability	Frequency
40.17	2-methyl-octane	21.4	3
40.31	1,1,3-trimethyl-cyclohexane	49.8	4
42.49	ethylbenzene	29.4	3
42.87	1,2,4-trimethyl-cyclohexane	21.3	4
43.54	1,1,2-trimethyl-cyclohexane	33.8	1
43.68	3,4-dimethyl-thiophene	67.2	1
43.92	p-xylene	34.7	2
44.09	ethinamate	35.4	4
44.72	3,4-dimethyl-thiophene	36.5	2
45.81	4-methyl-octane	56.4	3
46.25	3,4-dimethyl-thiophene	34.3	2
46.58	1,1,2-trimethyl-cyclohexane	21.2	1
46.7	3-ethyl-heptane	22.5	2
47.18	p-xylene	28.3	2
47.37	1,2,4-trimethyl-cyclohexane	37.3	3
49.02	1-ethyl-2-methyl-cyclohexane	29.7	1
50.85	nonane	22.9	3
53.87	propyl-cyclohexane	21.5	3
54.45	butyl-cyclopentane	32.6	2
55.24	2,6-dimethyl-octane	29.4	2
55.49	propyl-benzene	48.6	3
56.04	3-methyl-2-methyl-heptane	53.1	3
56.17	2-(1-methylethyl)-thiophene	40.8	3
56.45	1-ethyl-3-methyl-benzene	36.2	1
56.67	1-ethyl-3-methyl-benzene	25.5	1
57.13	2-(1-methylethyl)-thiophene	58.6	1
57.34	1,2,3-trimethyl-benzene	22.9	1
58.44	4-methyl-nonane	36.0	3

Naphtha_Cut 15_160 - 175 °C

Retention time (mins)	Name	Probability	Frequency
60.07	1,2,3-trimethyl-benzene	22.2	1
61.69	2,3,4-trimethyl-thiophene	45.2	1
62.54	decane	36.0	4
62.68	2,5-diethyl-thiophene	23.8	1
62.91	1-ethyl-3-methyl-benzene	18.6	1
63.23	trans-p-mentha-1(7),8-dien-2-ol	21.6	3
65.91	2-methyl-5-propyl-thiophene	24.7	1
66.19	1-methyl-3-propyl-benzene	34.6	2
66.95	2,5-diethyl-thiophene	58.6	2
67.18	2,5-diethyl-thiophene	22.5	2
68.04	2,5-diethyl-thiophene	54.4	2
68.28	5-methyl-decane	22.8	2
68.78	p-cymene	35.0	1
68.91	2-methyl-decane	20.6	2
69.48	3-methyl-decane	21.4	1
72.12	undecane	39.9	4

Naphtha_Cut 16_175 - 185 °C

Retention time (mins)	Name	Probability	Frequency
2.333	pentane	84.0	4
46.89	3-ethyl-heptane	30.5	1
54.43	butyl-cyclopentane	22.4	2
55.21	2,6-dimethyl-octane	38.0	2
55.49	propyl-benzene	28.1	3

Naphtha_Cut 16_175 - 185 °C

Retention time (mins)	Name	Probability	Frequency
56.01	3-methyl-2-methyl-heptane	42.7	3
56.15	2-(1-methylethyl)-thiophene	36.4	1
56.42	1-ethyl-3-methyl-benzene	32.7	1
56.65	1-ethyl-3-methyl-benzene	30.8	1
56.94	1,1,2,3-tetramethyl-cyclohexane	37.1	2
57.11	2-(1-methylethyl)-thiophene	44.8	1
57.33	1,2,3-trimethyl-benzene	23.4	1
58.43	4-methyl-nonane	34.7	3
60.05	1,2,3-trimethyl-benzene	25.9	1
61.12	1,4,6,6-tetramethyl-cyclohexene	19.2	1
61.68	2,3,4-trimethyl-thiophene	26.7	1
62.53	decane	36.3	4
62.67	2,5-diethyl-thiophene	25.4	2
62.91	mesytilene	22.4	2
65.91	2,5-diethyl-thiophene	22.6	1
66.19	1-methyl-3-propyl-benzene	30.3	2
66.96	2,5-diethyl-thiophene	49.9	2
68.04	2,5-diethyl-thiophene	54.7	2
68.29	5-methyl-decane	18.9	1
68.79	p-cymene	37.1	1
68.91	2-methyl-decane	19.4	2
69.48	3-methyl-decane	19.8	2
69.89	trans-p-mentha-1(7),8-dien-2-ol	26.1	2
72.15	undecane	37.3	4
76.05	2-ethyl-5-propyl-thiophene	67.9	2
80.61	dodecane	4.0	
81.88	2,6-dimethyl-undecane	25.9	2

Naphtha_Cut 17_185 - 195 °C

Retention			
time (mins)	Name	Probability	Frequency
2.253	2-methyl-butane	30.9	3
2.333	pentane	86.4	4
55.22	2,6-dimethyl-octane	20.9	2
56.02	3-methyl-2-methyl-heptane	24.4	
56.44	1-ethyl-3-methyl-benzene	43.8	1
56.96	1,1,2,3-tetramethyl-cyclohexane	29.1	1
58.44	4-methyl-nonane	28.1	3
60.05	1,2,3-trimethyl-benzene	22.4	1
62.51	decane	41.2	4
62.9	mesytilene	21.5	1
63.51	trans-p-mentha-1(7),8-dien-2-ol	34.6	2
65.3	(1-methylpropyl)-cyclohexane	19.7	1
65.91	2-methyl-5-propyl-thiophene	20.2	1
66.18	1-methyl-3-propyl-benzene	32.7	3
66.96	2,5-diethyl-thiophene	53.2	2
67.62	trans-p-mentha-1(7),8-dien-2-ol	23.9	2
68.04	2,5-diethyl-thiophene	58.1	2
68.79	p-cymene	32.6	1
68.91	2-methyl-decane	18.5	2
69.49	3-methyl-decane	22.3	2
69.89	trans-p-mentha-1(7),8-dien-2-ol	23.1	2
72.15	undecane	31.3	4
76.06	2-ethyl-5-propyl-thiophene	69.4	1
76.93	6-methyl-undecane	20.3	1
80.62	dodecane	25.7	4
81.88	2,6-dimethyl-undecane	29.7	3

APPENDIX F: Concentration of compounds identified in cracked naphtha

Peak	Retention time (mins)	Name	wt%
1	4.138	isobutane	0.12
2	4.310	2-butene	0.23
3	4.393	butane	0.91
5	4.482	2-butene	0.16
8	4.629	2-butene	0.13
9	5.041	3-methyl-1-butene	0.09
10	5.330	2-methyl-butane	1.89
11	5.597	ethyl-cyclopropane	0.54
12	5.688	ethanethiol	0.04
13	5.735	2-methyl-1-butene	0.37
14	5.837	pentane	3.98
16	6.005	2-pentene	0.66
18	6.201	2-pentene	0.34
19	6.328	1,2-dimethyl-cyclopropane	0.91
22	6.798	2,2-dimethyl-butane	0.03
23	7.154	2-propanethiol	0.07
24	7.389	cyclopentene	0.13
25	7.504	4-methyl-1-pentene	0.25
26	7.566	3-methyl-1-pentene	0.11
27	7.813	cyclopentane	0.39
28	7.872	2,3-dimethyl-butane	0.28
29	7.958	4-methyl-2-pentene	0.07
30	8.034	2-methyl-pentane	2.72
33	8.689	3-methyl-pentane	1.10
34	8.927	2-methyl-1-pentene	0.30
35	8.976	1-hexene	0.68
36	9.363	propyl mercaptan	0.07
37	9.598	n-hexane	4.12

Peak	Retention time (mins)	Name	wt%
38	9.710	3-hexene	0.20
39	9.781	3-hexene	0.07
40	9.870	2- hexene	0.50
41	10.009	2-methyl-2-pentene	0.70
42	10.155	3-methyl-cyclopentene	0.12
43	10.216	3-methyl-2-pentene	0.20
45	10.457	2-hexene	0.26
46	10.868	3-methyl-2-pentene	0.32
47	11.168	2,2-dimethyl-pentane	0.03
48	11.331	methyl-cyclopentane	1.48
56	12.958	2,4-dimethyl-1-pentene	0.03
58	13.161	3-methyl-cyclopentene	0.60
59	13.210	benzene	0.15
60	13.362	3-ethyl-2-pentene	0.07
61	13.587	thiophene	0.21
63	13.935	5-methyl-1-hexene	0.06
64	14.090	cyclohexane	0.50
65	14.330	2-methyl-3-hexene	0.06
68	14.656	4-methyl-1-hexene	0.18
69	14.921	4-methyl-2-hexene	0.18
70	15.074	2-methyl-hexane	1.24
71	15.233	2,3-dimethyl-pentane	0.50
72	15.513	1,1-dimethyl-cyclopentane	0.06
73	15.749	ethylidenecyclobutane	0.11
74	16.044	3-methyl-hexane	1.46
76	16.749	1,3-dimethyl-cyclopentane	0.41
77	17.088	1,3-dimethyl-cyclopentane	0.35
79	17.432	1,2-dimethyl-cyclopentane	0.52
80	17.664	1-heptene	0.58
82	18.510	3-methyl-3-hexene	0.09

Peak	Retention time (mins)	Name	wt%
83	19.008	3-heptene	0.58
84	19.294	heptane	4.32
86	19.612	2-methyl-2-hexene	0.22
87	19.763	2-heptene	0.14
88	20.033	2,3-dimethyl-2-pentene	0.40
89	20.257	4-methyl-2-hexene	0.03
91	20.691	3-methyl-2-hexene	0.37
94	21.843	3-ethyl-2-pentene	0.04
95	22.191	3-methyl-2-hexene	1.26
96	22.822	2-heptene	0.09
99	24.357	ethyl-cyclopentane	0.52
100	24.860	2,5-dimethyl-hexane	0.27
101	25.198	2,4-dimethyl-hexane	0.16
103	26.154	1,2,4-trimethyl-cyclopentane	0.20
107	27.708	1,2,3-trimethyl-cyclopentane	0.14
110	28.576	1-methylidene-cyclobutane	0.46
111	28.887	ethylidene-cyclopentane	0.20
112	29.103	toluene	0.72
113	29.540	2-methyl-thiophene	0.46
116	30.636	4-methyl-2-heptene	0.04
117	30.870	1-ethyl-2-methyl-cyclopentene	0.18
118	31.197	3-methyl-thiophene	0.39
119	31.338	3-ethyl-2-methyl-pentane	0.16
122	32.693	2-methyl-heptane	2.04
123	32.986	4-methyl-heptane	0.45
124	33.414	ethylidene-cyclopentane	0.11
125	33.900	6-methyl-2-heptene	0.11
126	34.112	1,3-dimethyl-cyclohexane	0.28
127	34.284	3-methyl-heptane	0.76
128	34.496	1,4-dimethyl-cyclohexane	0.21

Peak	Retention time (mins)	Name	wt%
132	35.530	1,1-dimethyl-cyclohexane	0.07
135	36.472	1-ethyl-3-methyl-cyclopentane	0.41
136	36.867	1-ethyl-3-methyl-cyclopentane	0.24
137	37.106	1-ethyl-3-methyl-cyclopentane	0.25
140	37.890	1,2-dimethyl-cyclohexane	0.16
143	38.971	1-ethyl-5-methyl-cyclopentene	0.15
144	39.139	1,4-dimethyl-cyclohexane	0.14
145	39.341	1-octene	0.37
146	39.589	octane	2.71
151	41.014	1-ethyl-5-methyl-cyclopentene	0.05
160	43.191	1,2-dimethyl-cyclohexane	0.09
162	43.619	2,4-dimethyl-heptane	0.10
165	44.116	ethyl-cyclohexane	0.53
167	44.694	2,6-dimethyl-heptane	0.54
168	44.979	1,1,3-trimethyl-cyclohexane	0.61
169	45.327	1-ethyl-5-methyl-cyclopentene	0.04
170	45.681	2,5-dimethyl-heptane	0.21
175	46.954	ethylbenzene	0.25
176	47.141	2-ethyl-thiophene	0.30
177	47.321	1,2,4-trimethyl-cyclohexane	0.20
178	47.494	2,6-dimethyl-1-heptene	0.17
180	47.909	1,2,4-trimethyl-cyclohexane	0.02
181	48.054	2,5-dimethyl-thiophene	0.25
182	48.264	m-xylene	0.66
183	48.375	p-xylene	0.32
185	48.708	3-ethyl-hexane	0.34
186	49.033	3,4-dimethyl-thiophene	0.39
187	49.216	1-methyl-3-(1-methyl-ethyl)-cyclopentane	0.10
188	49.388	4-ethyl-heptane	0.16
189	49.720	2,6-dimethyl-3-heptene	0.14

Peak	Retention time (mins)	Name	wt%
190	49.887	4-methyl-octane	0.34
191	50.040	2-methyl-octane	0.52
193	50.476	2,3-dimethyl-thiophene	0.36
194	50.753	3-ethyl-heptane	0.13
195	50.940	2,5-dimethyl-heptane	0.82
197	51.362	o-xylene	0.33
198	51.545	1,2,4-trimethyl-cyclohexane	0.13
199	51.774	3-(1-methylethyl)-cyclohexene	0.07
203	52.771	1,2-diethyl-cyclopentane	0.12
204	53.145	1-nonene	0.34
206	53.818	4-nonene	0.14
210	54.663	nonane	1.86
212	55.036	2-nonene	0.15
215	55.516	2-(1-methyl-ethyl)-thiophene	0.04
224	57.713	propyl-cyclohexane	0.19
226	58.253	butyl-cyclopentane	0.20
230	58.898	2,6-dimethyl-octane	0.55
232	59.192	2-propyl-thiophene	0.18
233	59.303	propyl-benzene	0.15
235	59.702	3-methyl-2-methyl-heptane	0.31
236	59.952	2-(1-methyl-ethyl)-thiophene	0.36
237	60.215	1-ethyl-3-methyl-benzene	0.32
238	60.431	1-ethyl-3-methyl-benzene	0.16
240	60.827	1,1,2,3-tetramethyl-cyclohexane	0.21
241	60.936	2-(1-methyl-ethyl)-thiophene	0.13
242	61.096	mesitylene	0.25
247	62.020	5-methyl-nonane	0.40
248	62.116	4-methyl-nonane	0.12
256	63.788	1,2,4-trimethyl-benzene	0.37
262	64.796	2,3,4-trimethyl-thiophene	0.36

Peak	Retention time (mins)	Name	wt%
269	66.028	decane	1.14
270	66.264	2,5-diethyl-thiophene	0.25
272	66.627	1,2,3-trimethyl-benzene	0.26
284	68.939	(1-methylpropyl)-cyclohexane	0.12
288	69.539	2-methyl-5-propyl-thiophene	0.28
289	69.796	1-methyl-3-propyl-benzene	0.13
293	70.587	2,5-diethyl-thiophene	0.23
295	70.960	2,5-diethyl-thiophene	0.11
297	71.431	2,5-diethyl-thiophene	0.11
298	71.727	5-methyl-decane	0.25
300	72.228	p-cymene	0.09
301	72.372	2-methyl-decane	0.23
304	72.949	3-methyl-decane	0.27
314	74.145	1-undecene	0.09
316	75.580	undecane	0.61
333	79.636	2-ethyl-5-propyl-thiophene	0.10
337	80.377	6-methyl-undecane	0.06
355	84.083	dodecane	0.31
360	85.352	2,6-dimethyl-undecane	0.14
390	91.872	tridecane	0.16
400	99.109	tetradecane	0.12
401	105.889	pentadecane	0.06